Attempts in improving low clouds, deep clouds and mean states of CFSv2

Partha Mukhopadhyay

Phani Murli Krishna, Medha Deshpande, M. Mahakur, Malay Ganai, Sahadat Sarkar, Snehlata Tirkey, Shilpa Malviya, Tanmoy Goswami, Kumar Roy

Student who worked : Abhik S. and Bidyut Goswami

Dr. V. S. Prasad and Dr. R. Ashrit (NCMRWF)

Work presented here are from the following papers

Goswami et al. 2014
Bidyut B. Goswami, R. P. M. Phani, P. Mukhopadhyay, Marat Khairoutdinov and B. N. Goswami, "Simulation of the Indian Summer Monsoon in the Superparameterized Climate Forecast System version 2: Preliminary Results", **J. of Climate**, 2015
Abhik et al. 2015, Clim Dyn.
Ganai Et al. 2014, Clim. Dyn on Revised SAS
Ganai et al. 2016, JGR, diurnal
Abhik et al. 2017 (JAMES under revision)

Outline

- Paradigm of Conventional Parameterization

- Issues of CFSv2 biases related to convection

- Recent approaches in dealing convection parameterization in CFSv2

- High resolution GFS/GEFS

- Future plans

Issues of cumulus Parameterization

The Cumulus Parameterization Problem: Past, Present, and Future

By Akio Arakawa, JOC, 2004, Arakawa et al. 2011, Arakawa and Wu 2013, Wu and Arakawa 2014

- "Major practical and conceptual problems in the conventional approach of cumulus parameterization, includes inappropriate separations of processes and scales".

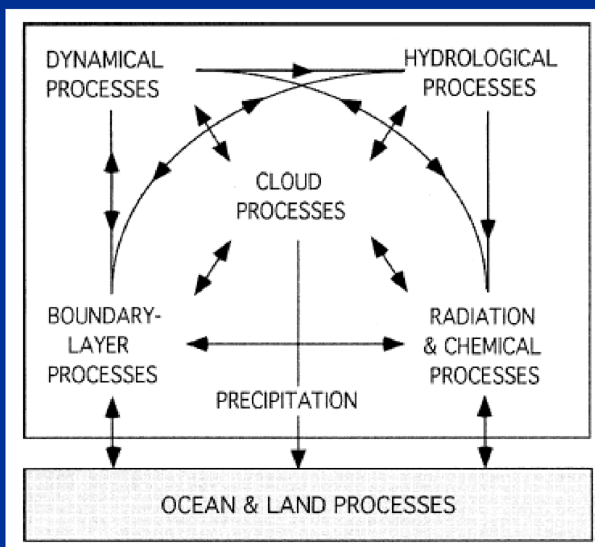

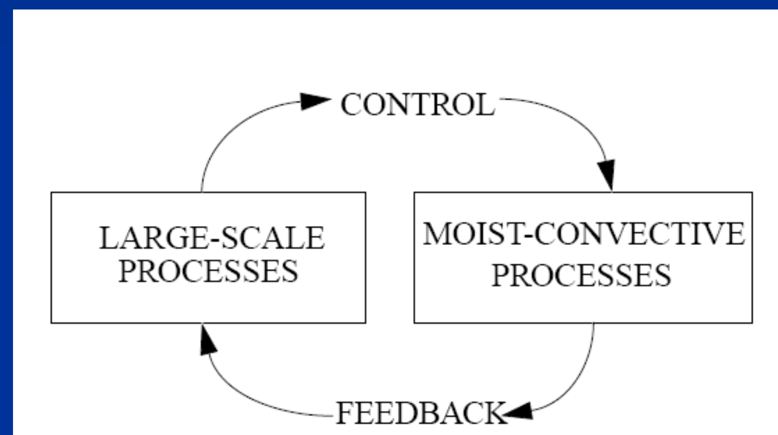

$$\sum_{j=1}^{N} K_{ij} \cdot M_{Bj} + F_i = 0$$

K_{ij} = effect of cloud j on cloud i,

F_i = environmental forcing for cloud i

M_{Bj} = mass flux at base of cloud j

Task of Conv. Param

To calculate the collective effects of an ensemble of convective clouds in a model column

$$Q_{1C} \equiv Q_1 - Q_R \equiv L(\bar{c} - \bar{e}) - \frac{\partial \overline{\omega' s'}}{\partial p}$$

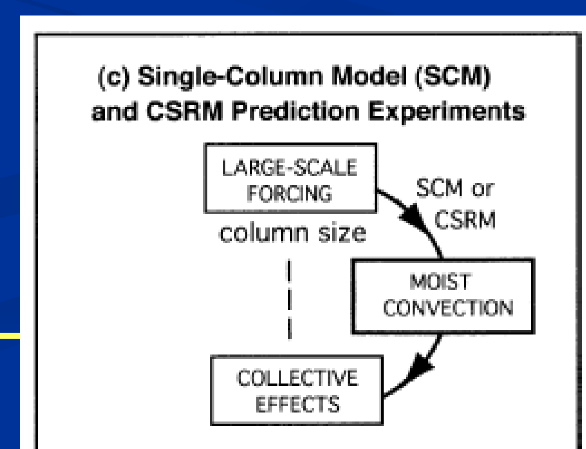

ISSUES

- CFSv2 T126 shows colder Tropospheric temperature bias and colder SST bias

- CFSv2 T382 shows warmer Tropospheric temperature and warmer SST bias

Inspite of contrasting bias, the rainfall bias in both the models are similar

- CFSv2T126 & CFSv2 T382 both produce too much frequency of lighter rainfall (drizzle) and shows dry bias over Indian land mass but northward propagation is reasonable in both.

- CFSv2T126 & CFSv2 T382 both underestimates synoptic variance and overestimates ISO variance

- Diurnal Convective lifecycle is equally incorrect in CFSv2T126 & CFSv2 T382. (Deep convection is lacking)

CFSv2 T126 bias

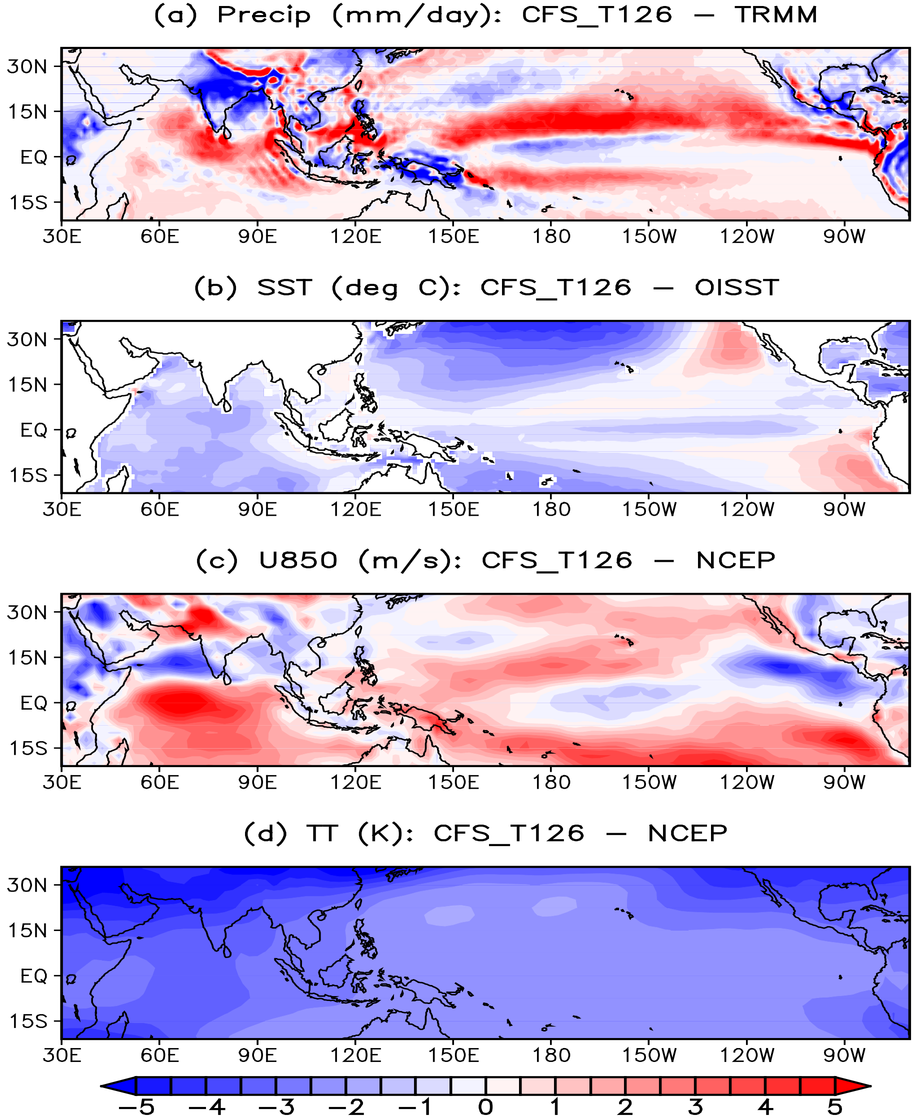

CFSv2 T382 bias

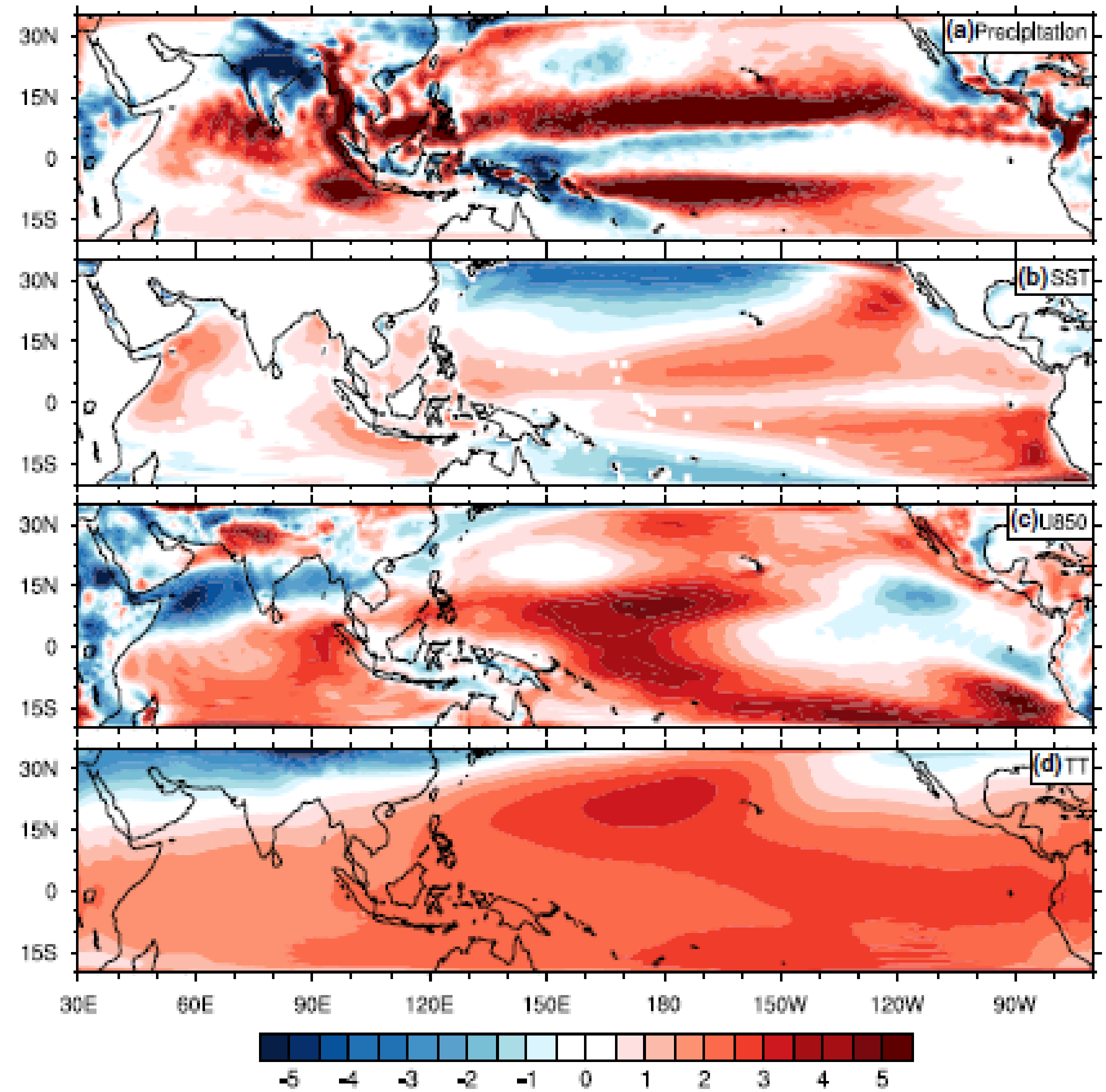

Seasonal mean bias in a) precipitation (mm day−1), b) SST (°C), c) zonal wind at 850 hPa (m s −1) and d) tropospheric temperature (TT, K) relative to TRMM, TMI and CFSR respectively

Abhik et al. Cli. Dyn. 2015,

Climatology of JJA Precipitation

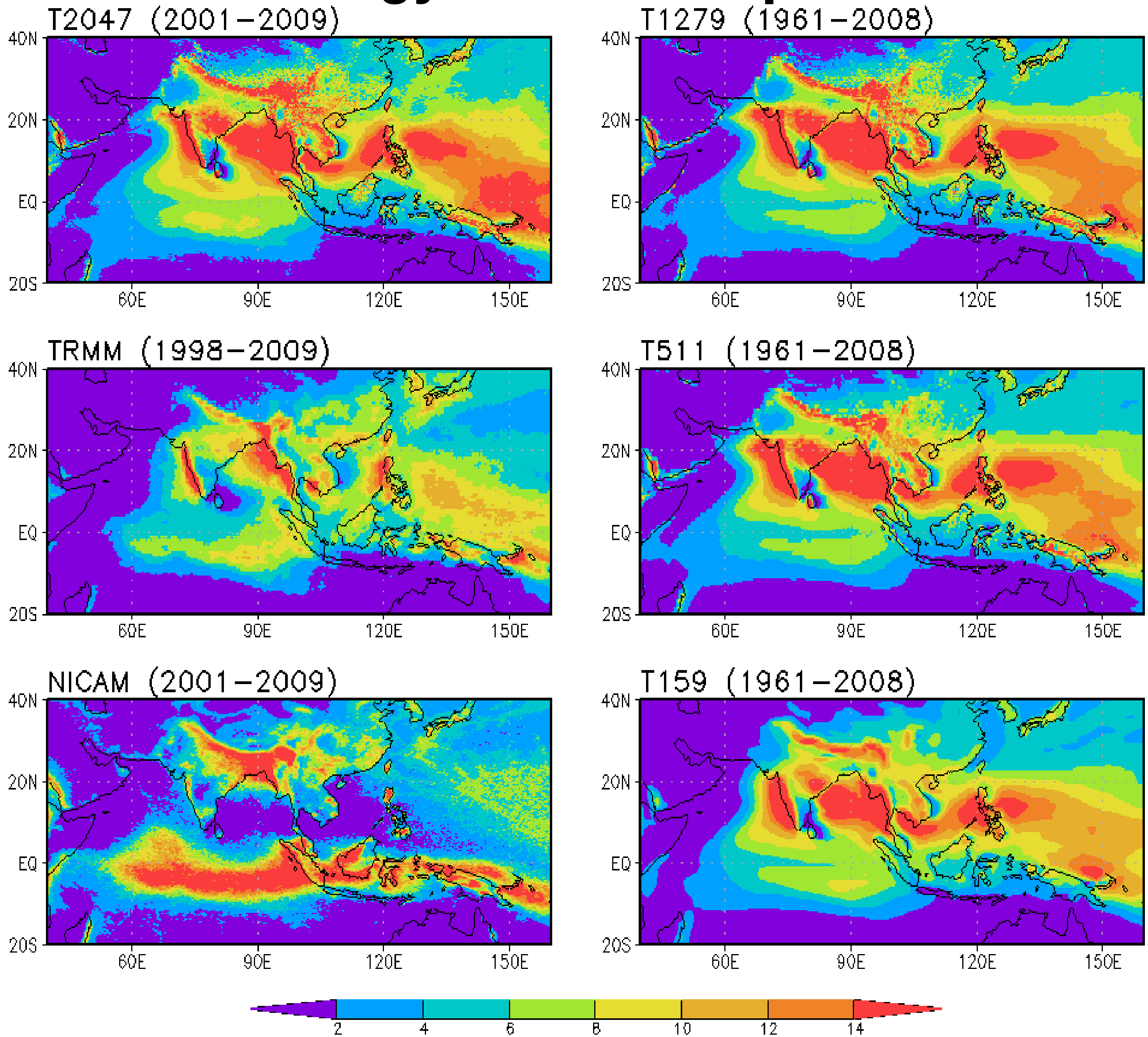

IFS T12047
10 km

IFS T1279
15 km

TRMM
25km

IFS T1511
39km

NICAM
7 km

IFS T1159
125 km

Slide courtesy Emilia Jin, Athena Workshop, ECMWF, 7-8 June 2010

Standard Deviation of JJA Precipitation Anomalies

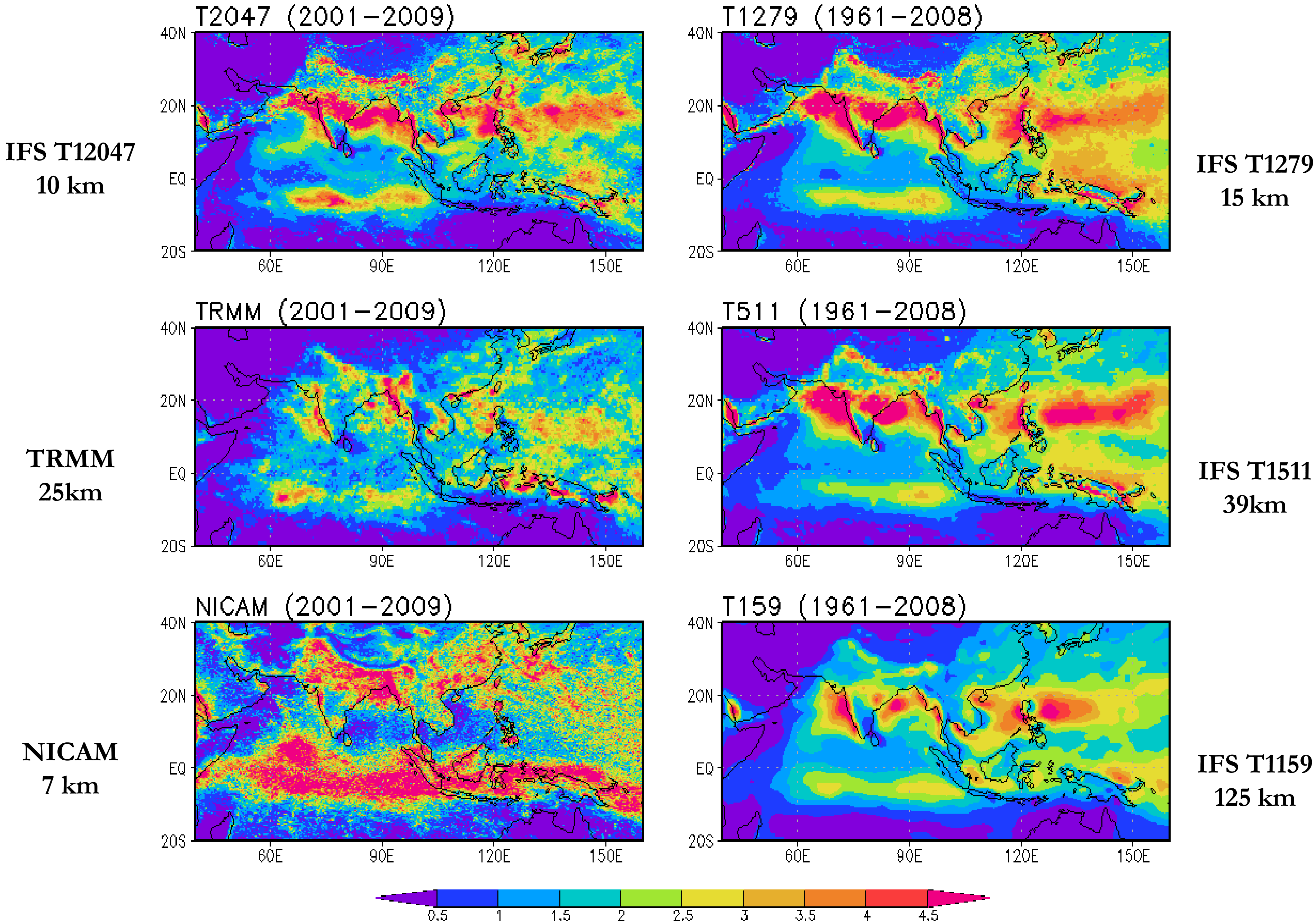

Slide courtesy Emilia Jin, Athena Workshop, ECMWF, 7-8 June 2010

Fig. 4 Probability distribution function (PDF) of daily rainfall (mm day^{-1}) during all JJAS seasons with a bin width of 5 mm day^{-1} in percentage over **a** central India (CI), **b** Bay of Bengal (BoB), **c** Arabian Sea (AS) and eastern equatorial Indian Ocean (EEIO). The regions are marked by *white boxes* in Fig. 3b

CFSv2T382

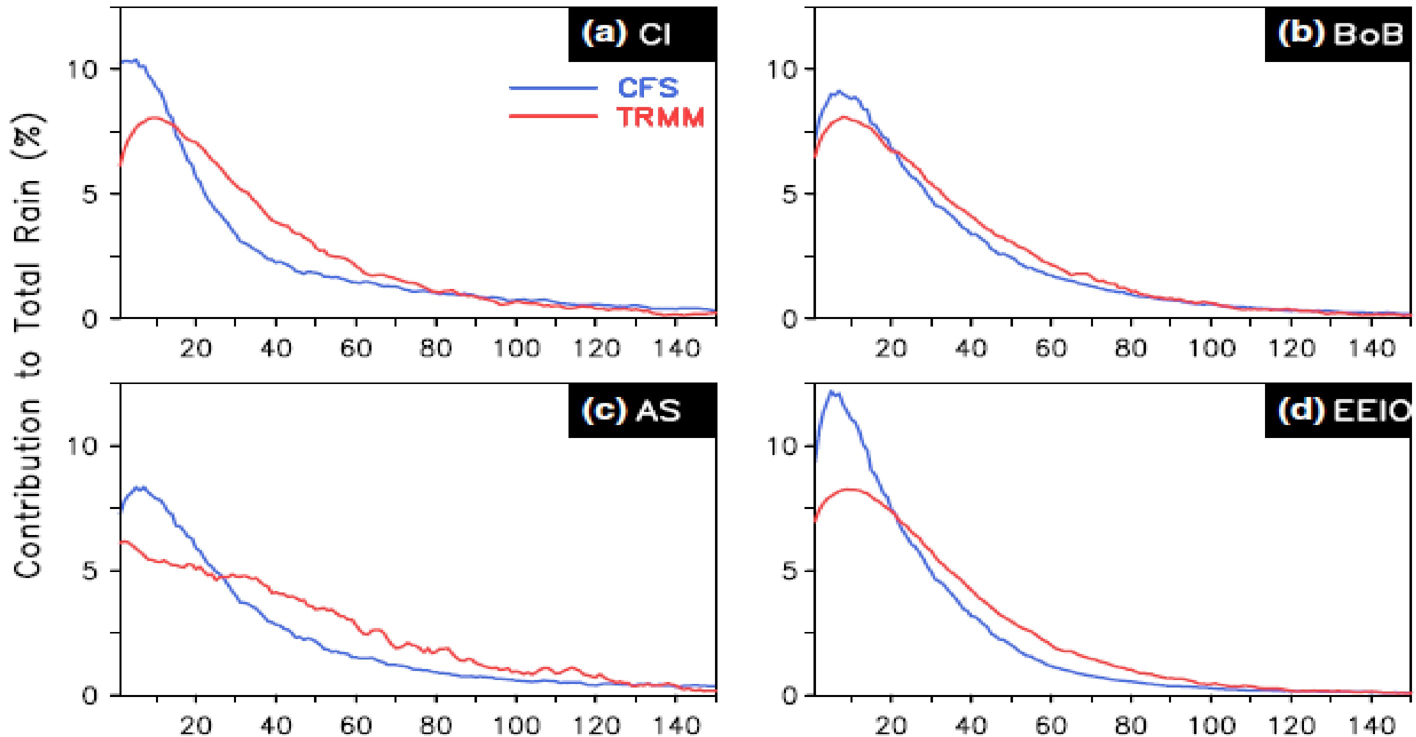

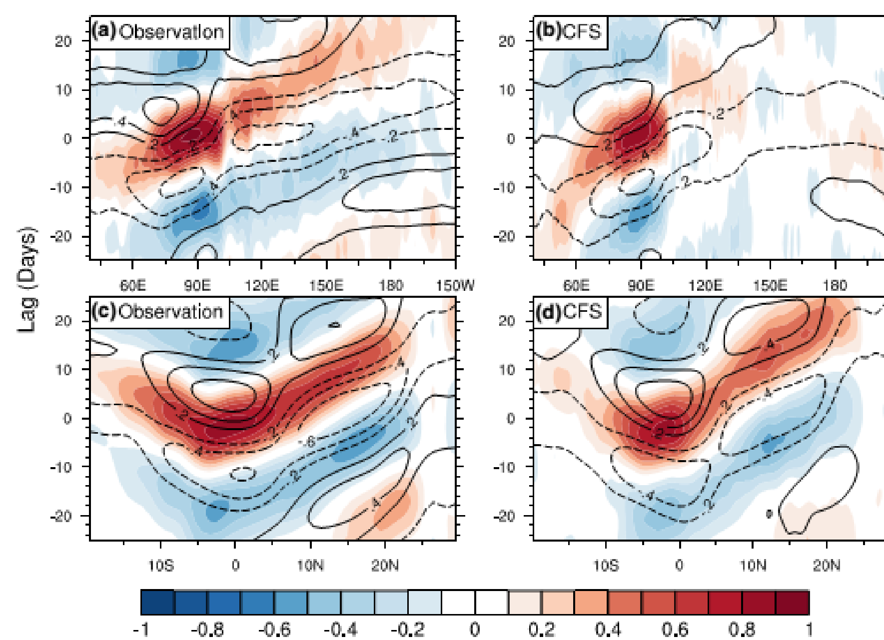

Fig. 8 **a, b** Longitude versus lag correlation and **c, d** latitude versus lag correlation of 20–100-day filtered precipitation (*shaded*) and U_{850} (*contour*) with base 20–100-day filtered precipitation time series over EEIO (10°S–5°N, 75°–100°E) for observation and CFS T382. For longitude-lag (latitude-lag) plot data are averaged between 70°E and 90°E (10°S and 10°N)

Abhik et al. 2015

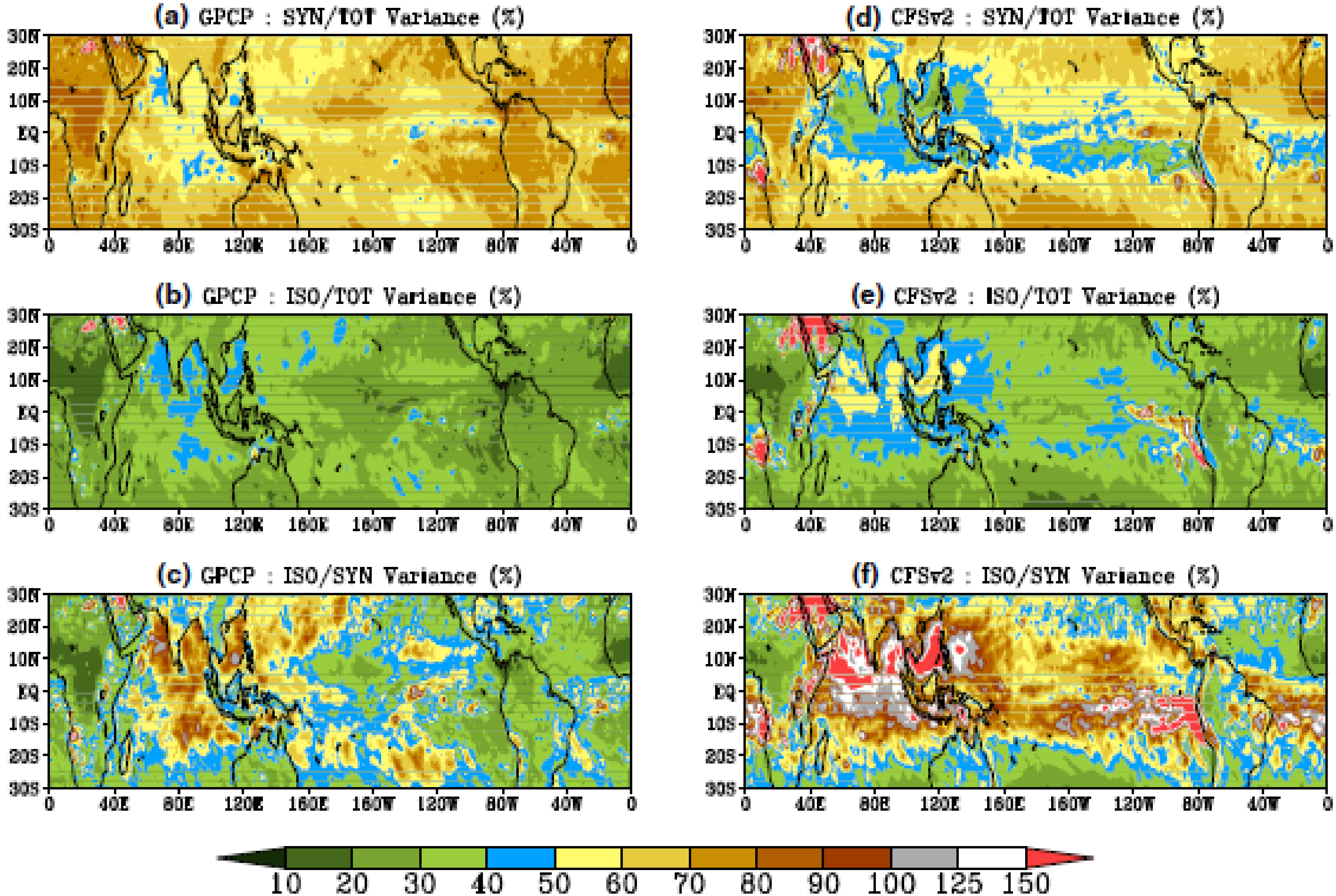

CFSv2 T126 (right panel) underestimates Synoptic variance and overestimates ISO variance over global tropics

Abhik et al. 2015

CFSv2 T382 ISO
10-90 days
variance

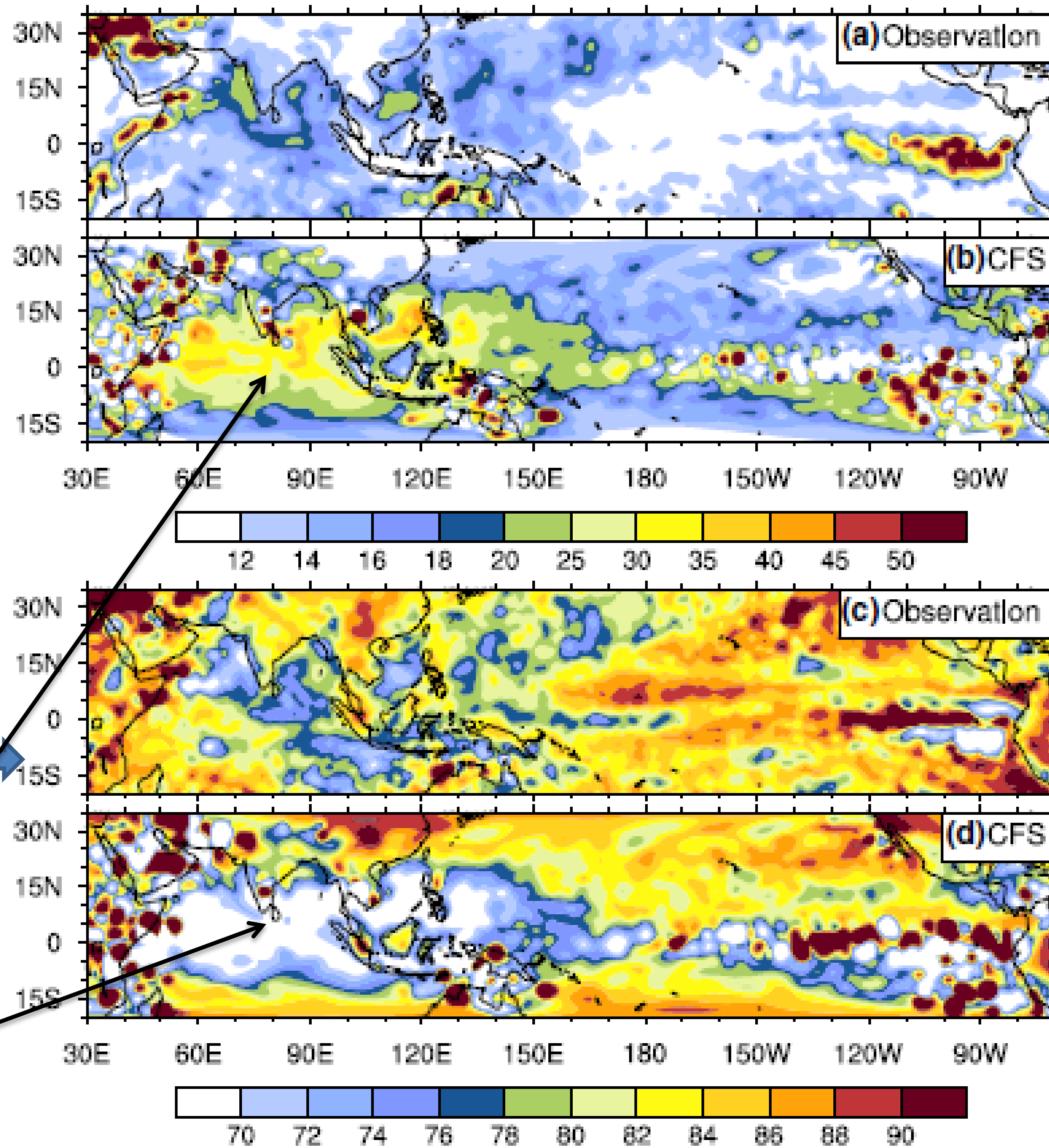

CFSv2 T382
Synoptic variance
(2-10 Days)

CFSv2 T382 overestimates ISO and underestimates Synoptic variance over tropics

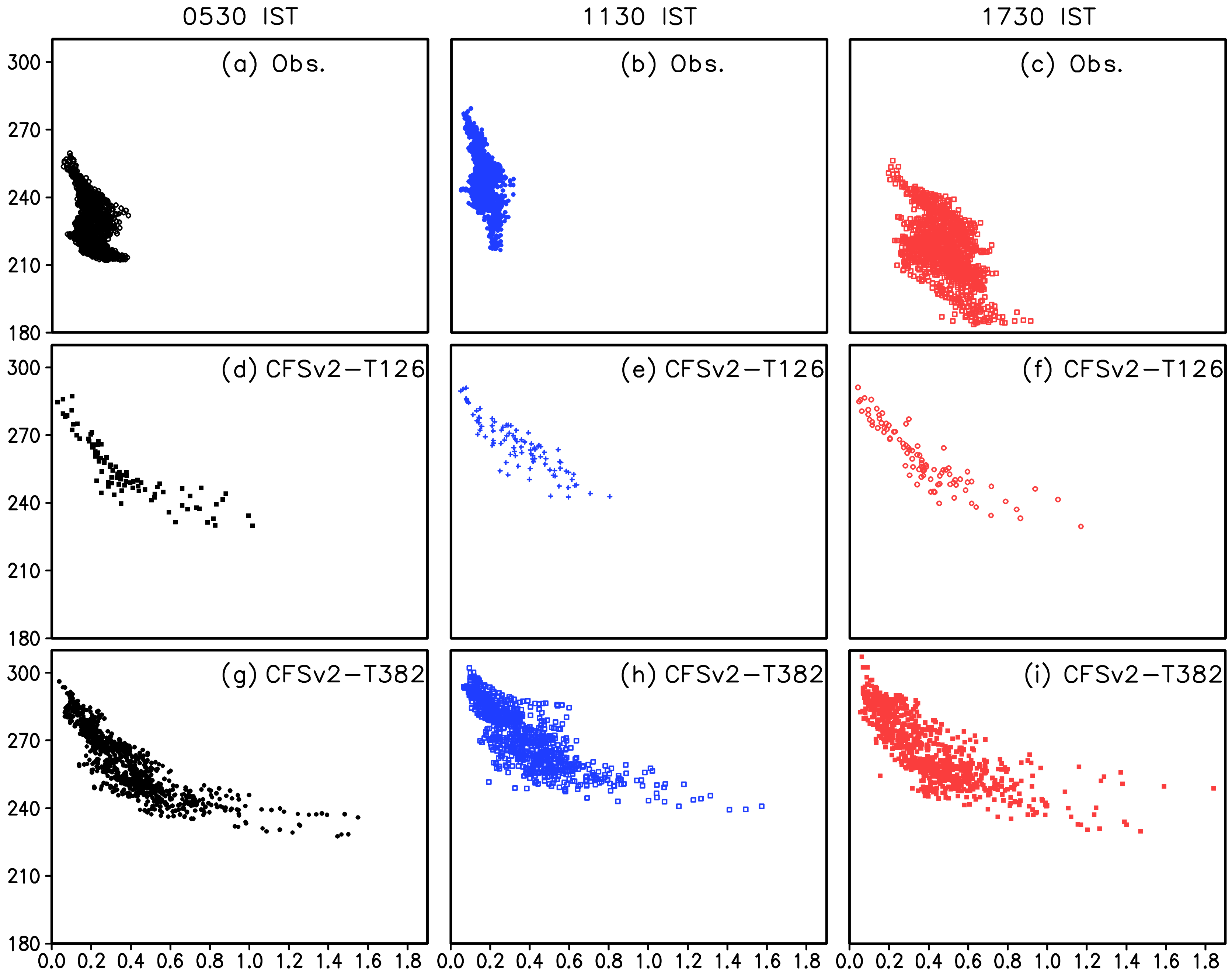

Scatter plot of OLR vs rainrate

Both the model do not produce deep convection consistent with too much of lighter precipitation

Ganai et al. 2015

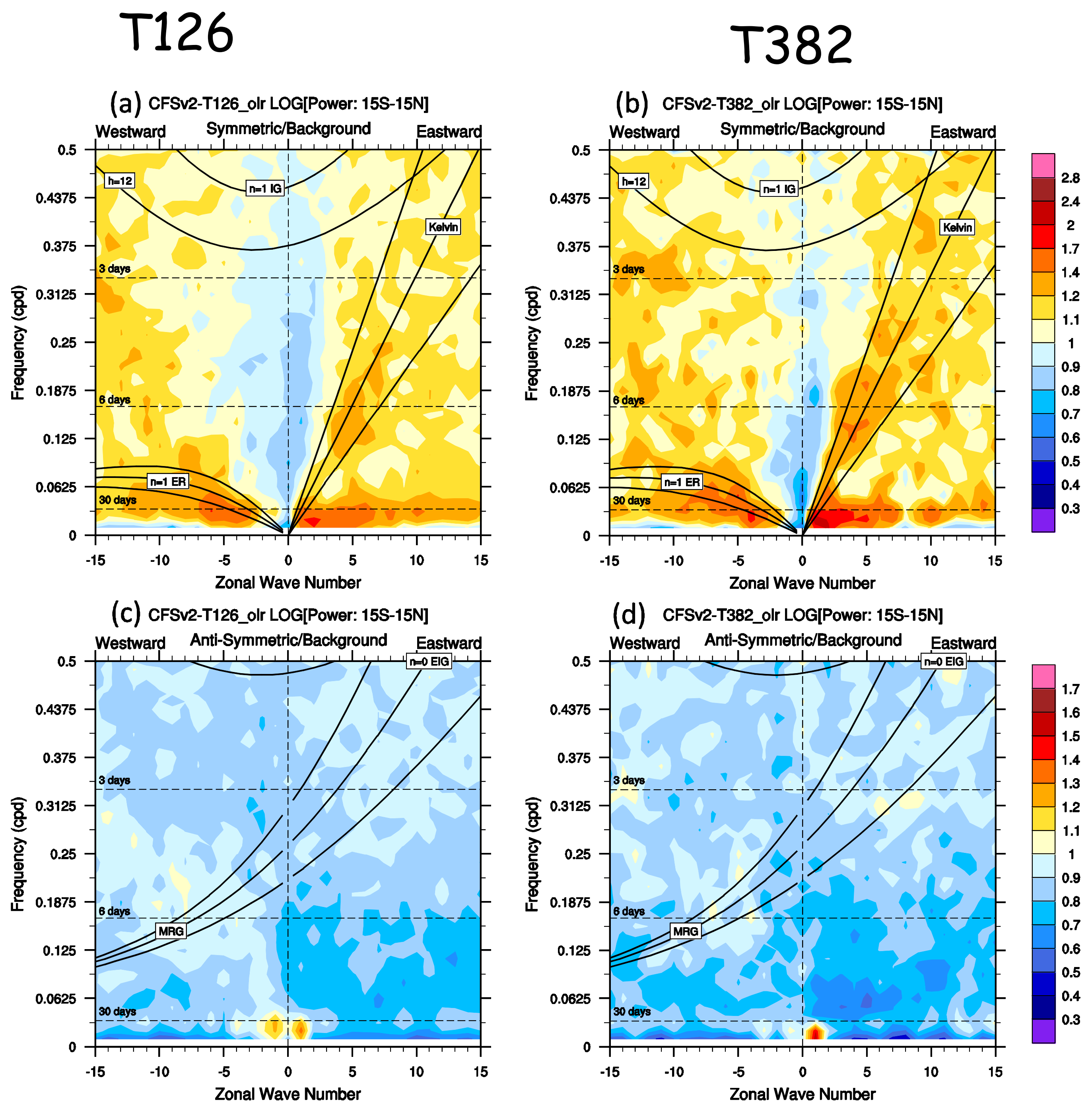

Space-Time spectra (Wheeler-Kiladis diagram [Wheeler and Kiladis, 1999]) of OLR showing the symmetric component for (a) CFSv2-T126, (b) CFSv2-T382 and the anti-symmetric component for (c) CFSv2-T126, (d) CFSv2-T382.

Goswami et al. 2015

CFSv2 T382

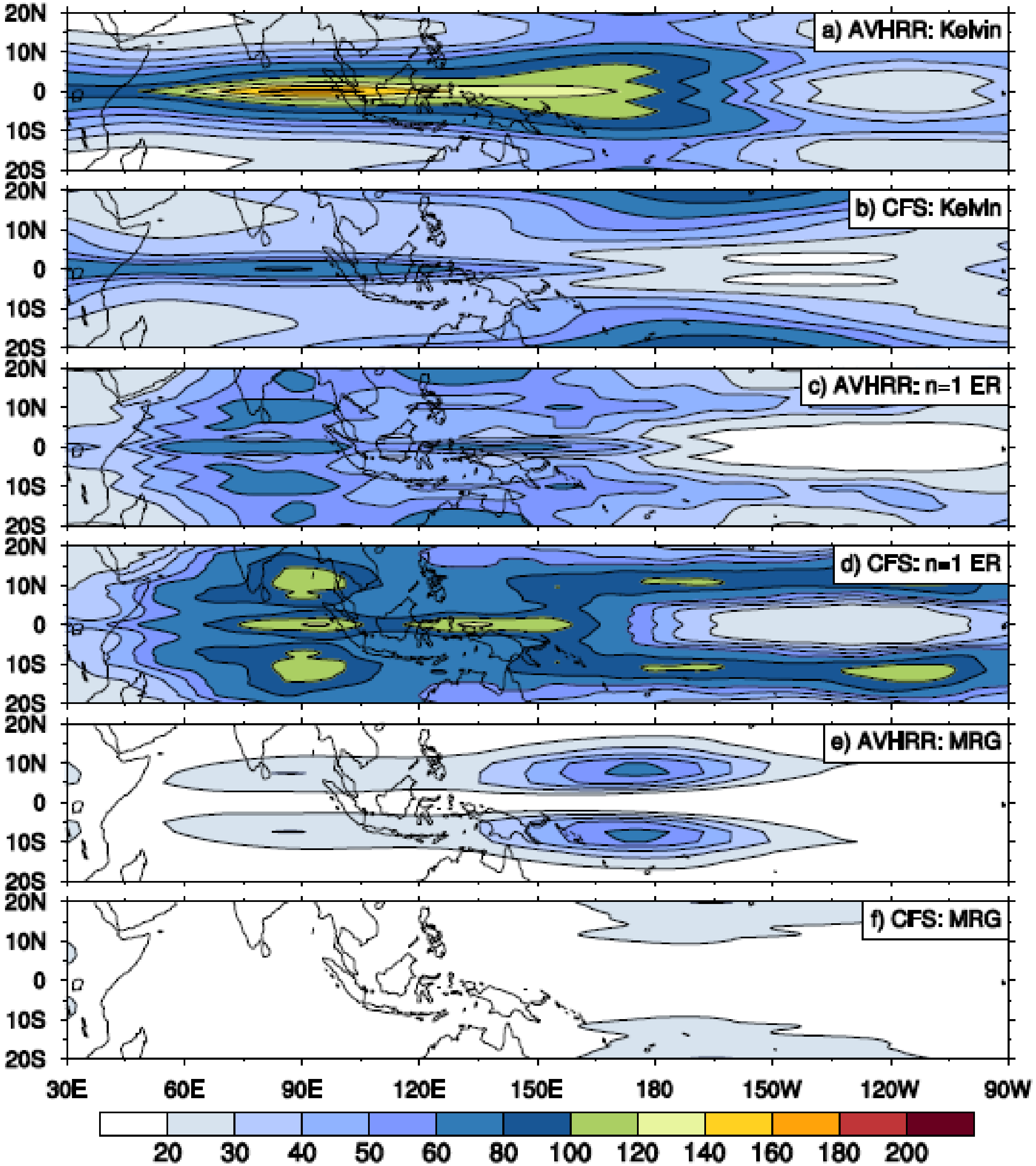

Fig. 13: Distribution of boreal summer time OLR variance ($W^2\ m^{-4}$) of (a), (b) Kelvin; (c), (d) n=1 ER and (e), (f) MRG waves for AVHRR and CFS.

Abhik et al., 2015

Arakawa and Wu, 2013

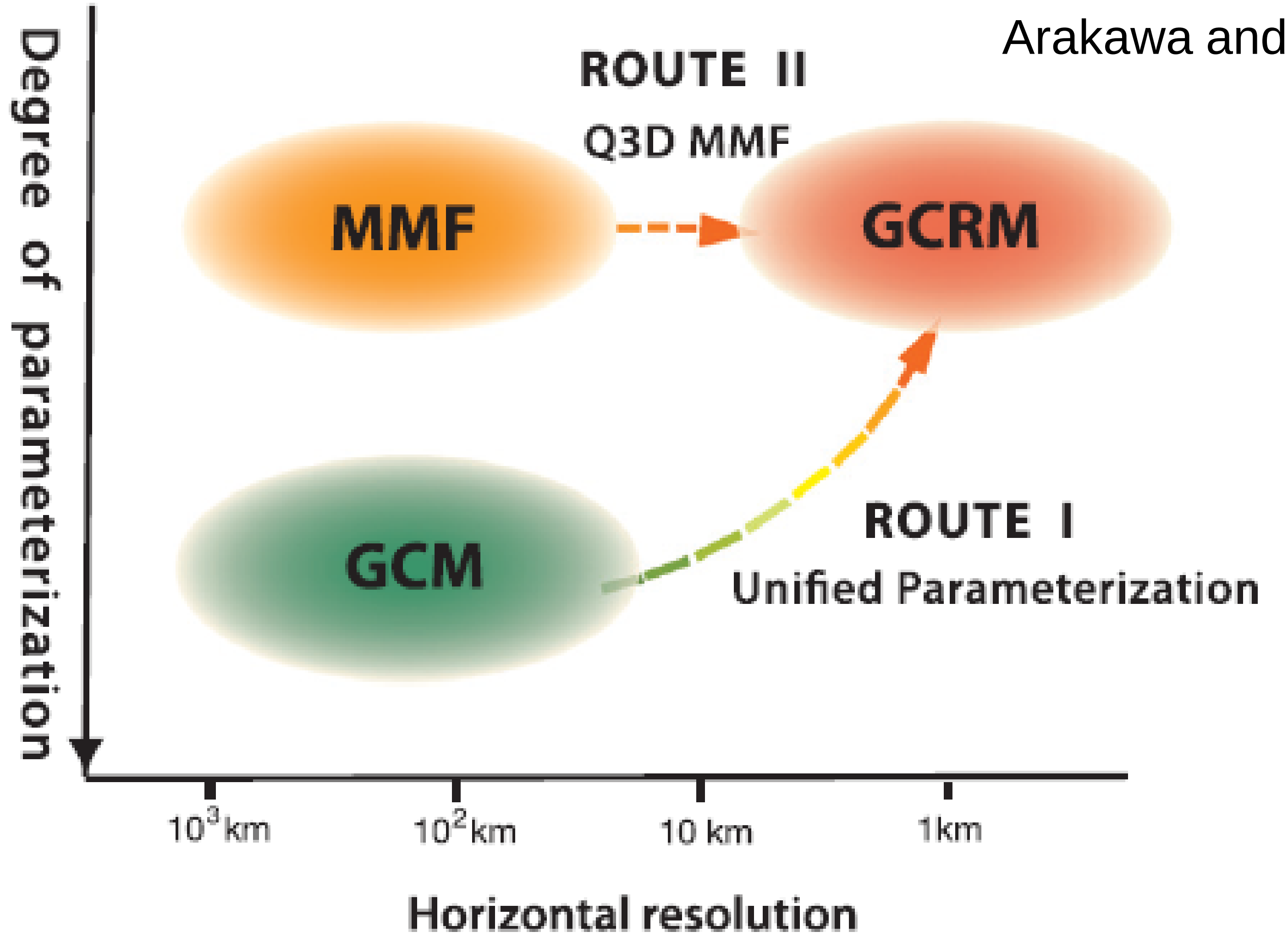

FIG. 3. Two routes for unifying the low- and high-resolution models.

Route II with 2D MMF: accomplished in IITM through development of SP-CFS

Attempts of Improving the biases of CFSv2 through Superparameterized CFS (SP-CFS)

Bidyut B. Goswami, R. P. M. Krishna, P. Mukhopadhyay, Marat Khairoutdinov, and B. N. Goswami, 2015: Simulation of the Indian Summer Monsoon in the Superparameterized Climate Forecast System Version 2: Preliminary Results. J. Climate, 28, 8988–9012

AMERICAN METEOROLOGICAL SOCIETY
AMS Journals Online

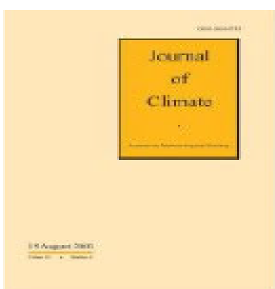

Journal Information
Online ISSN: 1520-0442
Print ISSN: 0894-8755
Frequency: Semimonthly

Journal of Climate 2015 ; e-View
doi: http://dx.doi.org/10.1175/JCLI-D-14-00607.1

Simulation of the Indian Summer Monsoon in the Superparameterized Climate Forecast System version 2: Preliminary Results

BIDYUT B. GOSWAMI,[1] R.P.M. KRISHNA,[2] P. MUKHOPADHYAY,[2] MARAT KHAIROUTDINOV,[3] and B. N. GOSWAMI[4]

[1] *Department of Mathematics and Statistics, University of Victoria, Canada*

[2] *Indian Institute of Tropical Meteorology, Pune-411008, INDIA*

[3] *School of Marine and Atmospheric Sciences, New York University, Stony Brook, USA*

[4] *Pisharoty Chair Professor, MoES, Indian Institute of Science Education and Research, Pune-411008, INDIA*

Superparameterized CFSv2-T62 (SPCFS) Analyses of 6.5 year free run

Convective tendencies are explicitly simulated with a **C**loud **R**esolving **M**odel running in each GCM grid column which replaces the traditional cumulus parameterization of the GCM.

- Model integrated for 6.5 years and five years are analyzed

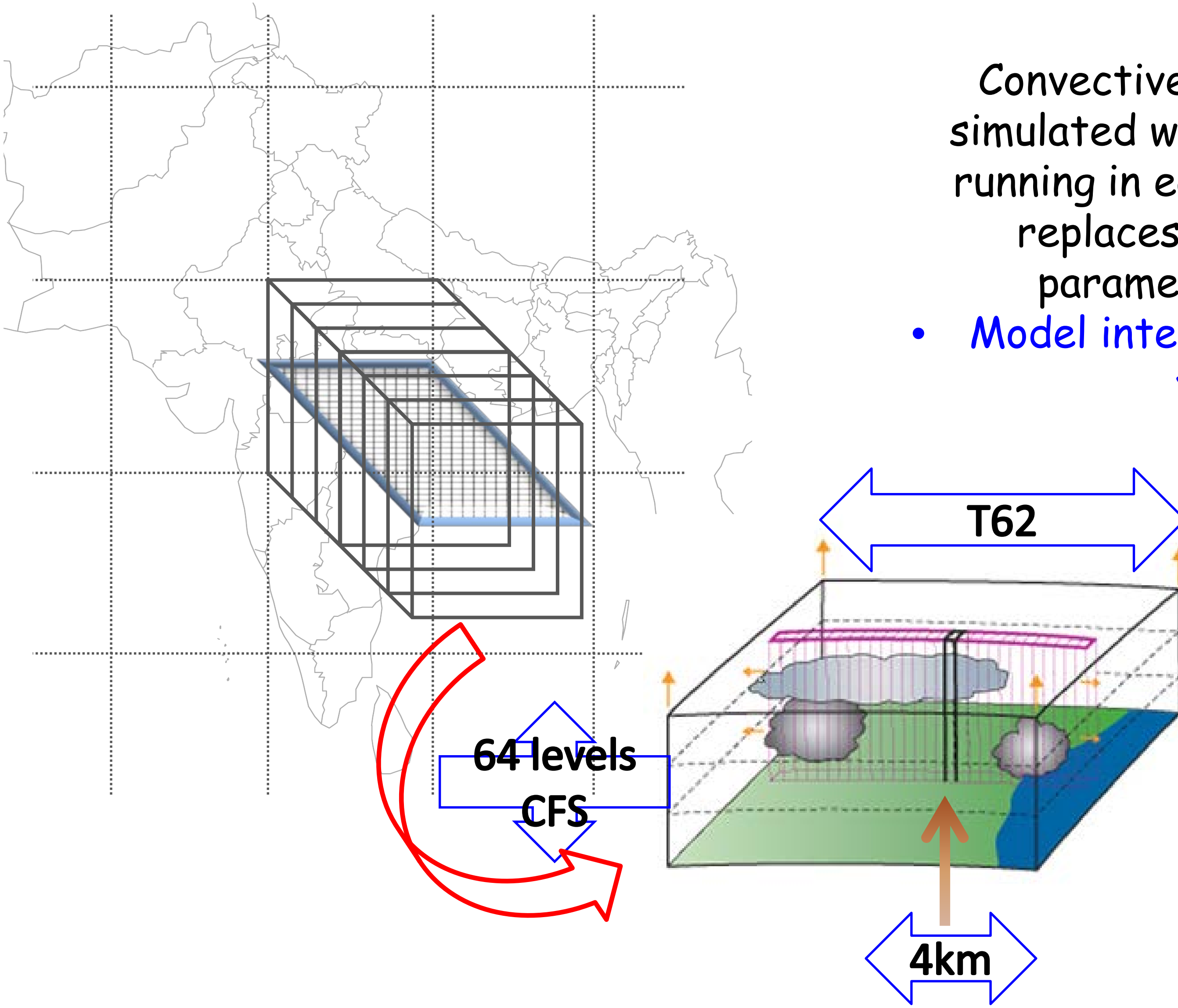

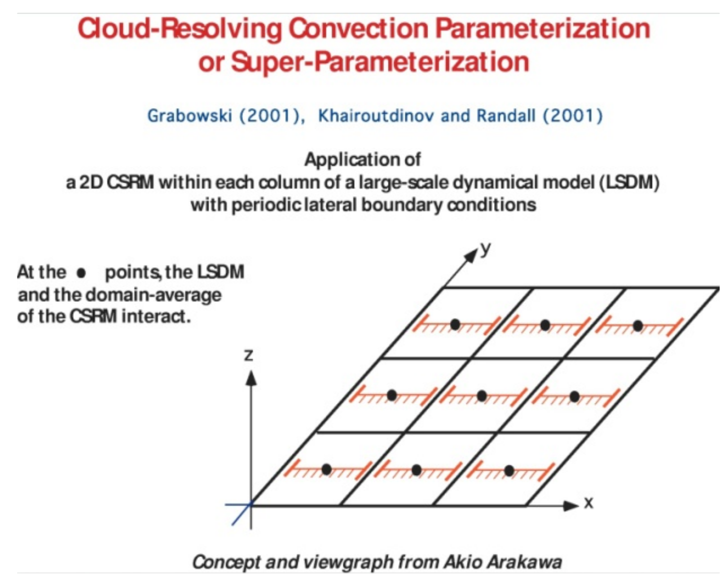

The rainfall is averaged over : 73-82E; 18-28N

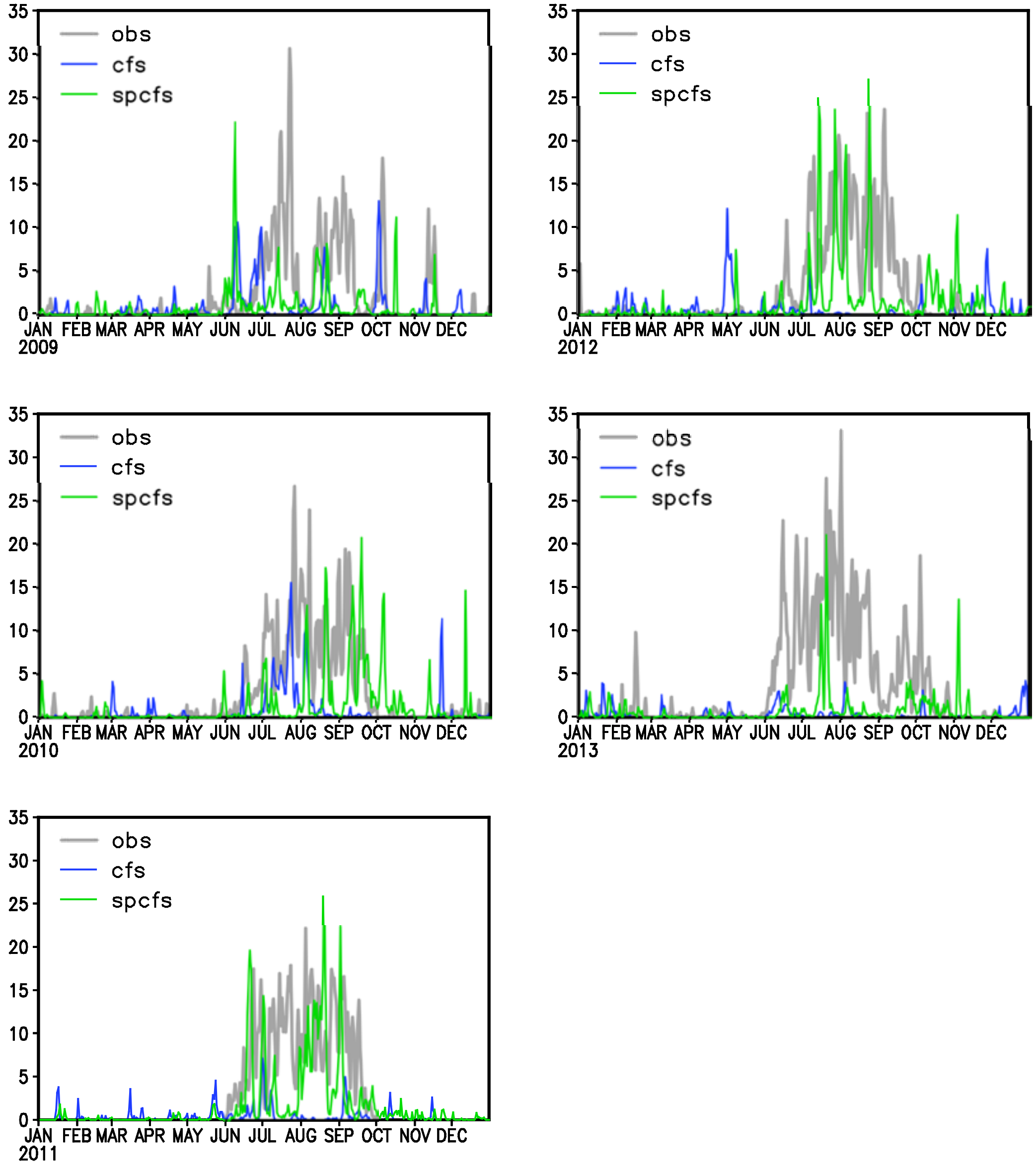

SP-CFS produces reasonable rain, CFS hardly rains

The Standard Dev for JJAS (5 years) :

IMD=5.01

SPCFS=4.33

CFS=1.8

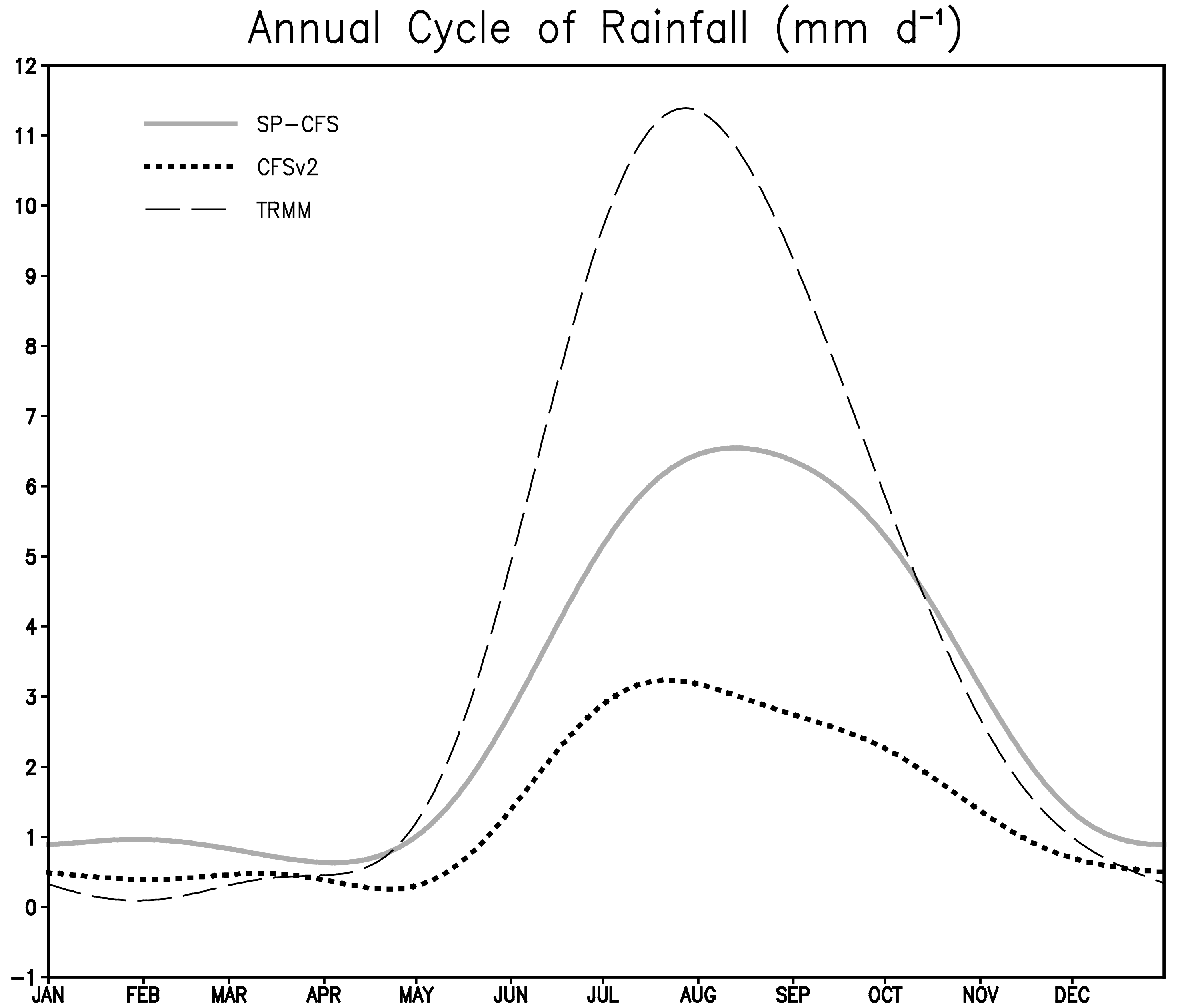

Annual cycle of the climatological mean rainfall (mm day^{-1}) averaged over the area: 15°N-25°N; 75°E-90°E.

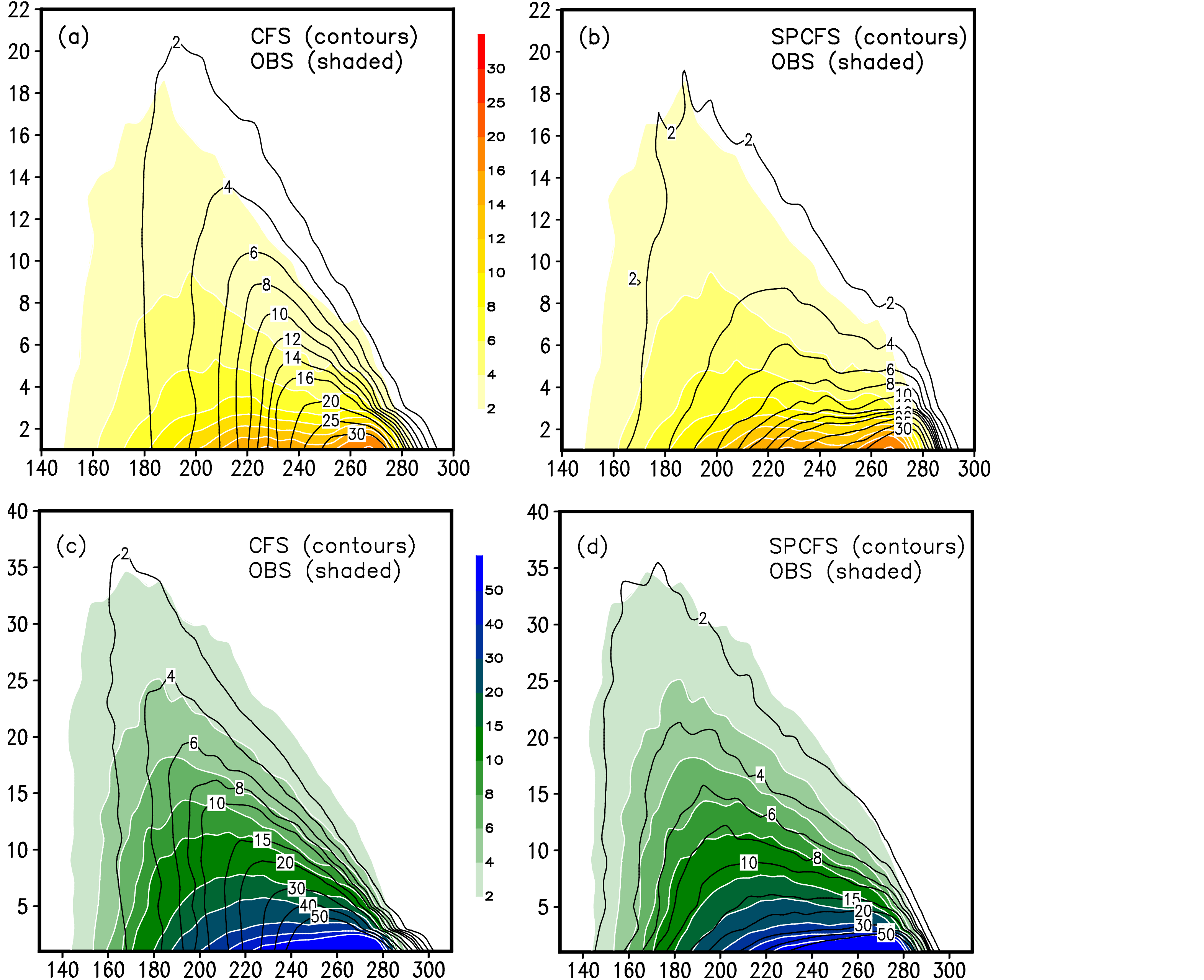

Joint distribution of rainfall (mm day^{-1}), along y-axis, and OLR (W m^{-2}), along x-axis, computed for each grid point, (a) & (b) over the monsoon domain bounded by 15°S-30°N and 50°E-110°E and (c) & (d) over the entire Tropics within 15°S-15°N, for the 5 boreal summers (JJAS). For observation we have taken TRMM rainfall and NOAA OLR. Model simulated values are contoured and overlaid on observation (in shading). The values are in multiples of 100.

North box : 40-100E; 5-35N
South box : 40-100E;15S-5N
600-200hPa (Xavier et. al. 2007)

Right result due to wrong reason in CFSv2

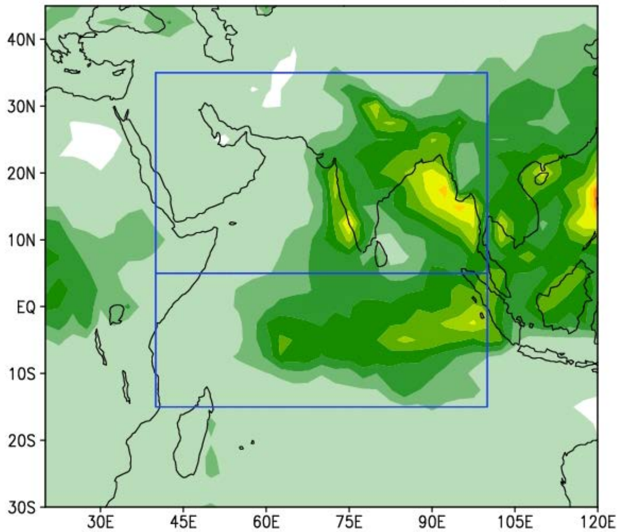

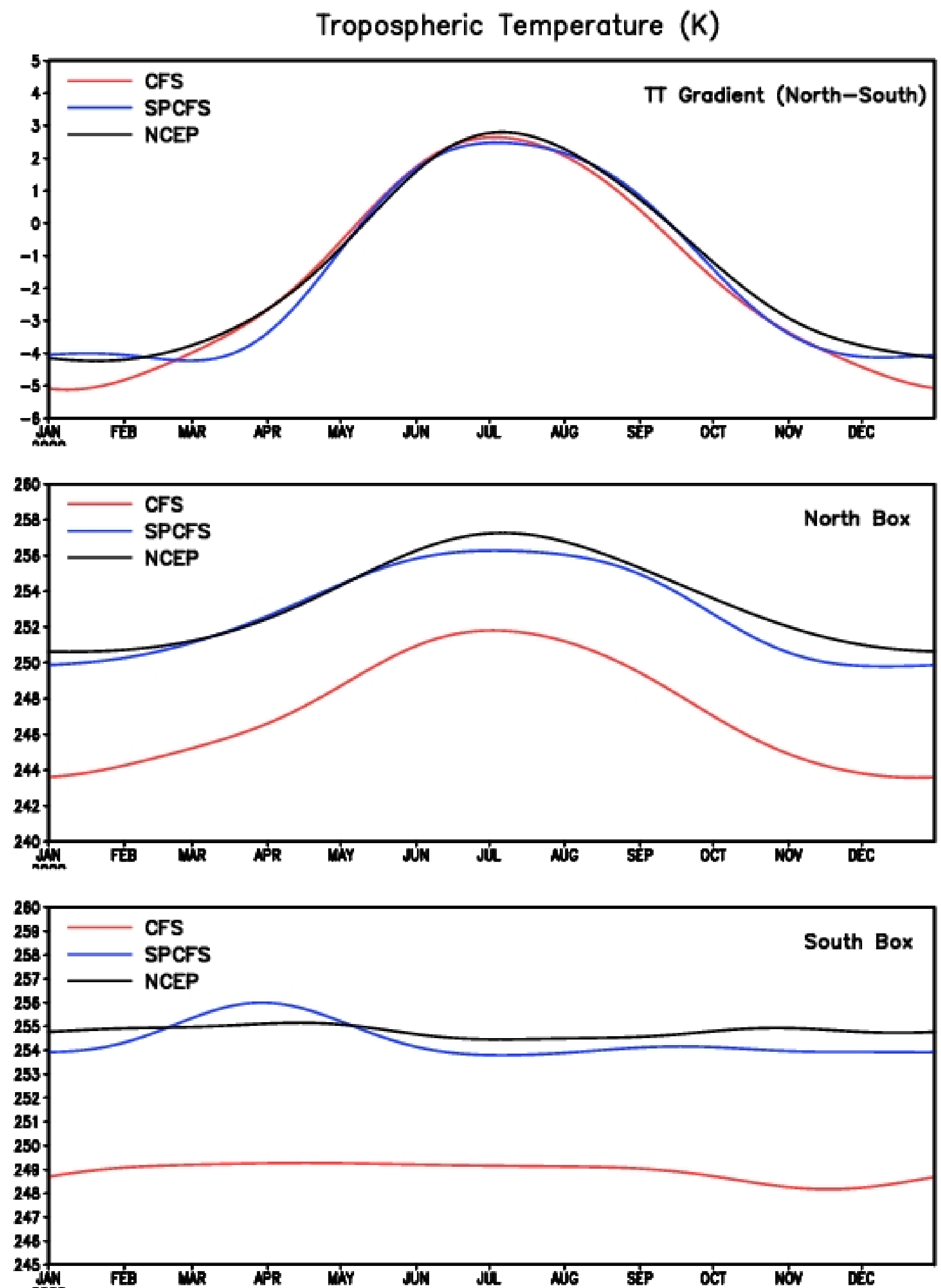

Improvement in tropospheric temperature bias is seen in TT gradient. Even though the Gradient looks reasonable in both CFS and SPCFS, but the bias is seen when we see the North and South boxes individually. The TT-gradient in a cooler background in CFS perhaps is consistent with reasonable circulation pattern (Fig-12 in manuscript) but deficient moisture (Fig-13b in manuscript) leading to dry monsoon.

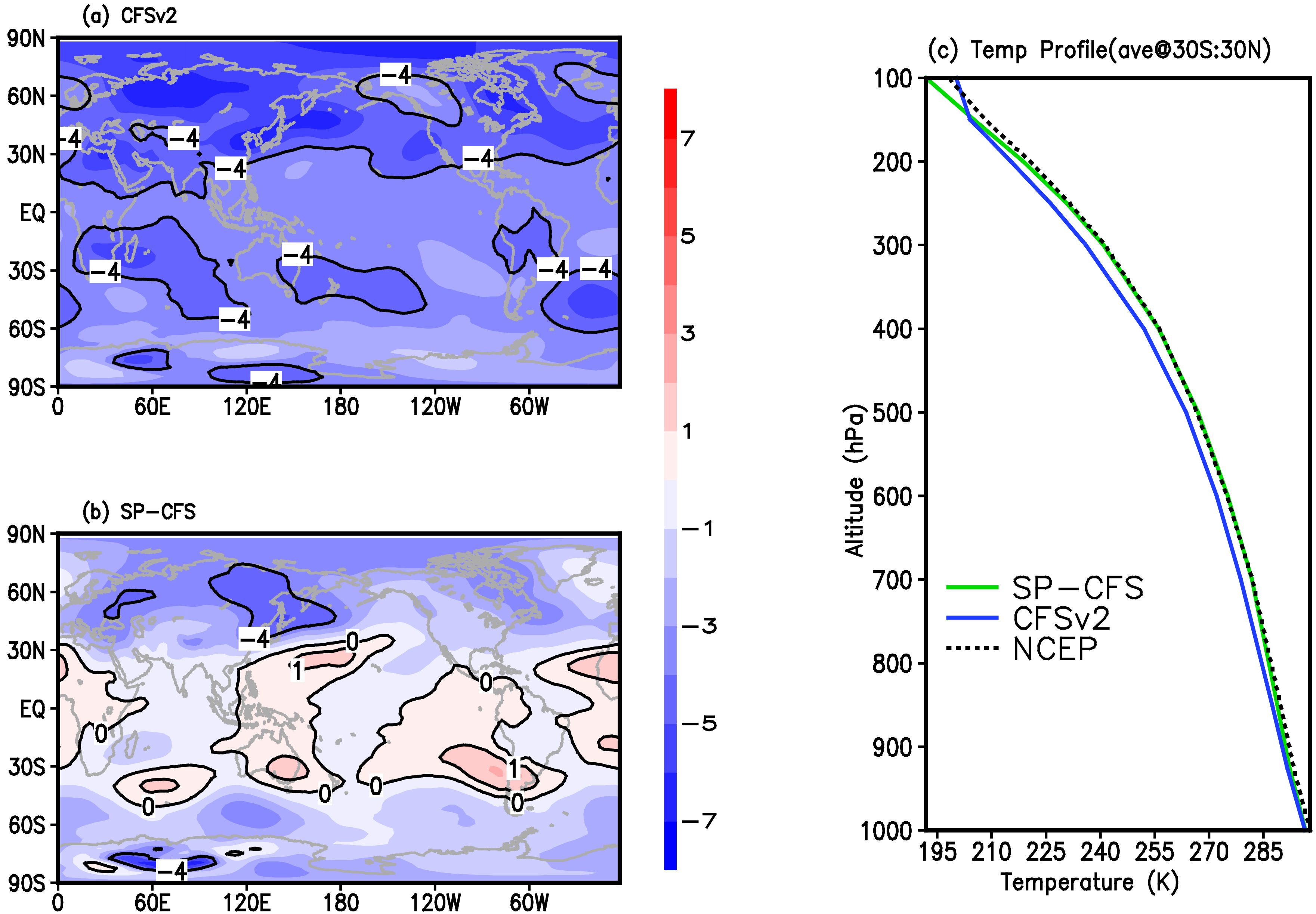

Boreal summer (JJAS) climatological Tropospheric temperature bias of (a) CFSv2 and (b) SP-CFS, relative to NCEP. (Averaged between 600hPa-300hPa). (c) Vertical profile of JJAS mean climatological temperature for tropics (30°S-30°N; 0°E-360°E).

Mean state in SP-CFS has improved due to improvement in moist instability and convective coupling as evident in the subsequent slides

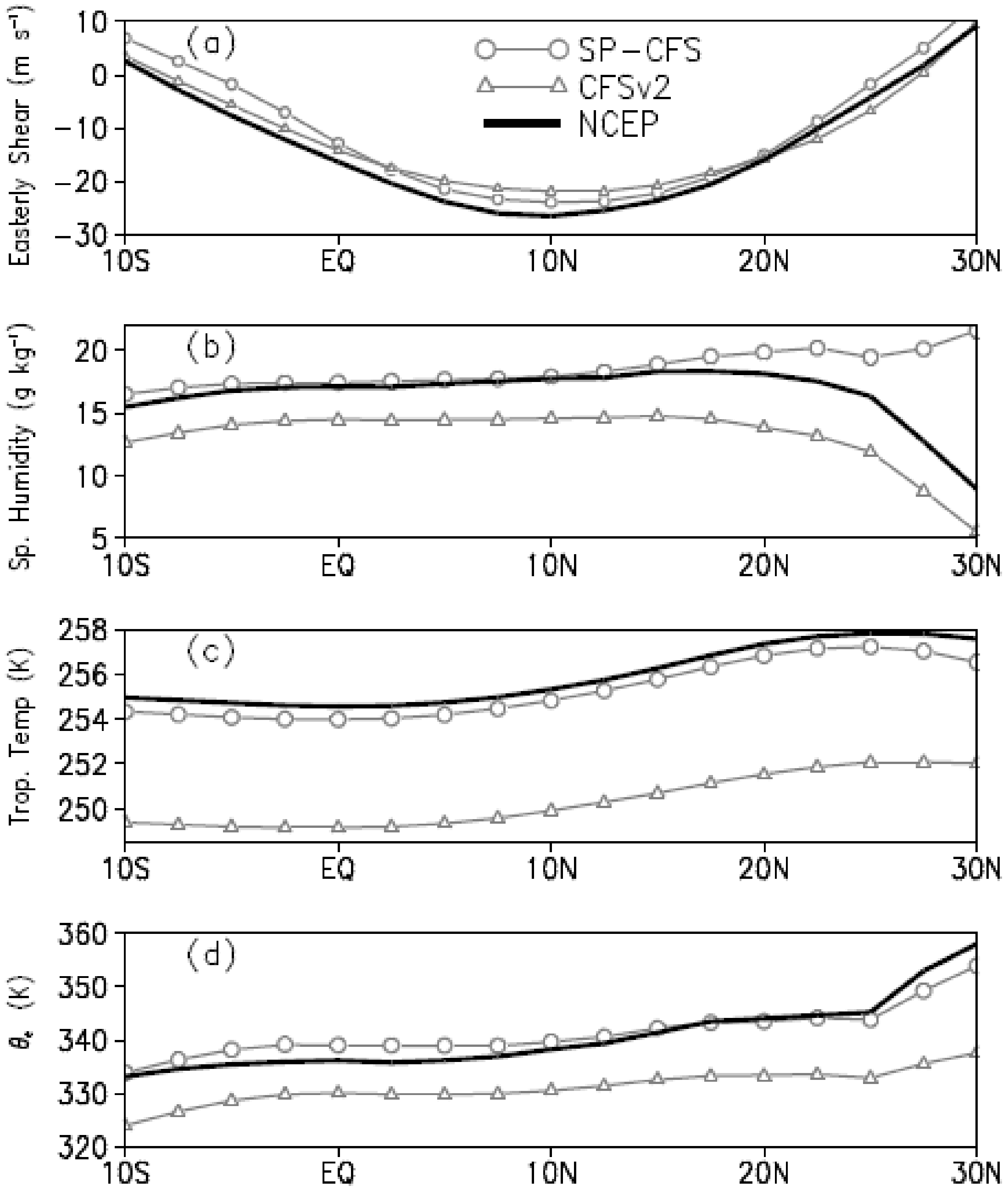

Climatological Seasonal mean meridional distribution of (a) easterly wind shear (U200–U850, m s-1), (b) surface level specific humidity (g kg-1), (c) tropospheric temperature (averaged between 200 and 600 hPa) and (d) equivalent potential temperature (averaged between 1000 to 850 hPa and 65° to 95°E.

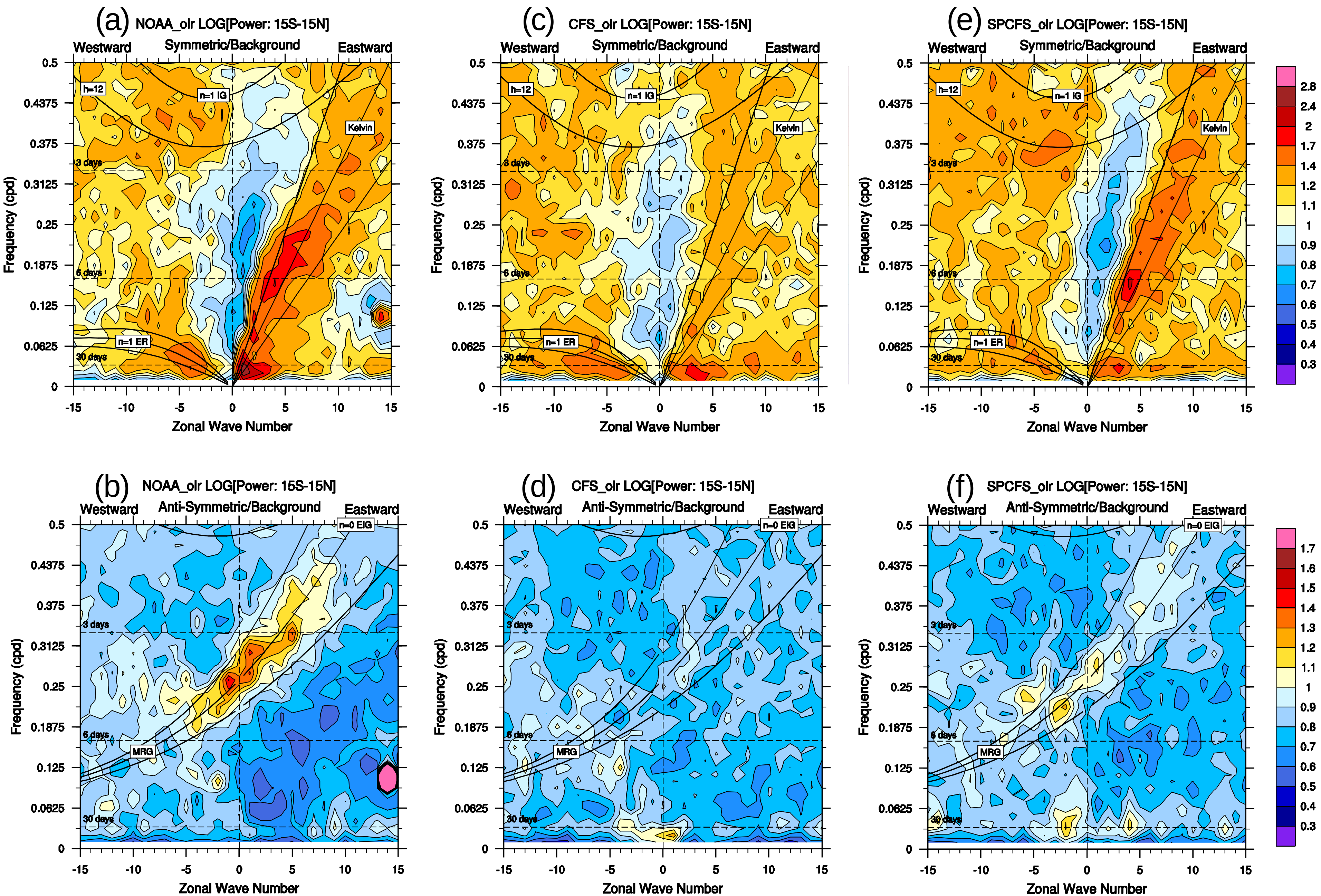

Space-Time spectra (Wheeler-Kiladis diagram [Wheeler and Kiladis, 1999]) of OLR showing the symmetric component for (a) NOAA OLR, (c) CFSv2 and (e) SP-CFS and the anti-symmetric component for (b) NOAA OLR, (d) CFSv2 and (f) SP-CFS.

Ratio of Synoptic to ISO variance.

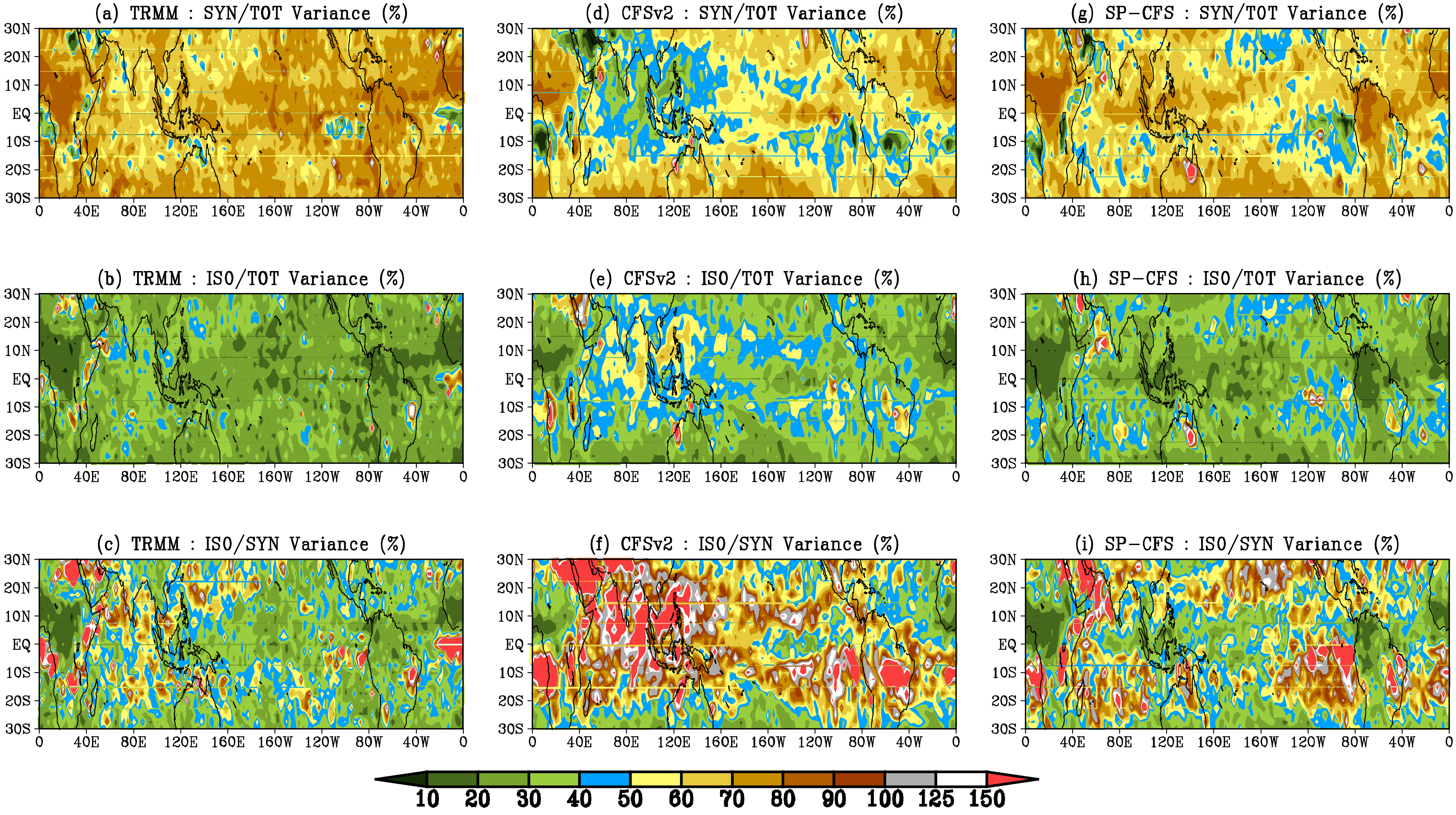

SP-CFS has improved the bias in synoptic and ISO variance

Arakawa and Wu, 2013

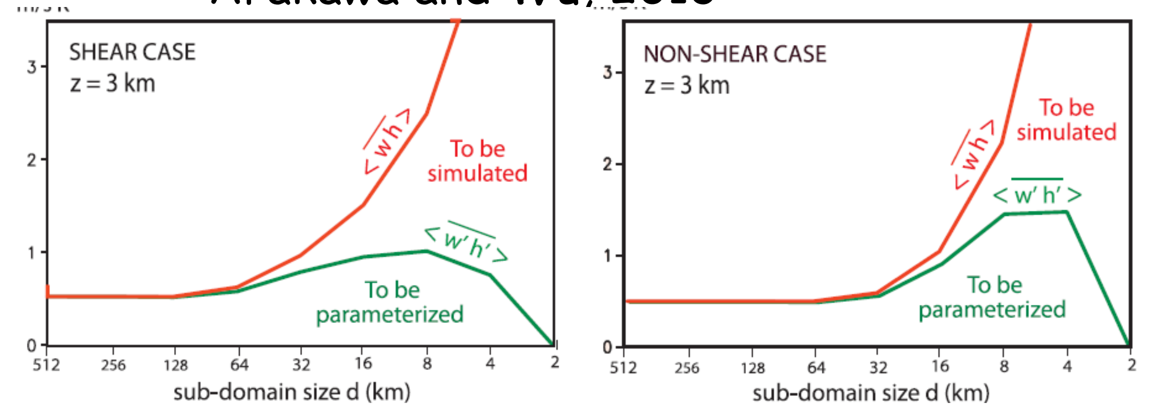

$\sigma \sim 1$

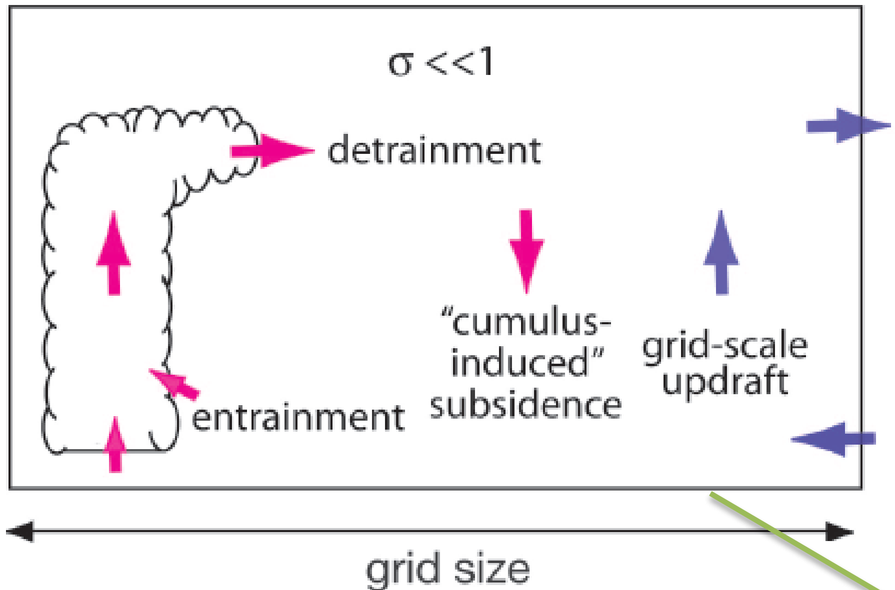

Arakawa et al. 2011, ACP

σ is the fractional area covered by all convective clouds in the grid cell

AS "Consider a horizontal area – large enough to contain an ensemble of cumulus clouds but small enough to cover a fraction of a large-scale disturbance. The existence of such an area is one of the basic assumptions of this paper." In reality, the GCM grid cells are not large enough and, at the same time, not small enough.

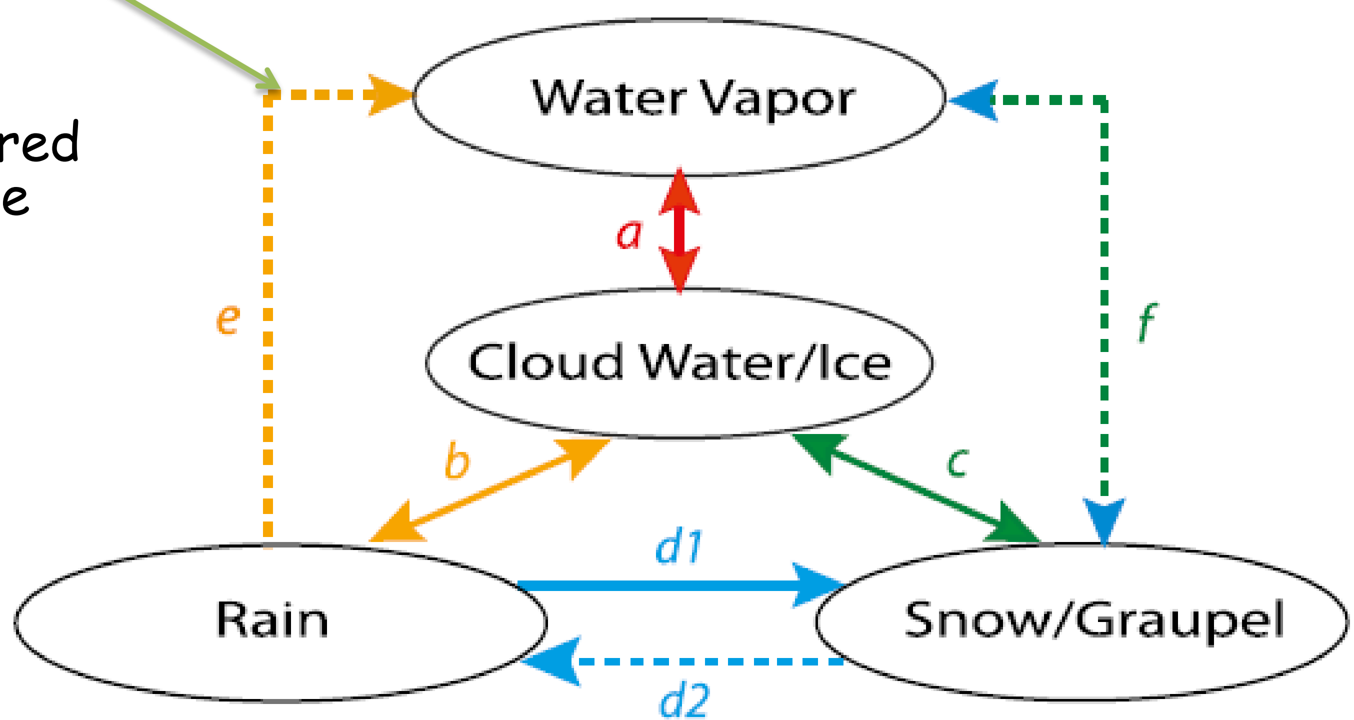

FIG. 9. A simplified view of the cloud microphysical conversions included in the CRM simulation used in this paper. See text for

Arakawa and Wu, 2014

Pros

- Superparameterized CFS (SP-CFS) demonstrates the merits of resolving cloud processes in a GCM

- Can be a good test bed

- Short run to for extreme events feasible (Li et al. 2014)

Cons

- Operationally not feasible (ensemble will be a challenge)

Impact of Revising Subgrid scale convection only RevSAS

JJAS Mean precip

JJAS precip bias

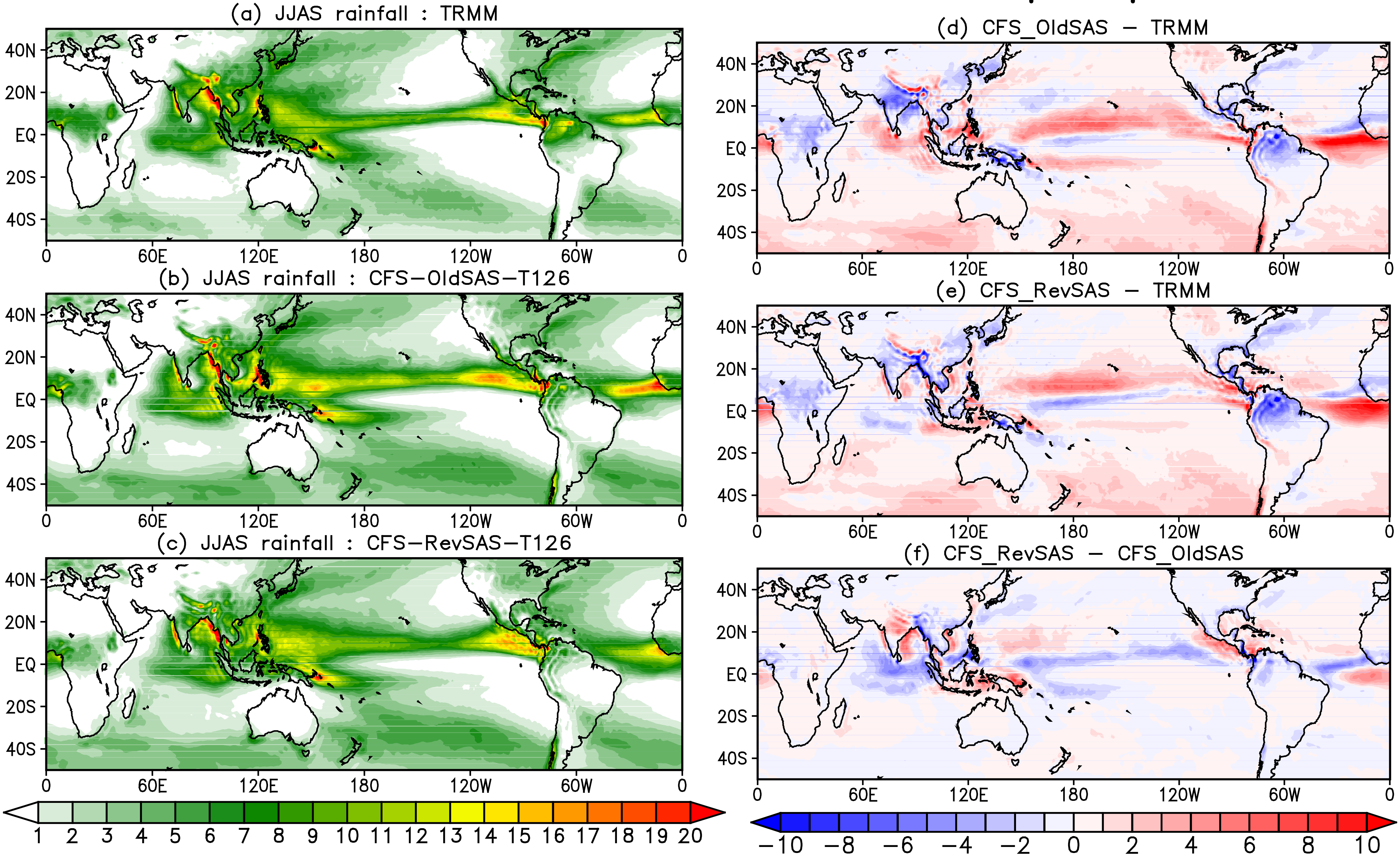

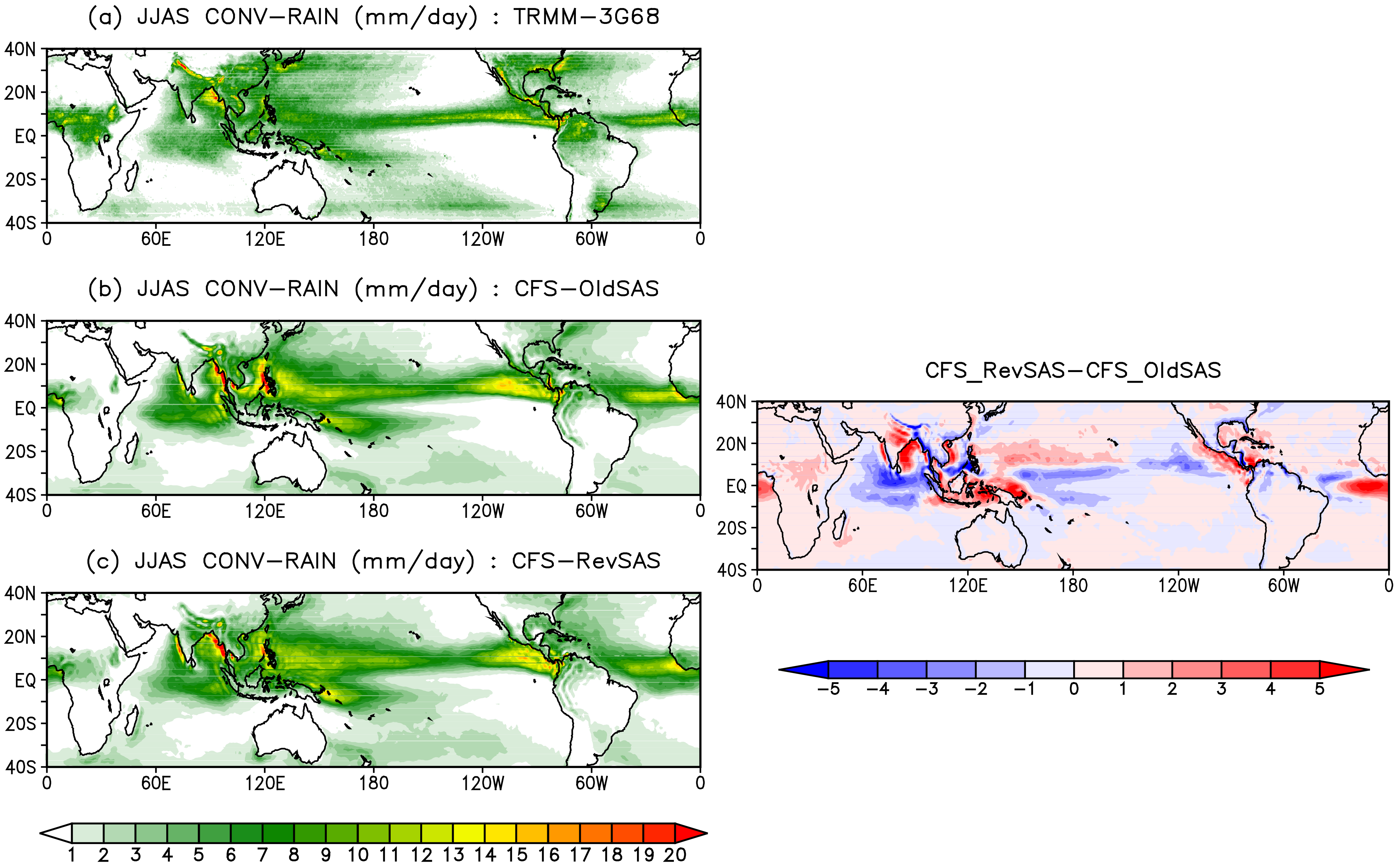

Convective Rain

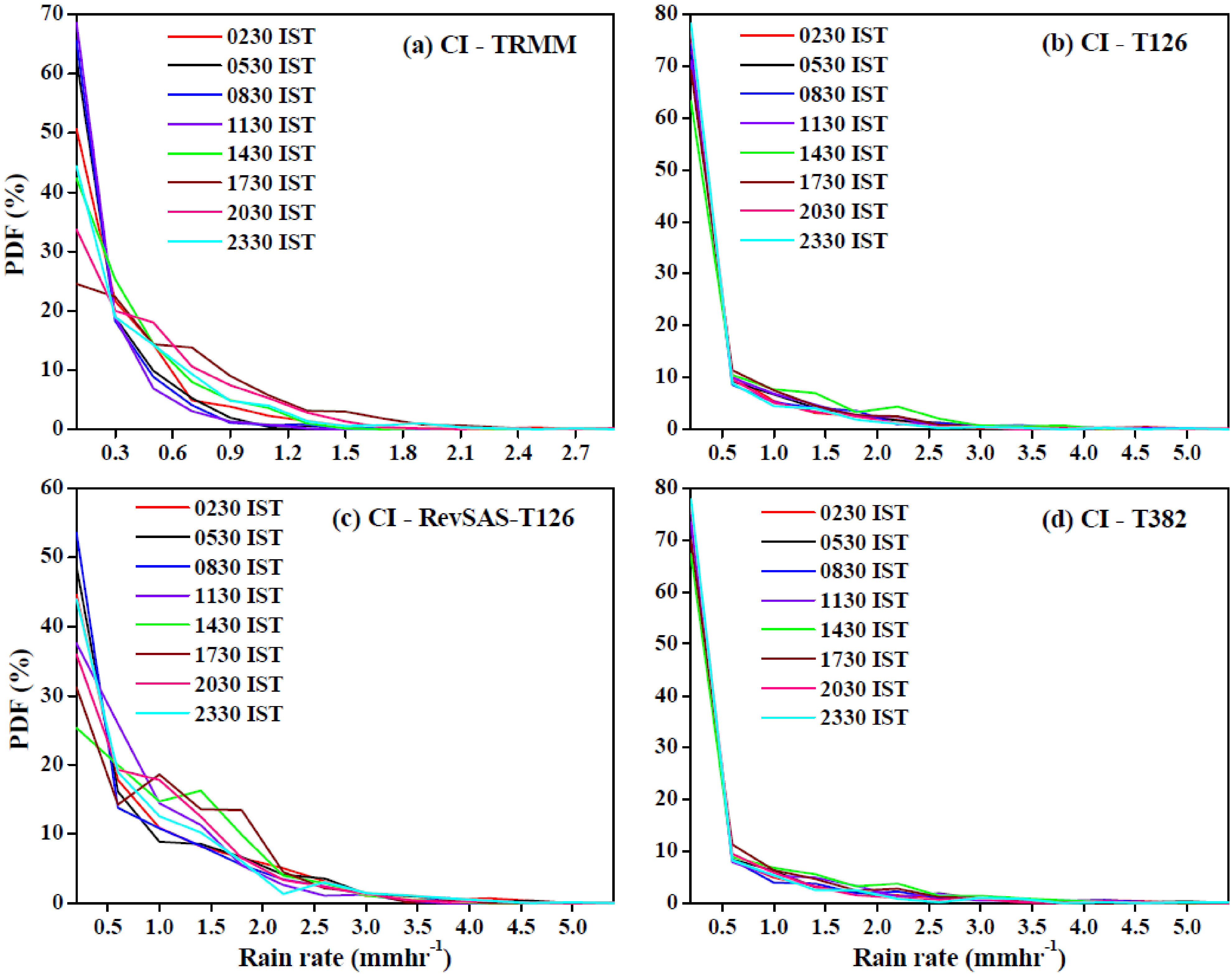

(a) CI - TRMM
(b) CI - T126
(c) CI - RevSAS-T126
(d) CI - T382
0230 IST
0530 IST
0830 IST
1130 IST
1430 IST
1730 IST
2030 IST
2330 IST
PDF (%)
Rain rate (mmhr^{-1})

Convective-rain OldSAS

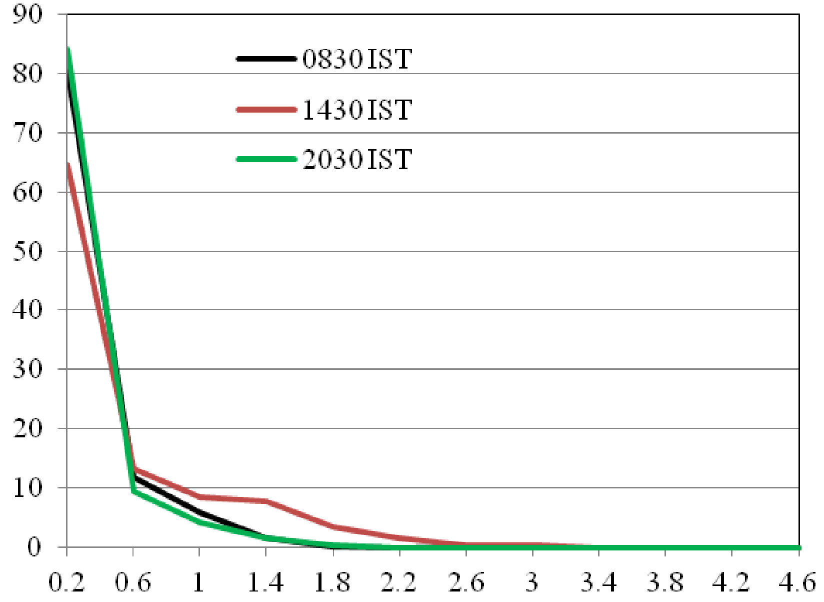

Convective-rain-RevSAS

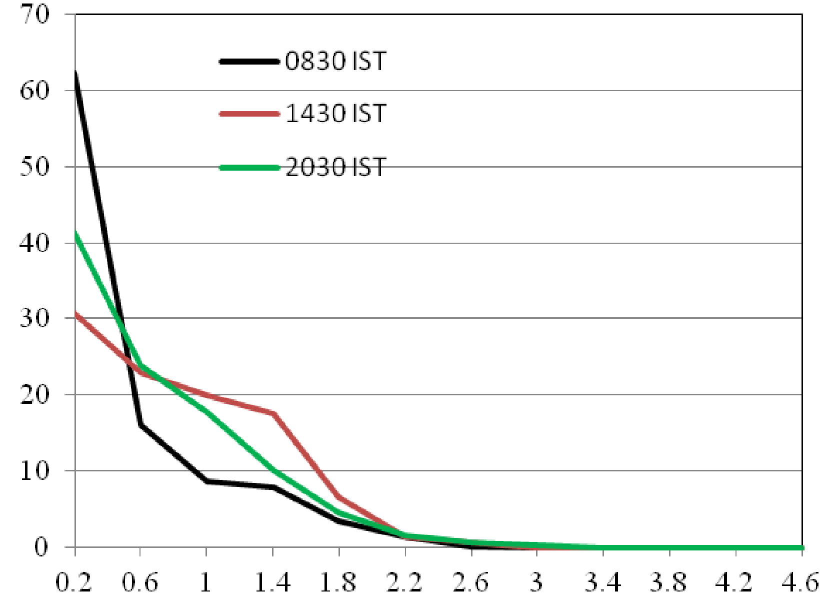

Stratiform-rain-OldSAS

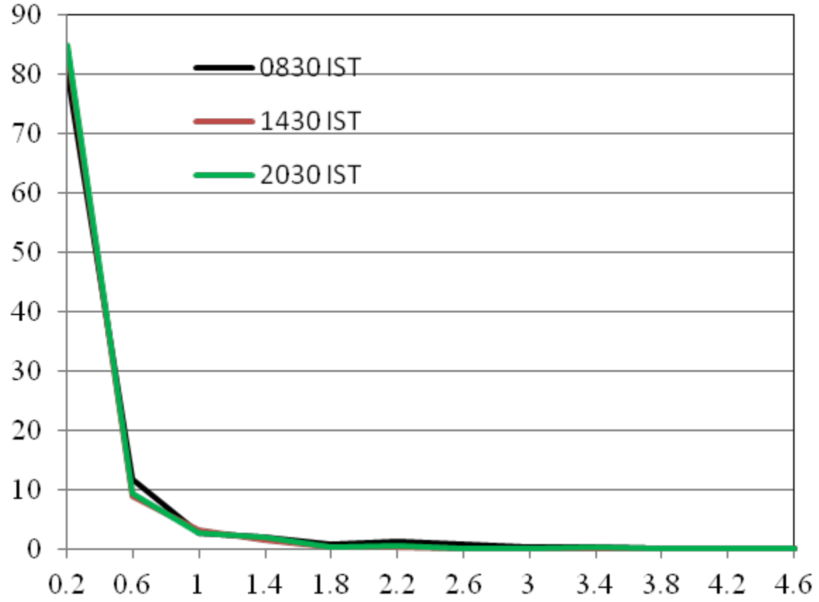

Stratiform-rain RevSAS

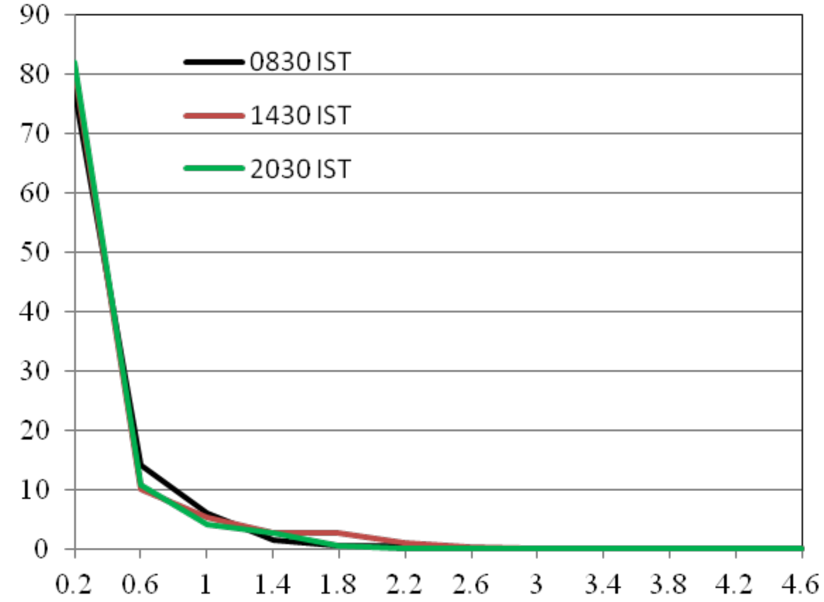

Log of RF (X-axis) along with vertical distribution of RH (Shaded)

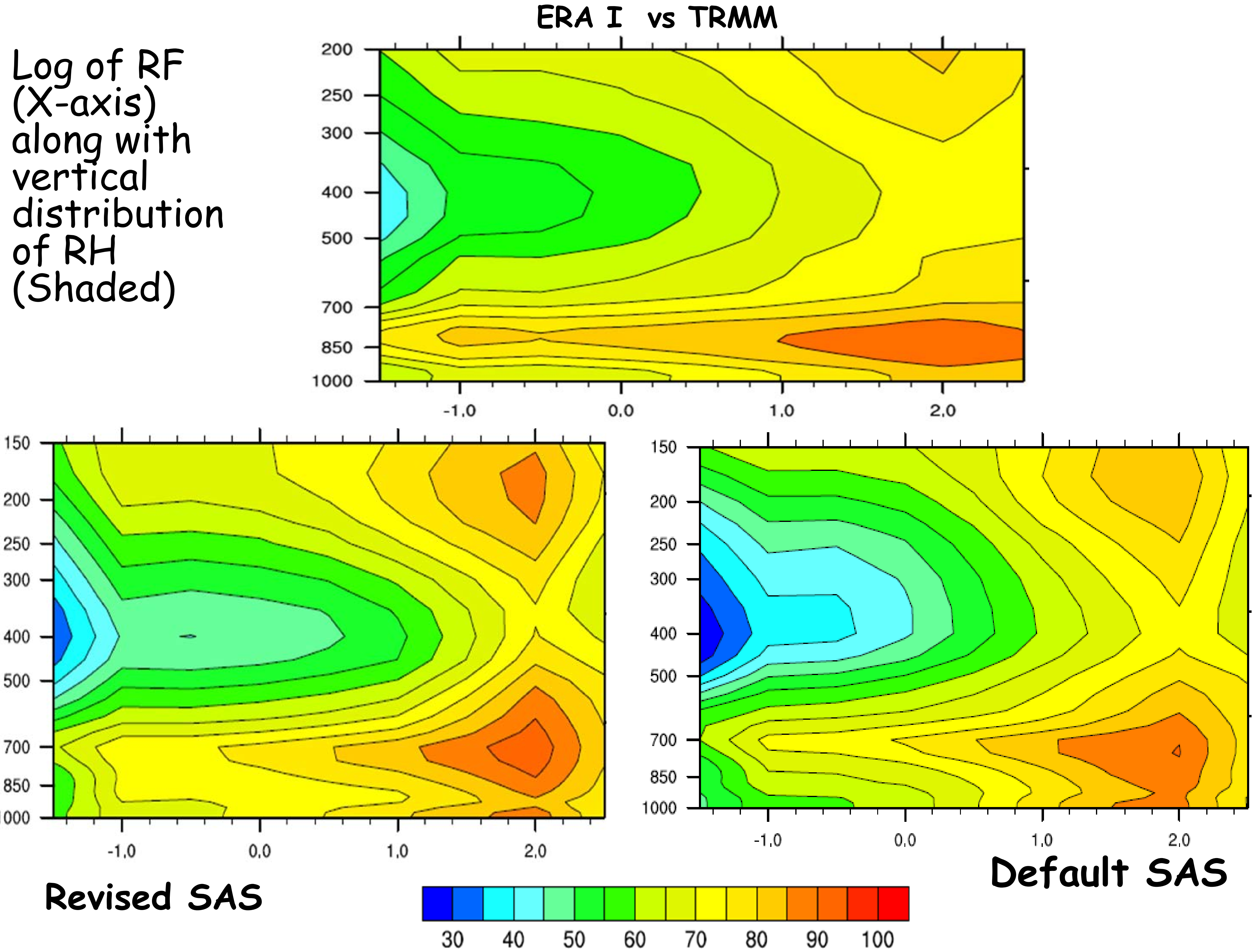

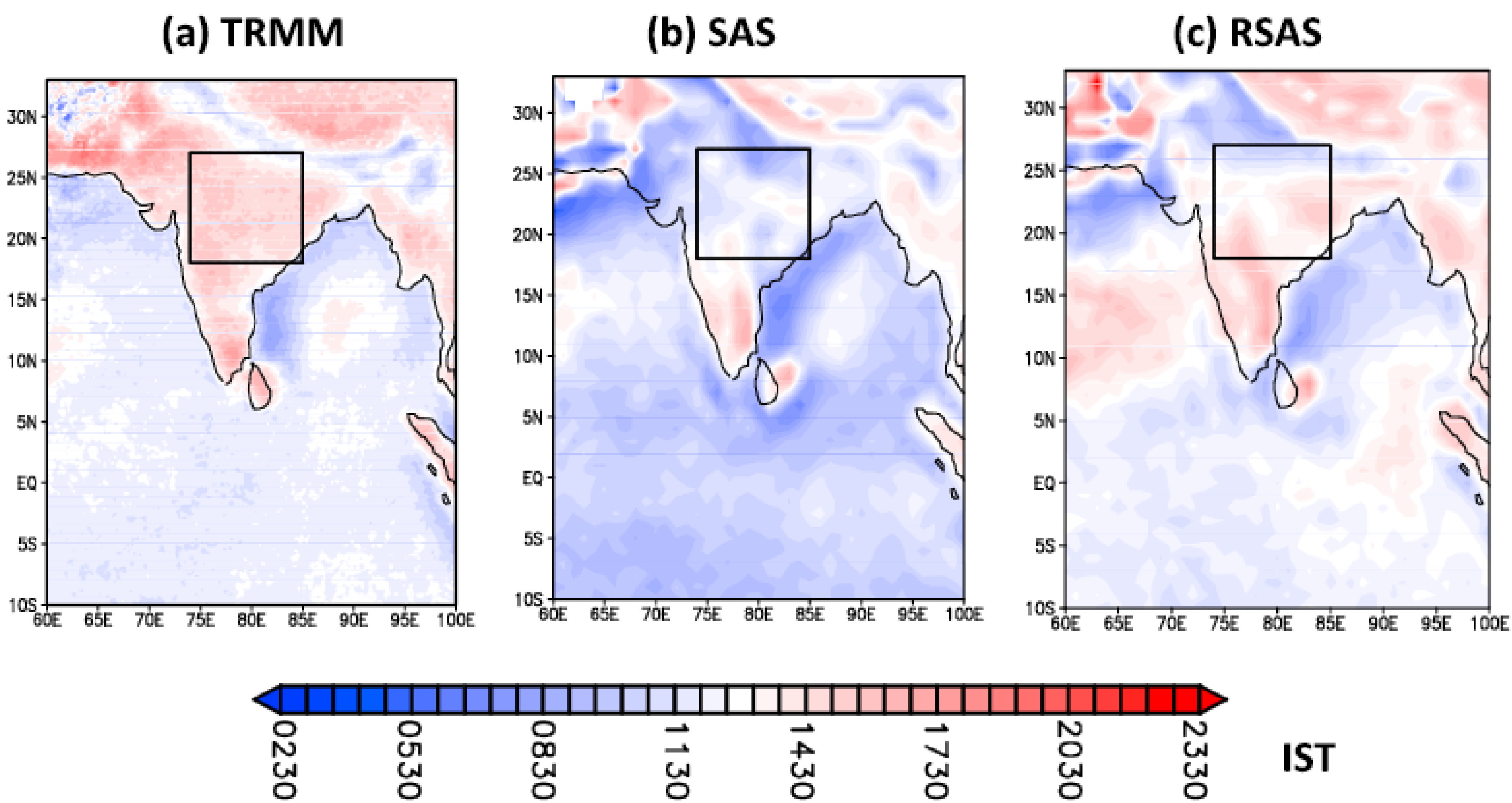

Seasonal (JJAS) mean distribution of diurnal phase (IST (h)) when maximum precipitation occurs for (a) TRMM, CFSv2 with (b) SAS and (c) RSAS scheme. Black box represents central India (CI) (18°N–27°N, 74°E–85°E) region.

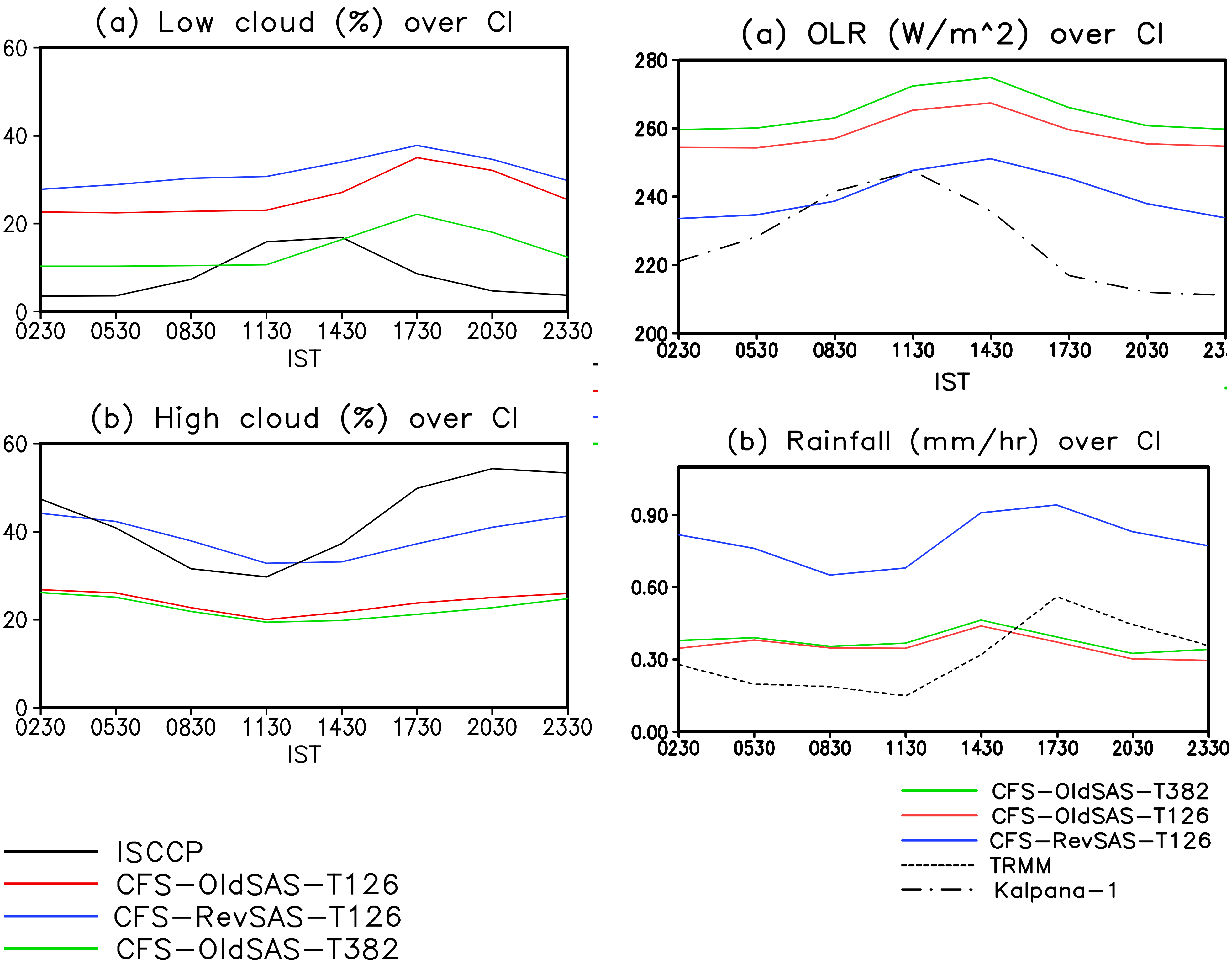
(a) Low cloud (%) over CI
60
40
20
0
0230 0530 0830 1130 1430 1730 2030 2330
IST
(b) High cloud (%) over CI
60
40
20
0
0230 0530 0830 1130 1430 1730 2030 2330
IST
ISCCP
CFS−OldSAS−T126
CFS−RevSAS−T126
CFS−OldSAS−T382
(a) OLR (W/m^2) over CI
280
260
240
220
200
0230 0530 0830 1130 1430 1730 2030
IST
(b) Rainfall (mm/hr) over CI
0.90
0.60
0.30
0.00
0230 0530 0830 1130 1430 1730 2030 2330
CFS−OldSAS−T382
CFS−OldSAS−T126
CFS−RevSAS−T126
TRMM
Kalpana−1

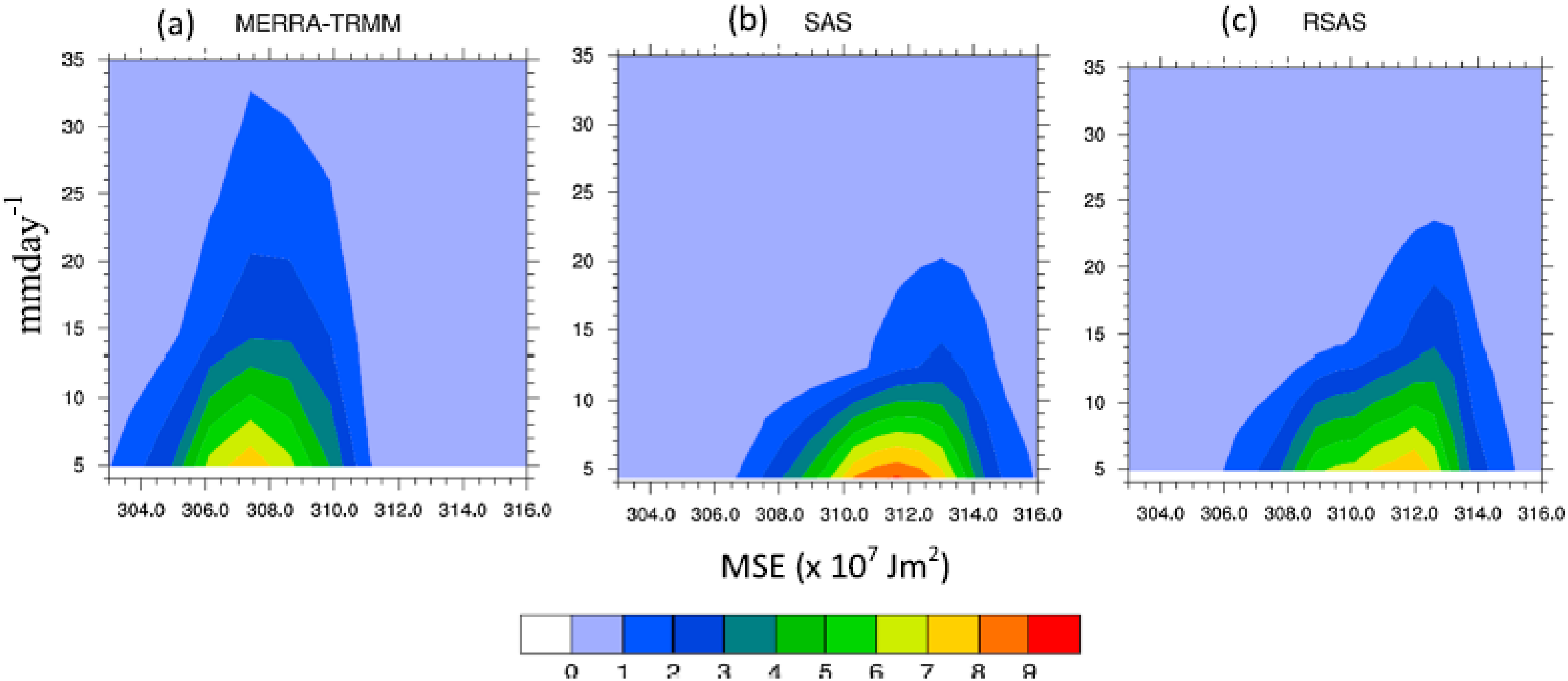

Joint probability distribution function of rainfall (mm d-1), along the y axis, and column integrated (surface to 100 hPa) MSE (× 10 7Jm-2), along the x axis, over CI region for (a) observation (TRMM and MERRA), CFSv2 with (b) SAS and (c) RSAS scheme during JJAS.

WHAT NEXT

CFST382 (RED line), CFST126 (BLACK line), TRMM & MERRA (Dotted BLUE line)
OLR (INSAT) from Mahakur et al.

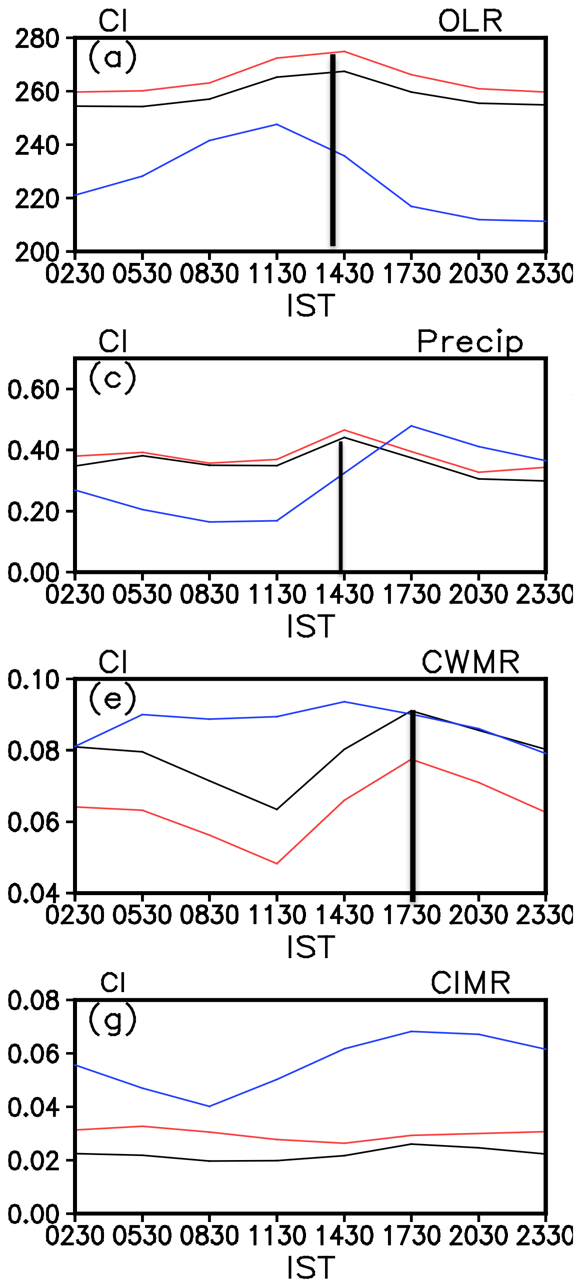

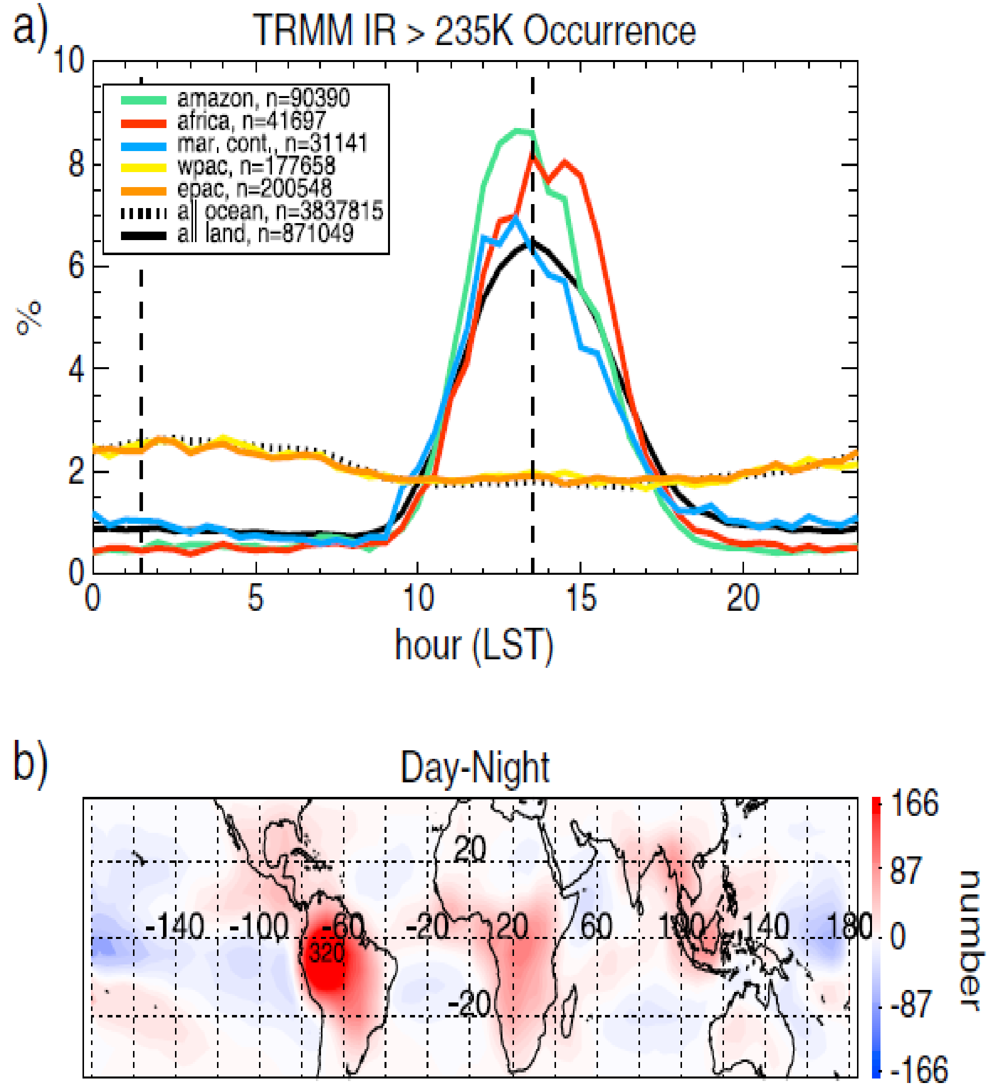

Diurnal variation of population of TRMM VIRS congestus for different regions. The black dashed lines indicate the times of CloudSat overpass.

Wall et al., 2013

Ganai et al.

Diurnal variation of population of TRMM VIRS congestus for different regions over Indian monsoon region

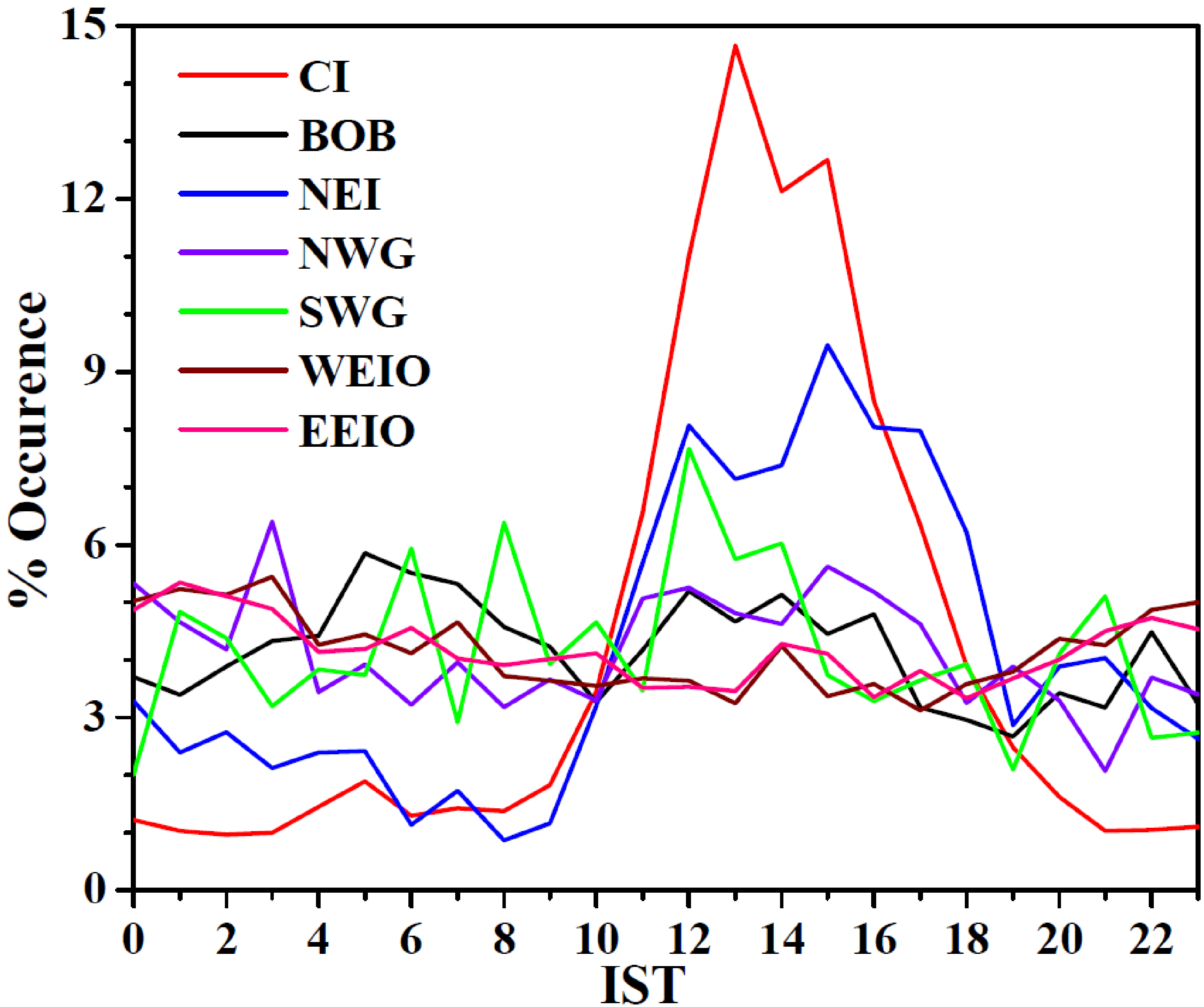

Mahakur et al.

ISCCP estimated low cloud (%) (black line) and high cloud (%) (Red line)

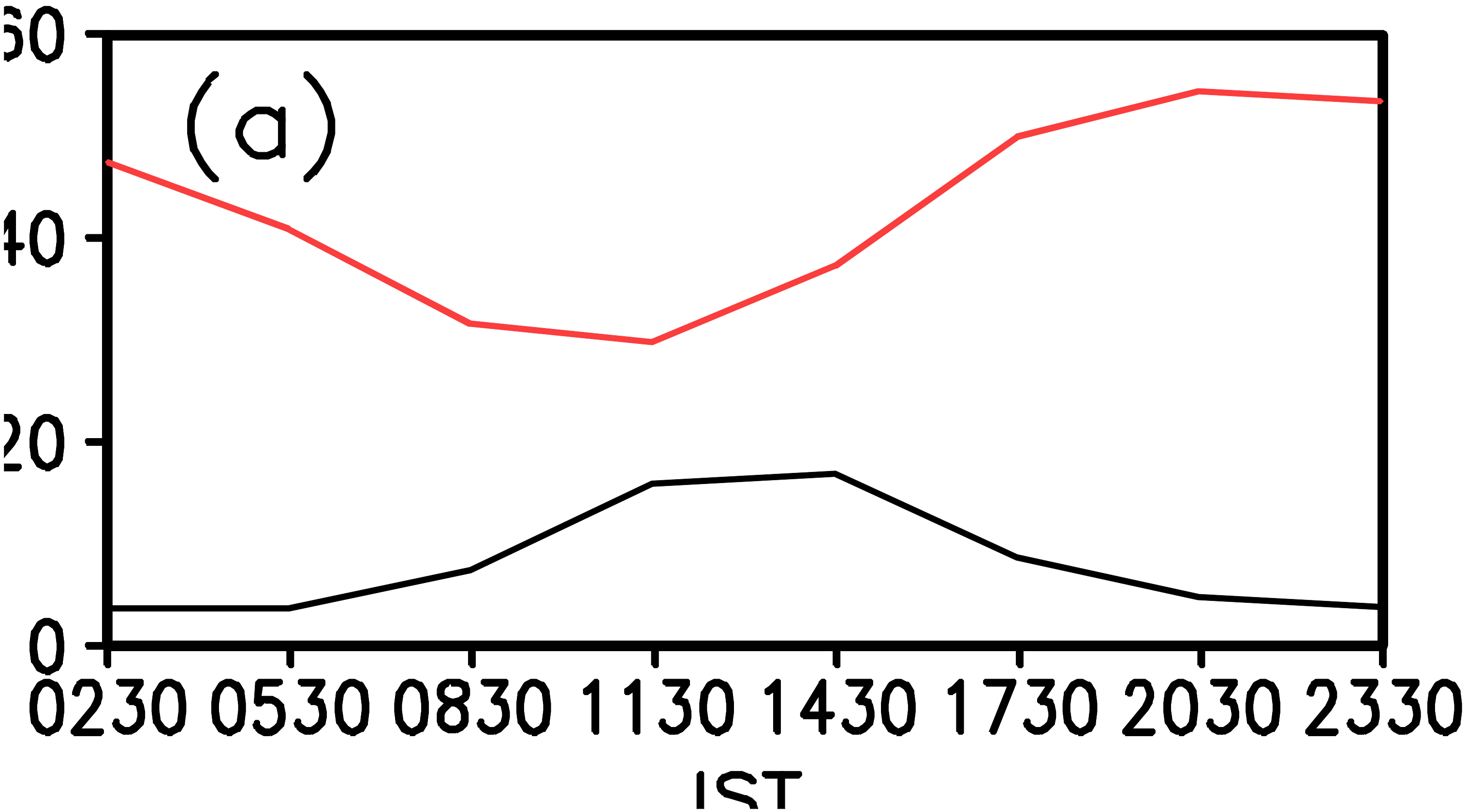

a) CI

Hypothesis based on observation for northward propagation BSISO (Abhik et al, 2013)

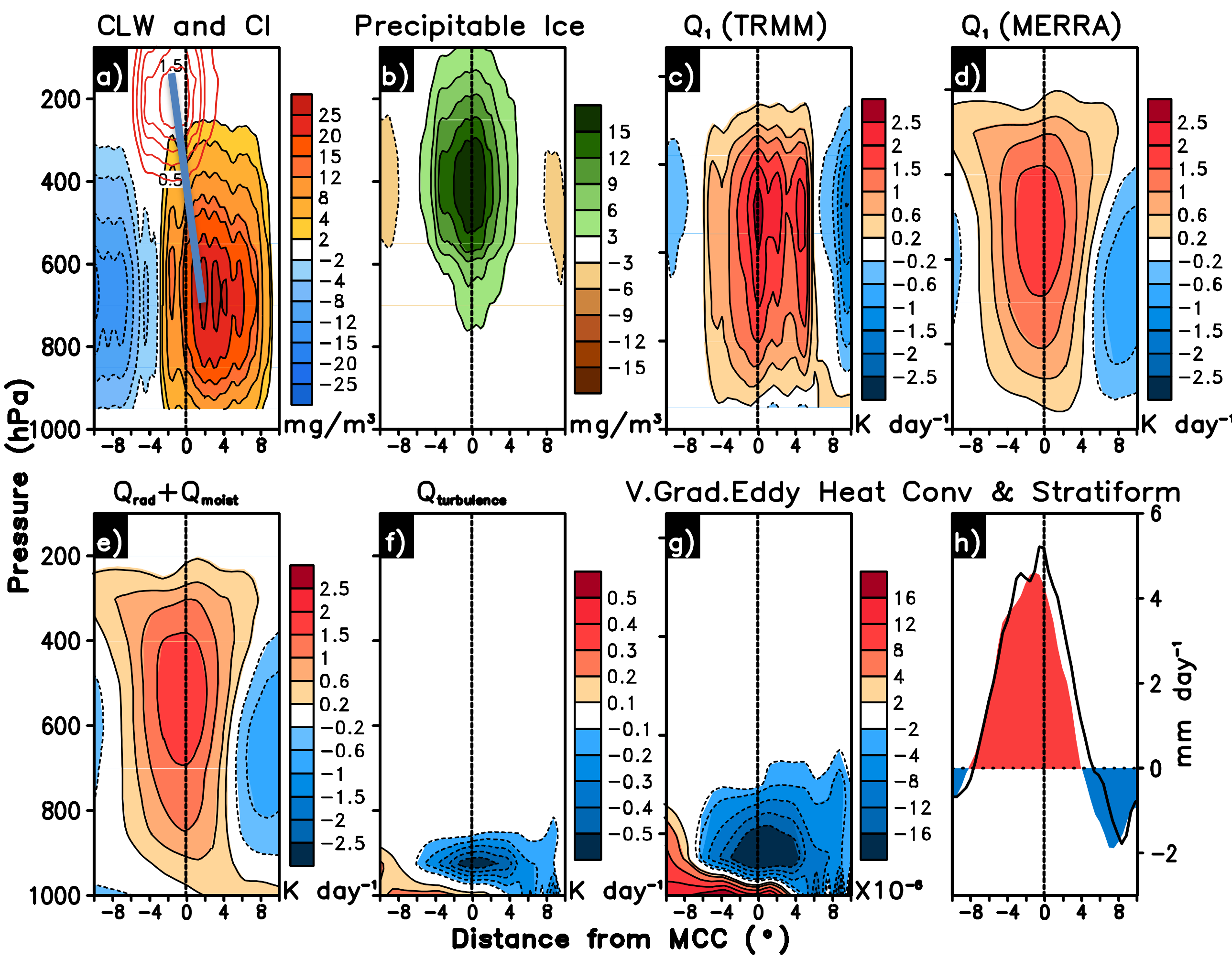

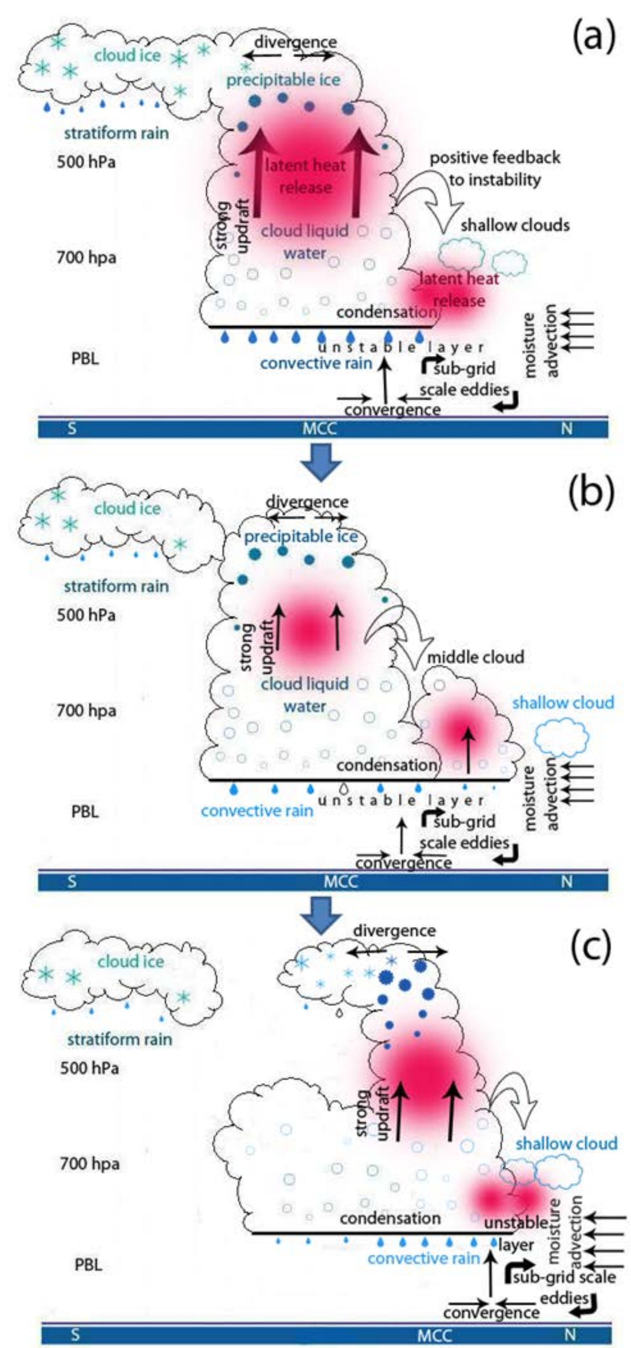

Our results are supplemented by few recent studies e. g.

Preconditioning Deep Convection with Cumulus Congestus by Hohenegger and Steven, 2013

A climatology of tropical congestus using CloudSat by Wall et al. 2013

To simulate better stratiform clouds a spectrum of cumulus clouds is necessary.

Model tuning via coupled convective and stratiform clouds

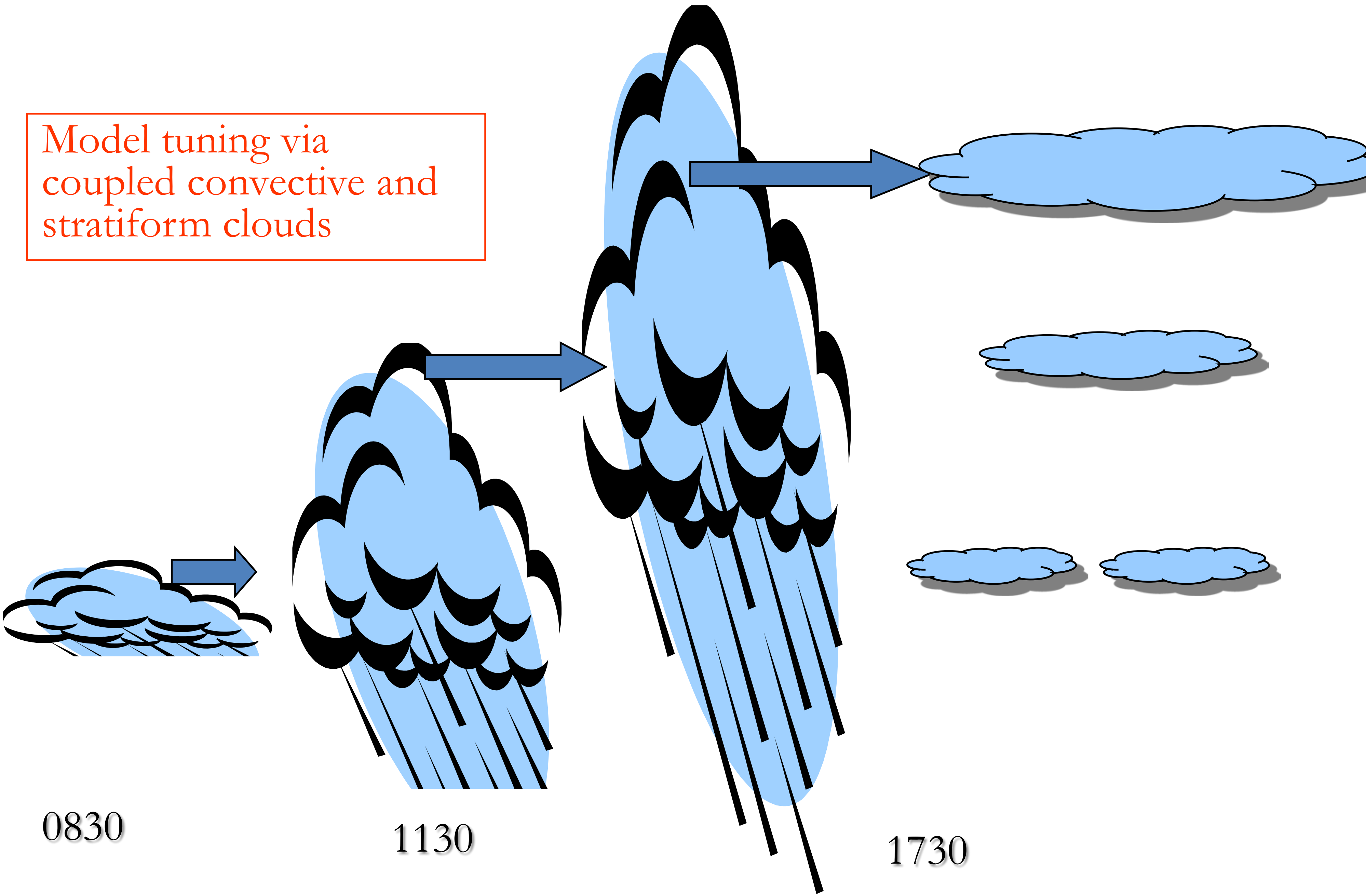

Separation into stratiform and convective clouds, detraining water from convective clouds is source for stratiform clouds => radiative effects

If convective clouds change so do stratiform.

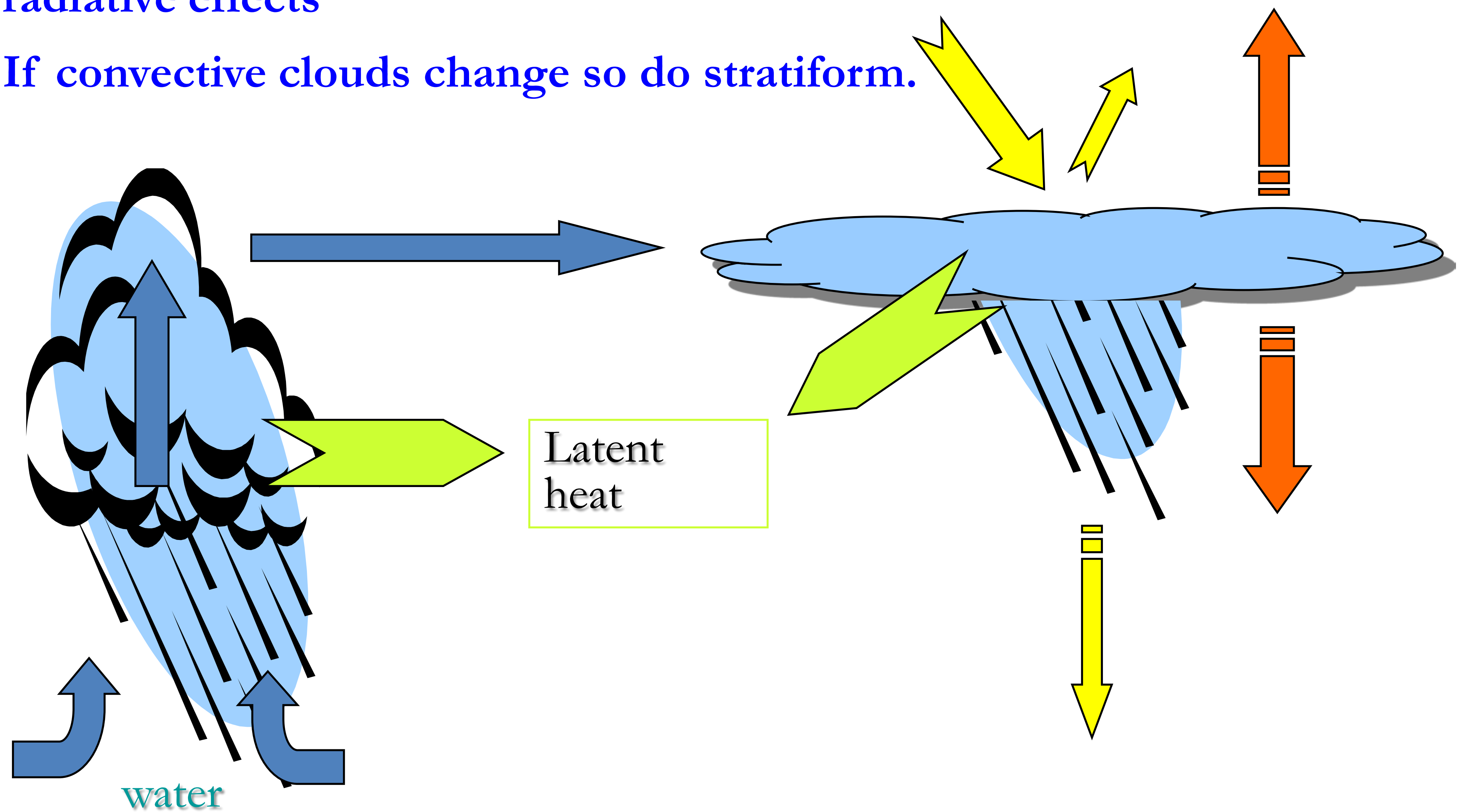

Two-moment bulk stratiform cloud microphysics in the GFDL AM3 GCM: description, evaluation, and sensitivity tests

M. Salzmann[1,*], Y. Ming[2], J.-C. Golaz[2], P. A. Ginoux[2], H. Morrison[3], A. Gettelman[3], M. Krämer[4], and L. J. Donner[2]

NCEP Initiative

Sun and Han, AGU 2014 "Zhao and Carr microphysics scheme has been implemented into the NCEP Global Forecasting System (GFS) for many years. It predicts total cloud condensate (cloud water or ice). We are testing several sophisticated microphysics schemes from the Weather Research and Forecasting Model (WRF) in the GFS. These schemes have more cloud species and more physically-based parameterized processes."

3074 JOURNAL OF THE ATMOSPHERIC SCIENCES VOLUME 59

Interactions between Cloud Microphysics and Cumulus Convection in a General Circulation Model

LAURA D. FOWLER AND DAVID A. RANDALL

Department of Atmospheric Science, Colorado State University, Fort Collins, Colorado

(Manuscript received 1 May 2001, in final form 17 May 2002)

Clim Dyn
DOI 10.1007/s00382-014-2376-1

GCMs with implicit and explicit representation of cloud microphysics for simulation of extreme precipitation frequency

In-Sik Kang · Young-Min Yang · Wei-Kuo Tao

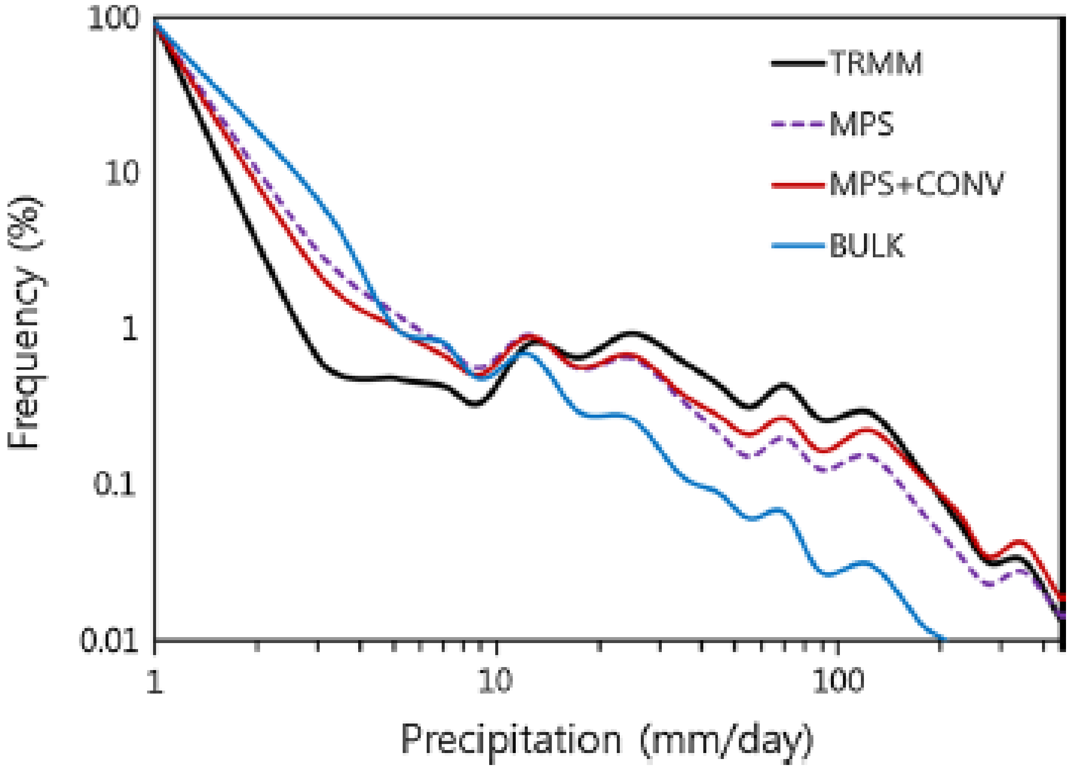

TECHNICAL MEMORANDUM

649

A new prognostic bulk microphysics scheme for the IFS

Richard M. Forbes[1], Adrian M. Tompkins[2] and Agathe Untch[1]

Research Department

[1]ECMWF [2]ICTP, Italy

September 2011

European Centre for Medium-Range Weather Forecasts
Europäisches Zentrum für mittelfristige Wettervorhersage
Centre européen pour les prévisions météorologiques à moyen terme

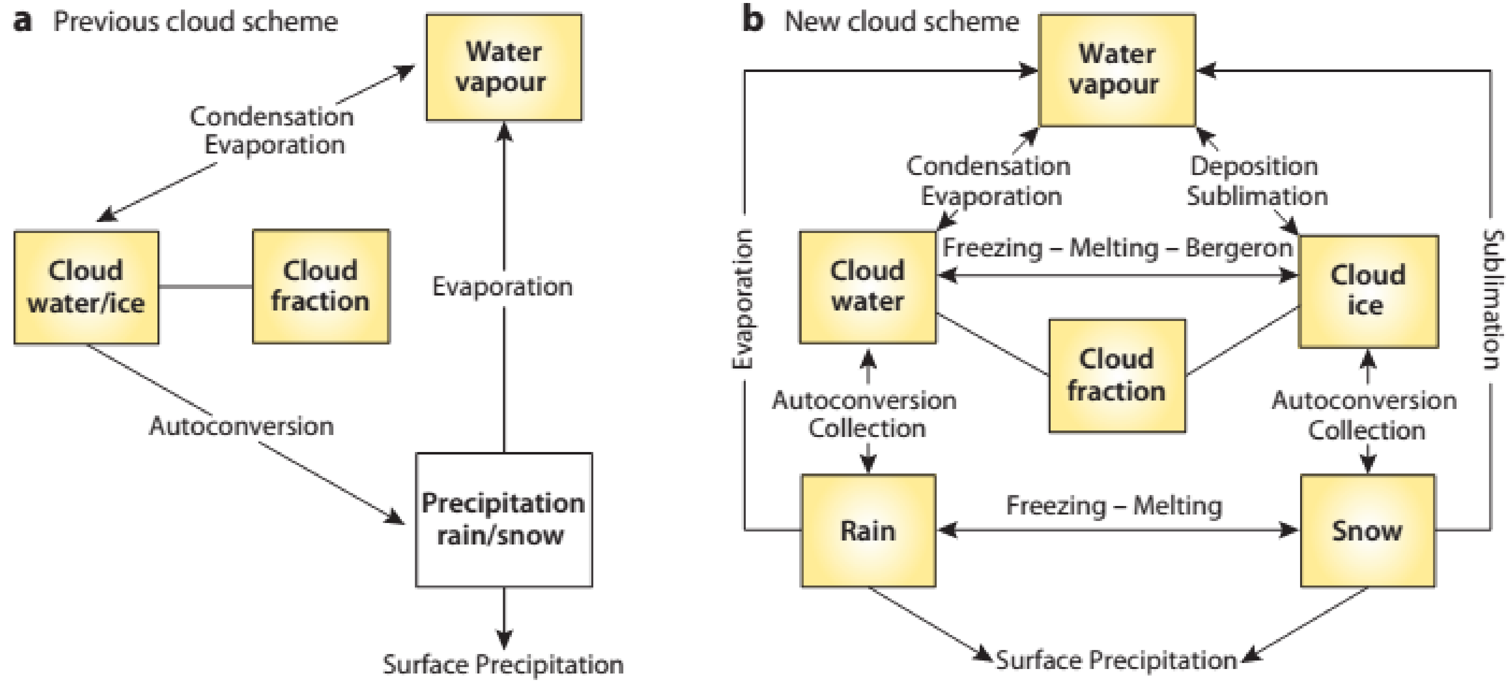

Figure 1: *Schematic of the IFS cloud scheme: (a) the Tiedtke scheme with three moisture related prognostic variables operational from 1995 to 2010 (before IFS Cy36r4) and (b) the new cloud scheme with six moisture related prognostic variables (Cy36r4 onwards). Yellow boxes indicate prognostic variables.*

2.2 Numerical framework

The new scheme is a multi-species prognostic microphysics scheme, with $m = 5$ prognostic equations for water vapour, cloud liquid water, rain, cloud ice and snow. The equation governing each prognostic cloud variable within the cloud scheme is

$$\frac{\partial q_x}{\partial t} = S_x + \frac{1}{\rho}\frac{\partial}{\partial z}(\rho V_x q_x), \quad (1)$$

where q_x is the specific water content for category x ($x = 1$ for cloud liquid droplets, $x = 2$ for rain, and so on), S_x is the net source or sink of q_x through microphysical processes, and the last term represents the sedimentation of q_x with fall speed V_x.

Zhao & Carr 1997

Default CFS Microphysics

Hong & Lim 2006

WSM6

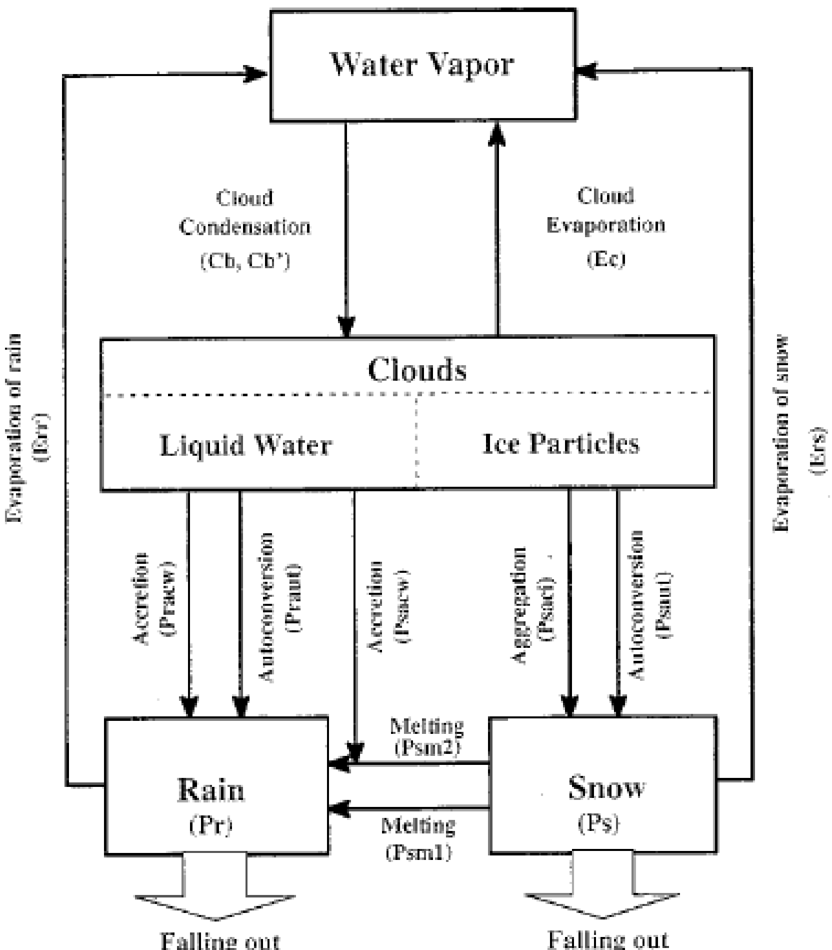

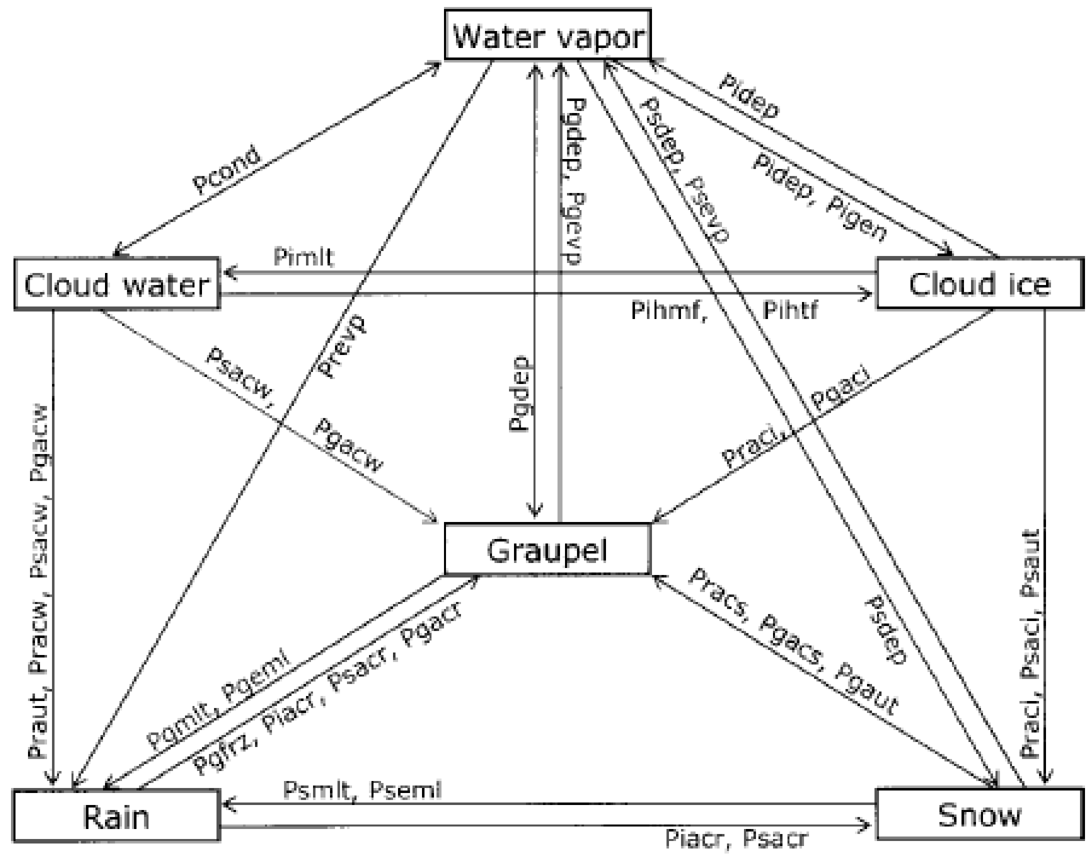

Tendencies

$$\frac{\partial}{\partial t}(n) = \mathrm{ADV}(n) + \mathrm{TURB}(n) + \mathrm{SEDIM}(n) + \mathrm{SOURCE}(n)$$

where n = *[n_r, n_i, n_s, n_{clw}, n_g, n_v] represents the concentration of rain, ice* crystals, snow, graupel, cloud water, water vap.

The Convective and Microphysical Scheme Communication

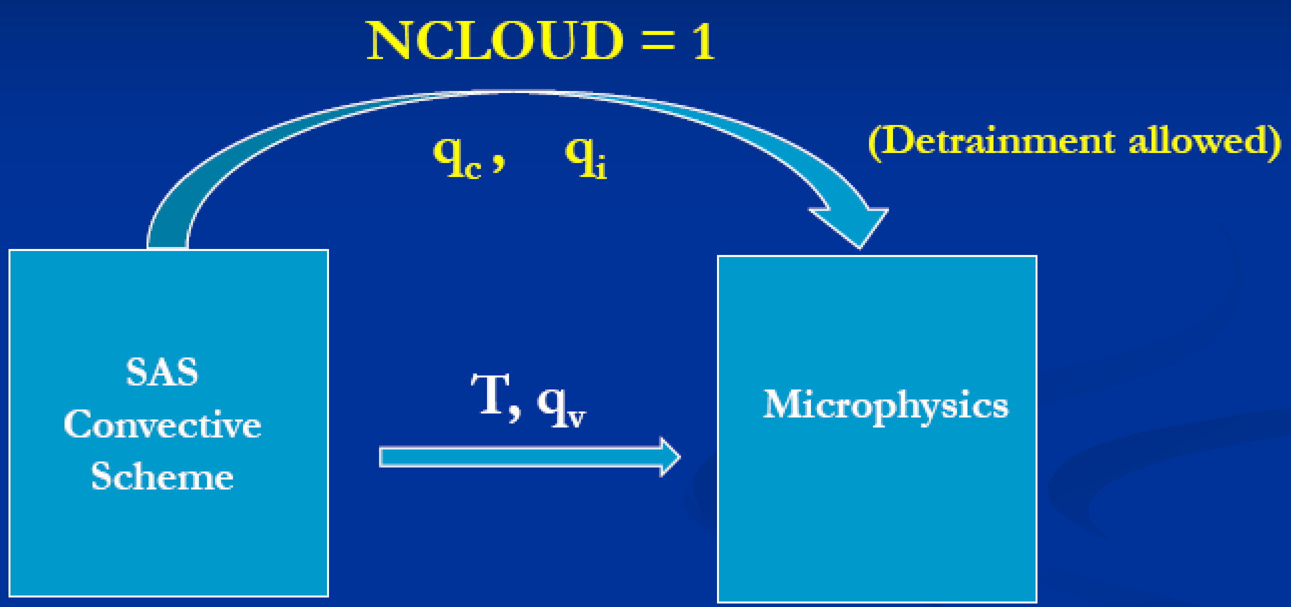

Revised Cloud-Convective-Radiation in CFSv2 T126

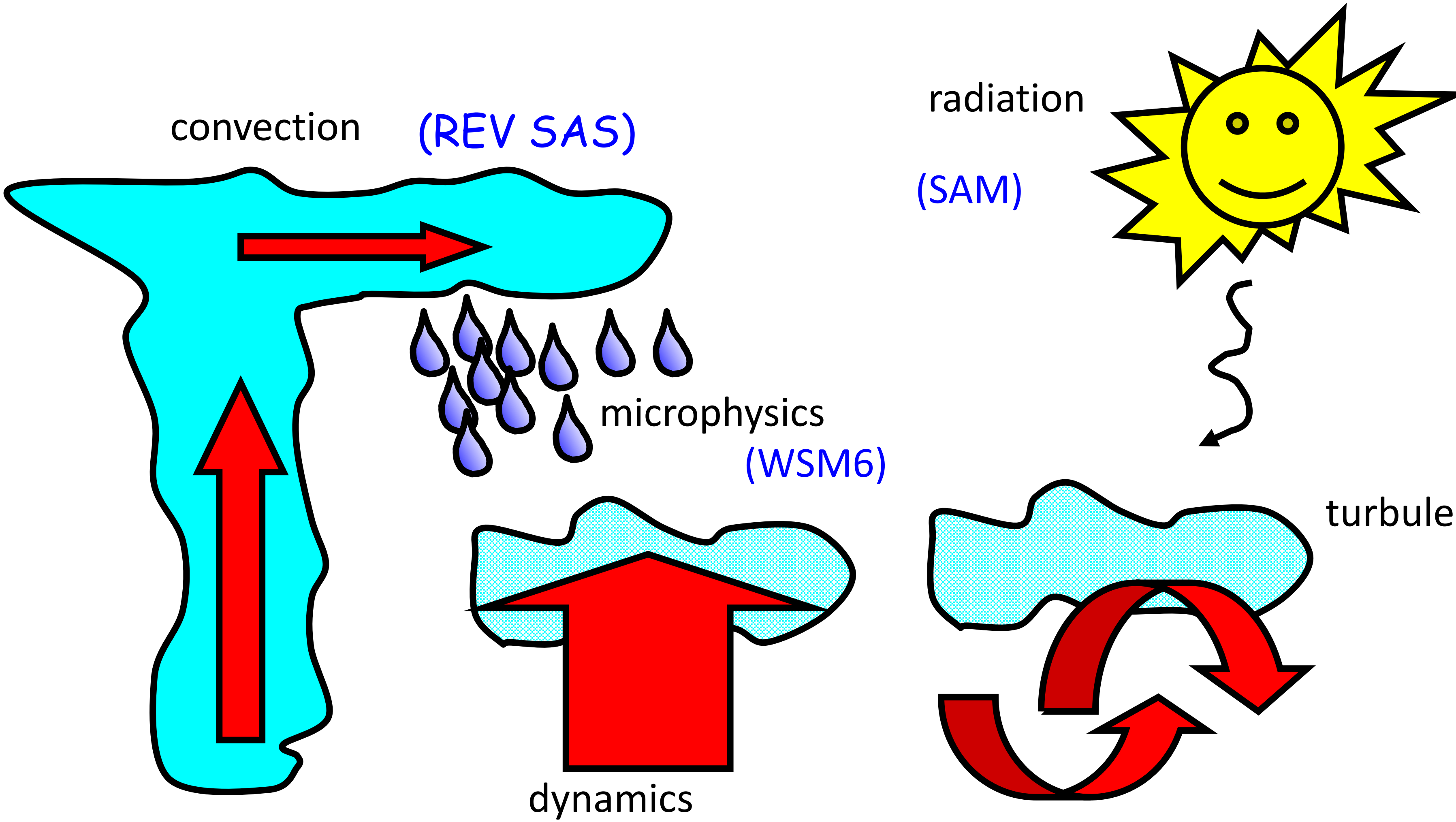

Clouds are the result of complex interactions between a large number of processes

SAM: System of Atmospheric Model

CloudSat IWC/LWC Retrieval

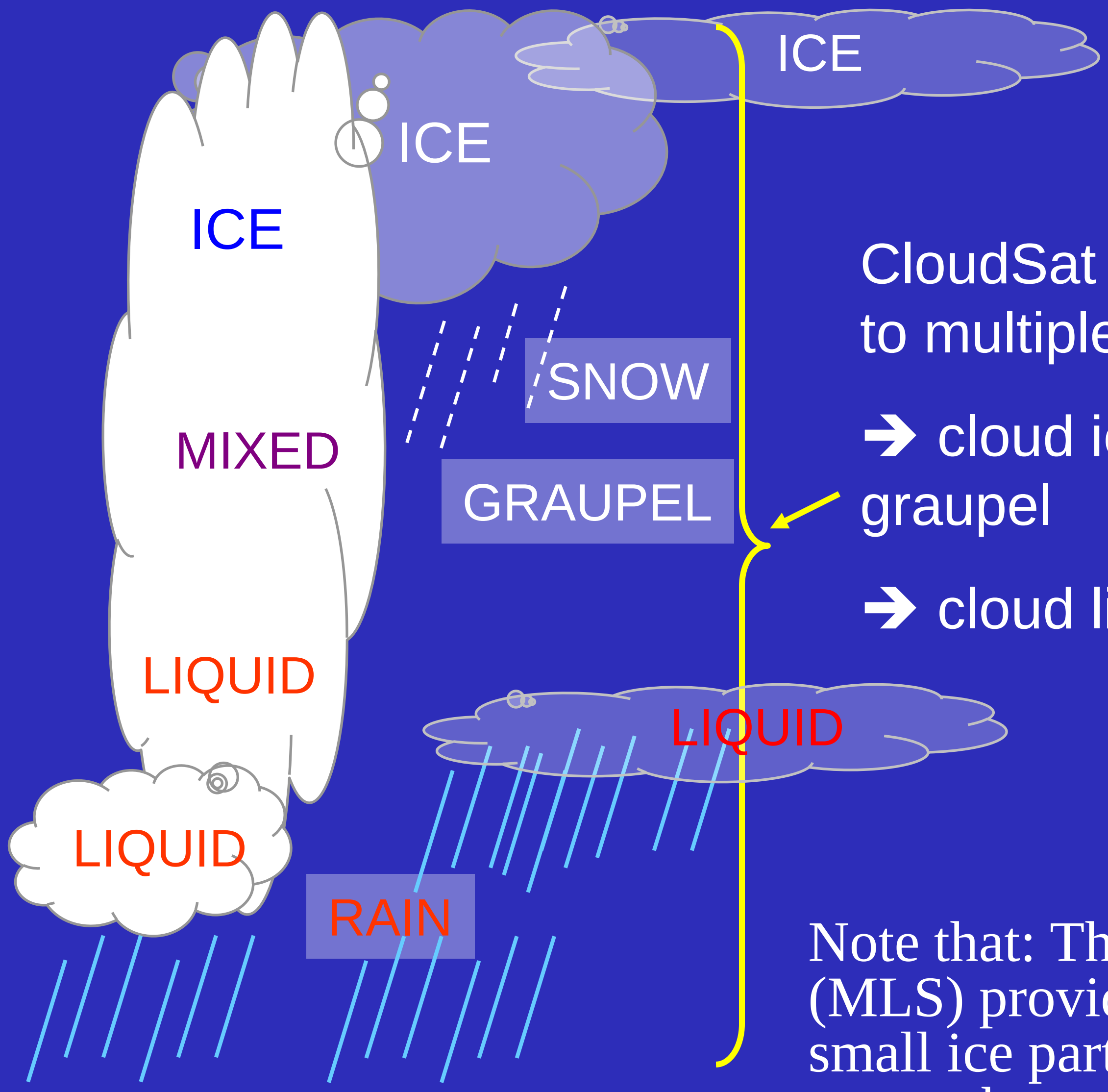

CloudSat measurements are sensitive to multiple particle types:

➔ cloud ice (~small particle), snow, graupel

➔ cloud liquid (~small particle), rain

Note that: The Micro Wave Limb Sounder (MLS) provides IWC estimates described as small ice particles at levels in the upper-troposphere

Slide Courtesy: Frank Li, JPL

Precip bias (JJAS)

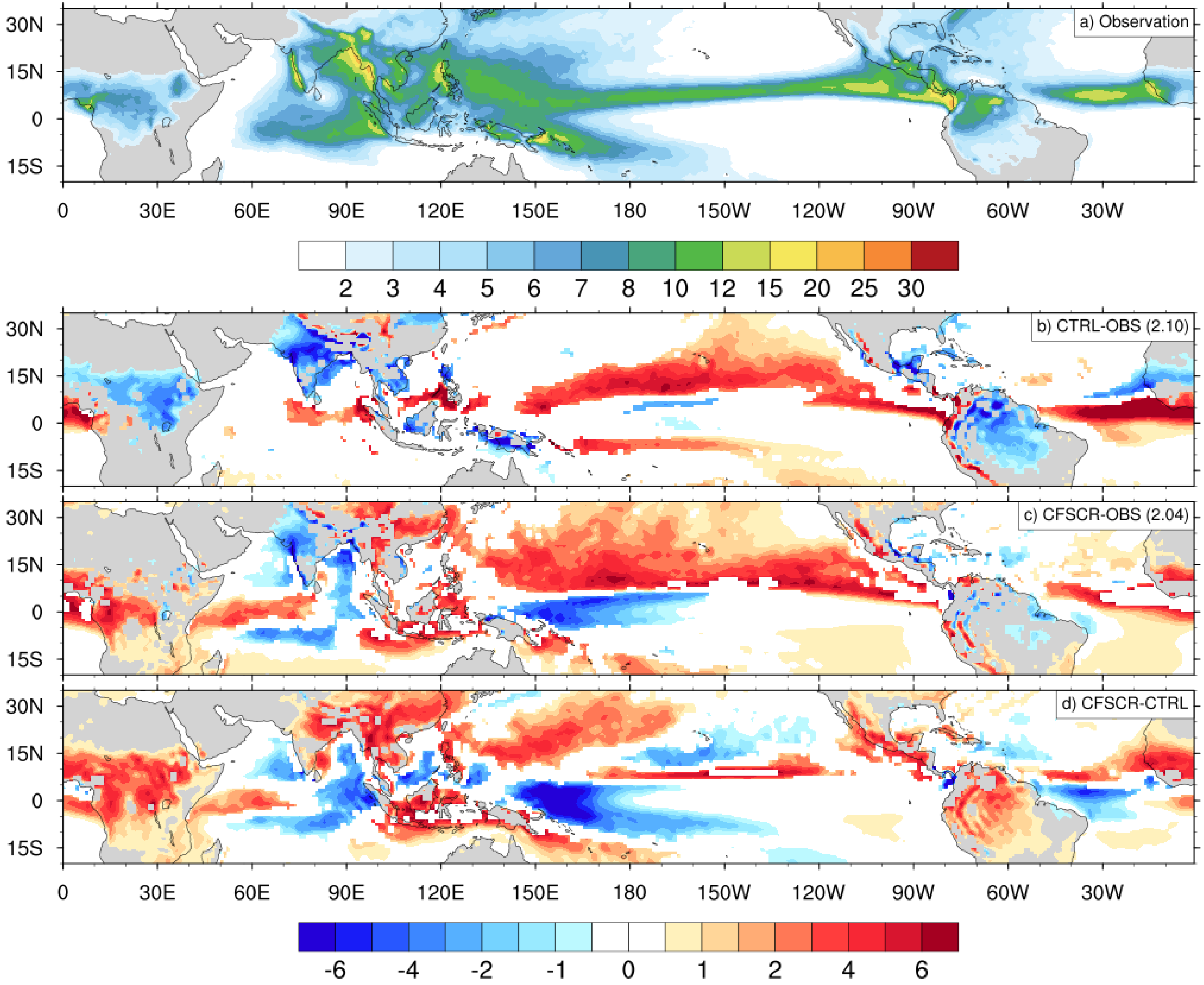

SST bias

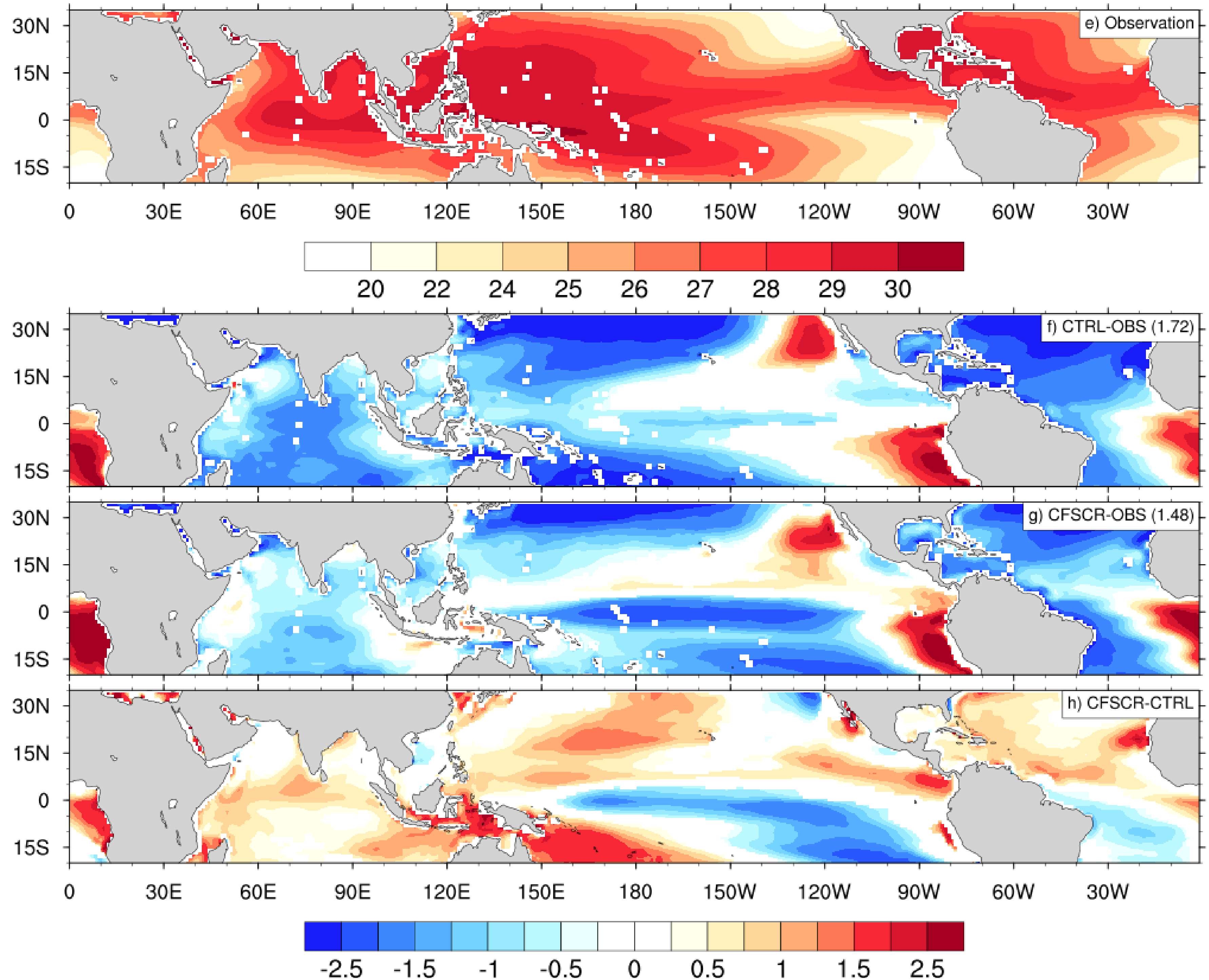

e) Observation
f) CTRL-OBS (1.72)
g) CFSCR-OBS (1.48)
h) CFSCR-CTRL
30N
15N
0
15S
0
30E
60E
90E
120E
150E
180
150W
120W
90W
60W
30W
20
22
24
25
26
27
28
29
30
-2.5
-1.5
-1
-0.5
0
0.5
1
1.5
2.5

Revised convection, modified microphysics and radiation is able to improve the mean state and Intraseasonal variability of CFSv2T126

Annual Rainfall Cycle <73°-85°E,15°-25°N>

Annual TT Difference <40°-100°E,5°-35°N> - <40°-100°E,15°S-5°N>

<40°-120°E, 15°S-30°N>

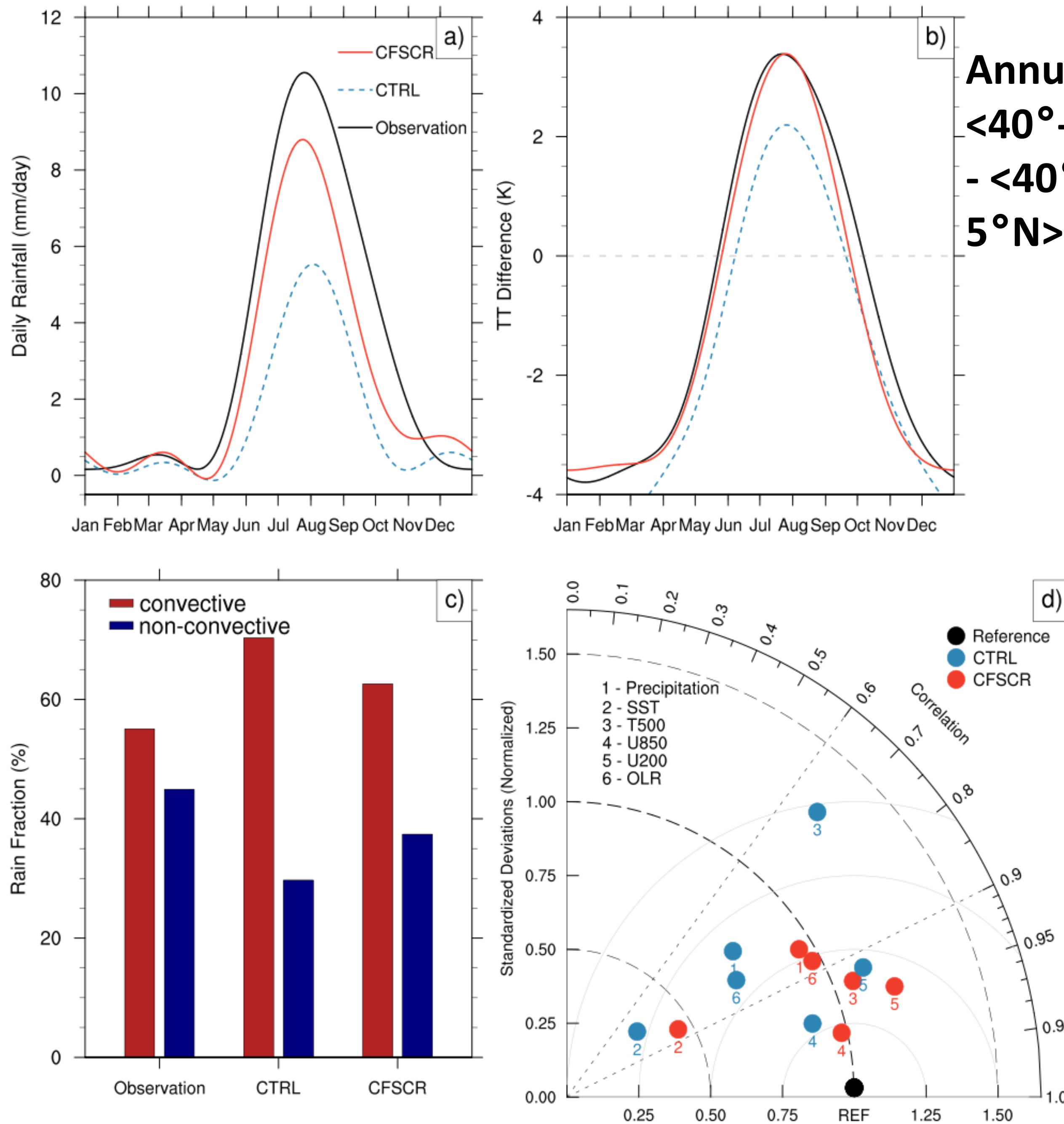

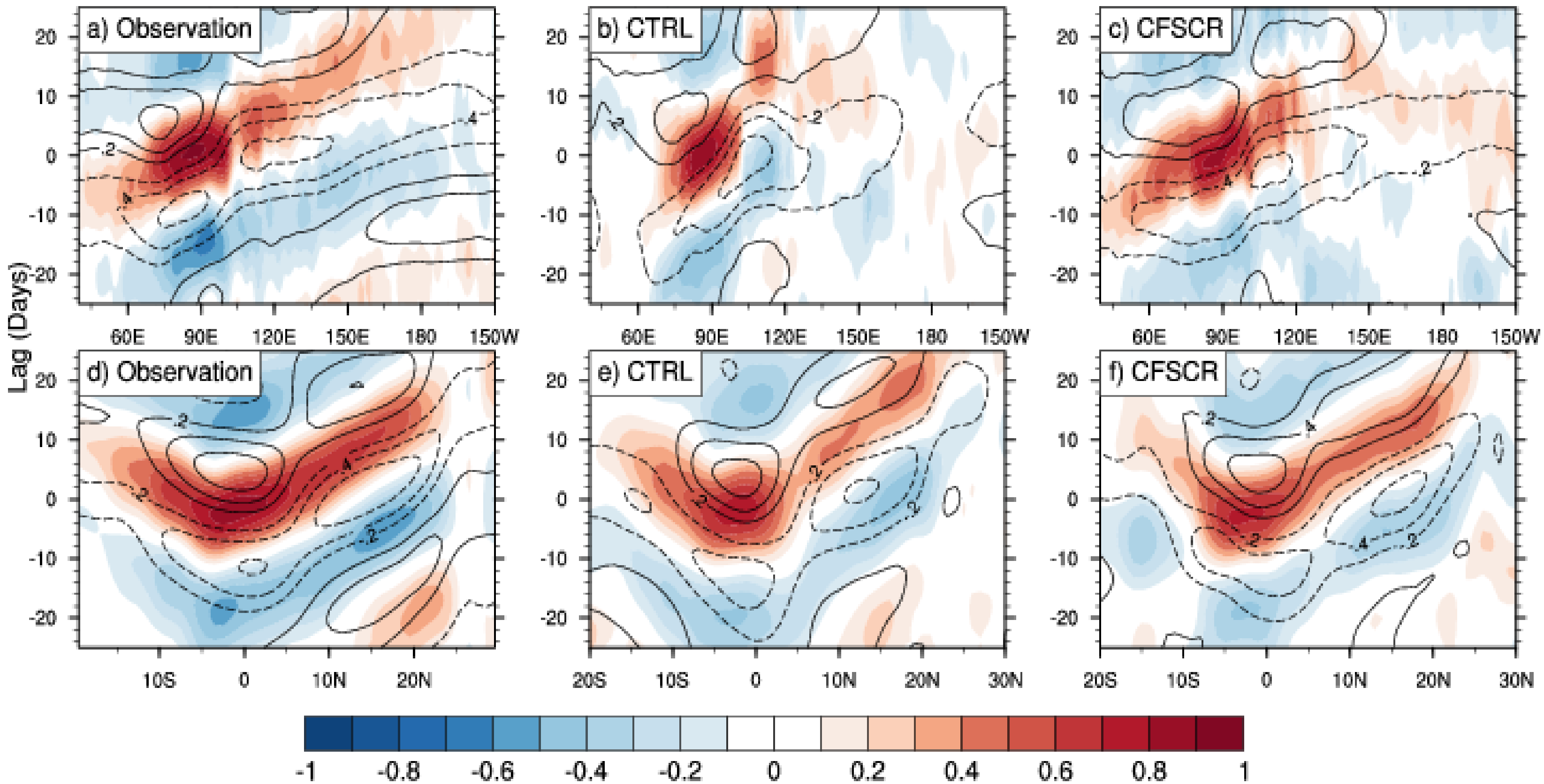

Longitude (Latitude) vs lag correlation of 20–100-day filtered precipitation (shaded) and U_{850} (contour) with base 20-100-day filtered precipitation time series over EEIO (10°S–5°N, 75°–100°E).

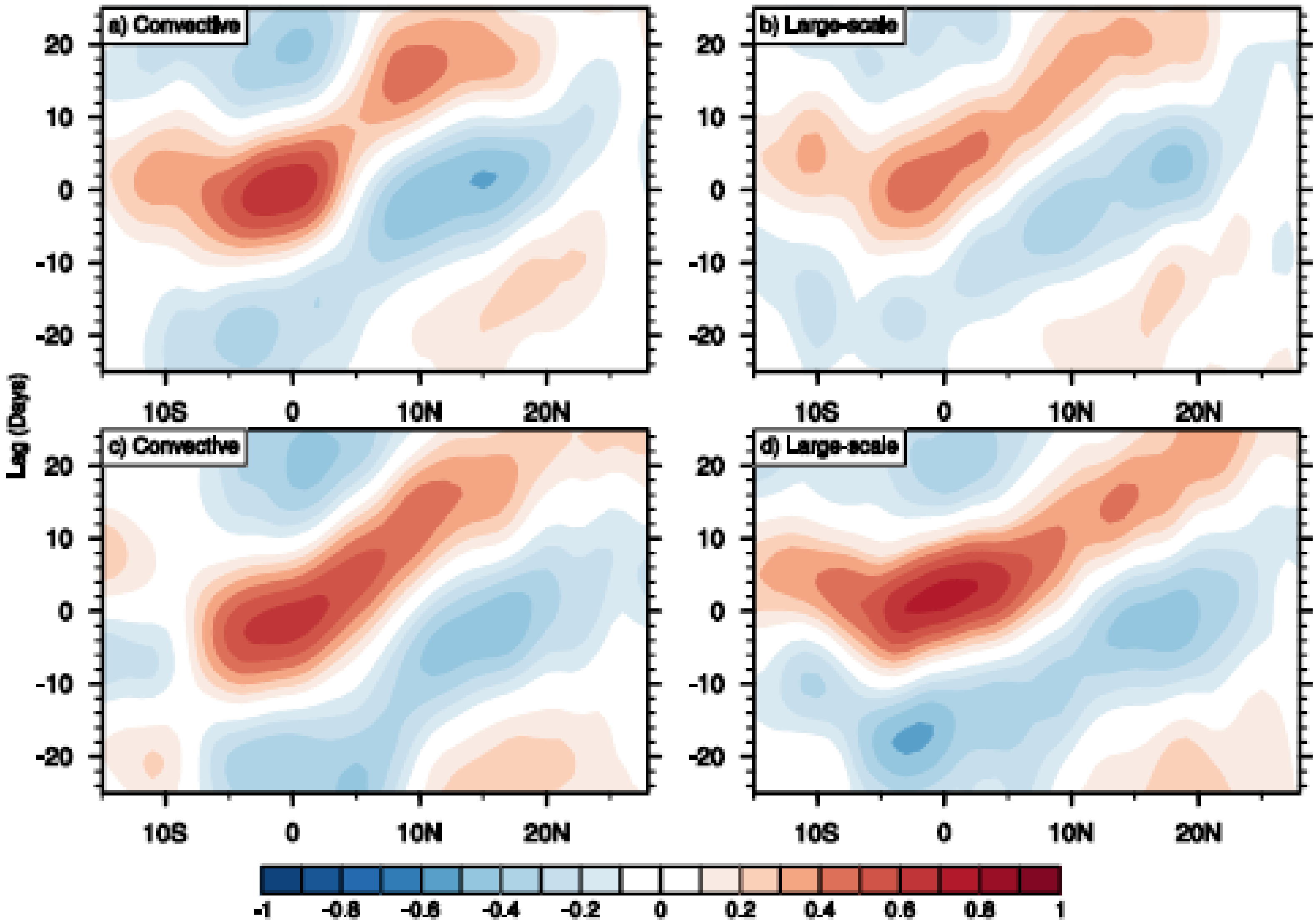

Longitude (Latitude) vs lag correlation of 20–100-day filtered convective and large-scale precipitation from CTRL and CFSCR

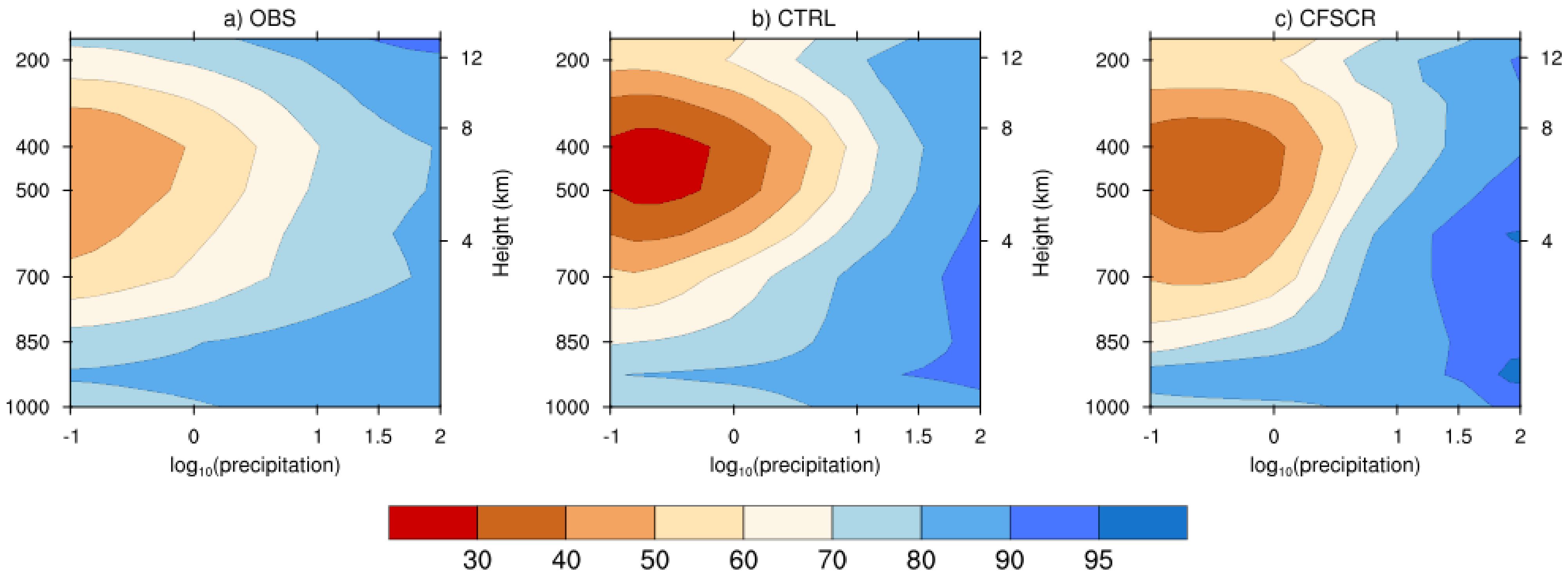

Composite profile of relative humidity as a function of rain rate over ISM domain (40° -120° E, 15° S-30° N) during all JJAS seasons from (a) observation (ERA-Interim vs TRMM), (b) CTRL and (c) CFSCR. The rain rate at the x-axis is plotted in $\log_{10}$ scale.

GCM Cloud Ice Water Content (IWC)

Annual Mean Values

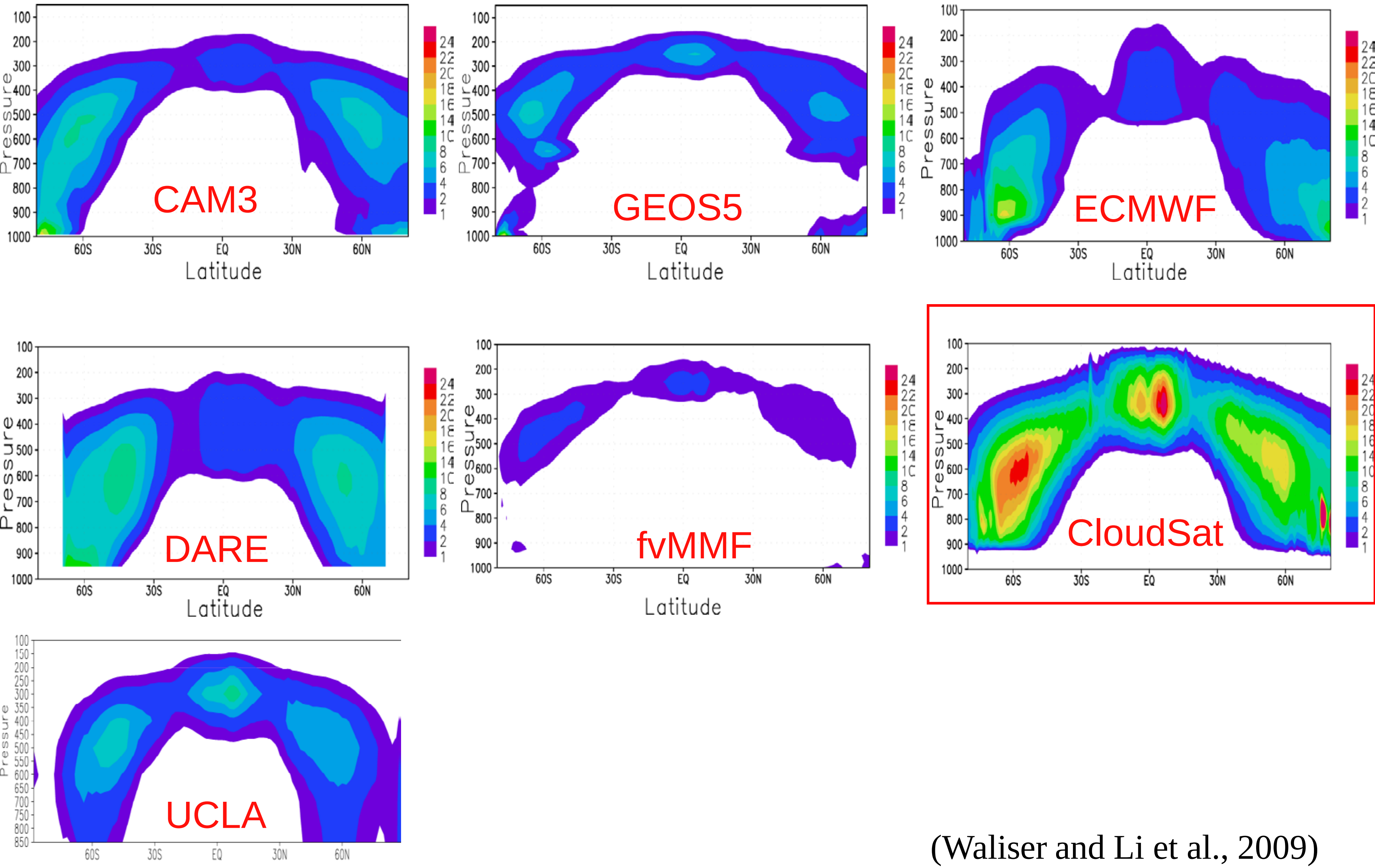

(Waliser and Li et al., 2009)

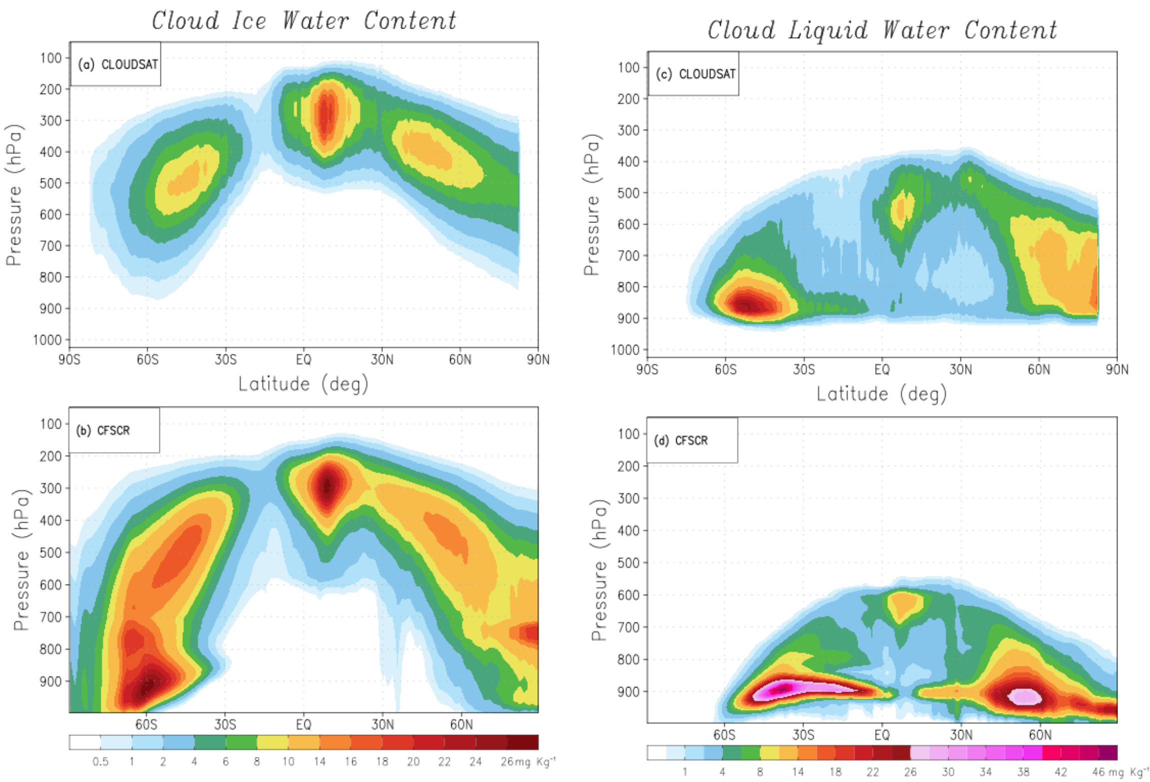

ECMWF IFS cloud ice Betchold+Bulk (comp)

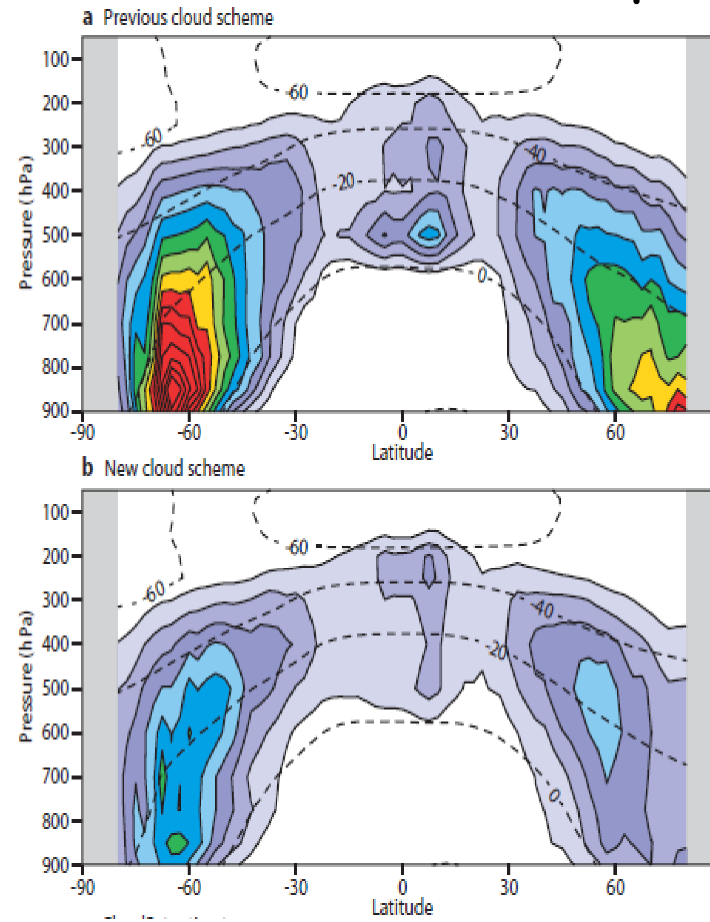

GFDL AM3+Morrisson

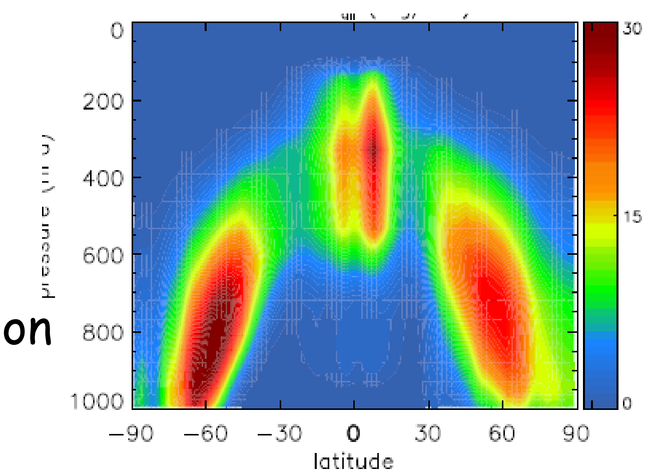

Zonally averaged annual mean vertical distribution of cloud ice water content (mg kg^{-1}) obtained from (a) CFSCR; and cloud liquid water content (mg kg^{-1}) from (b) CFSCR model.

CFSCR: Modified CFSv2 with revised Cloud Microphysics, Convection and radiation

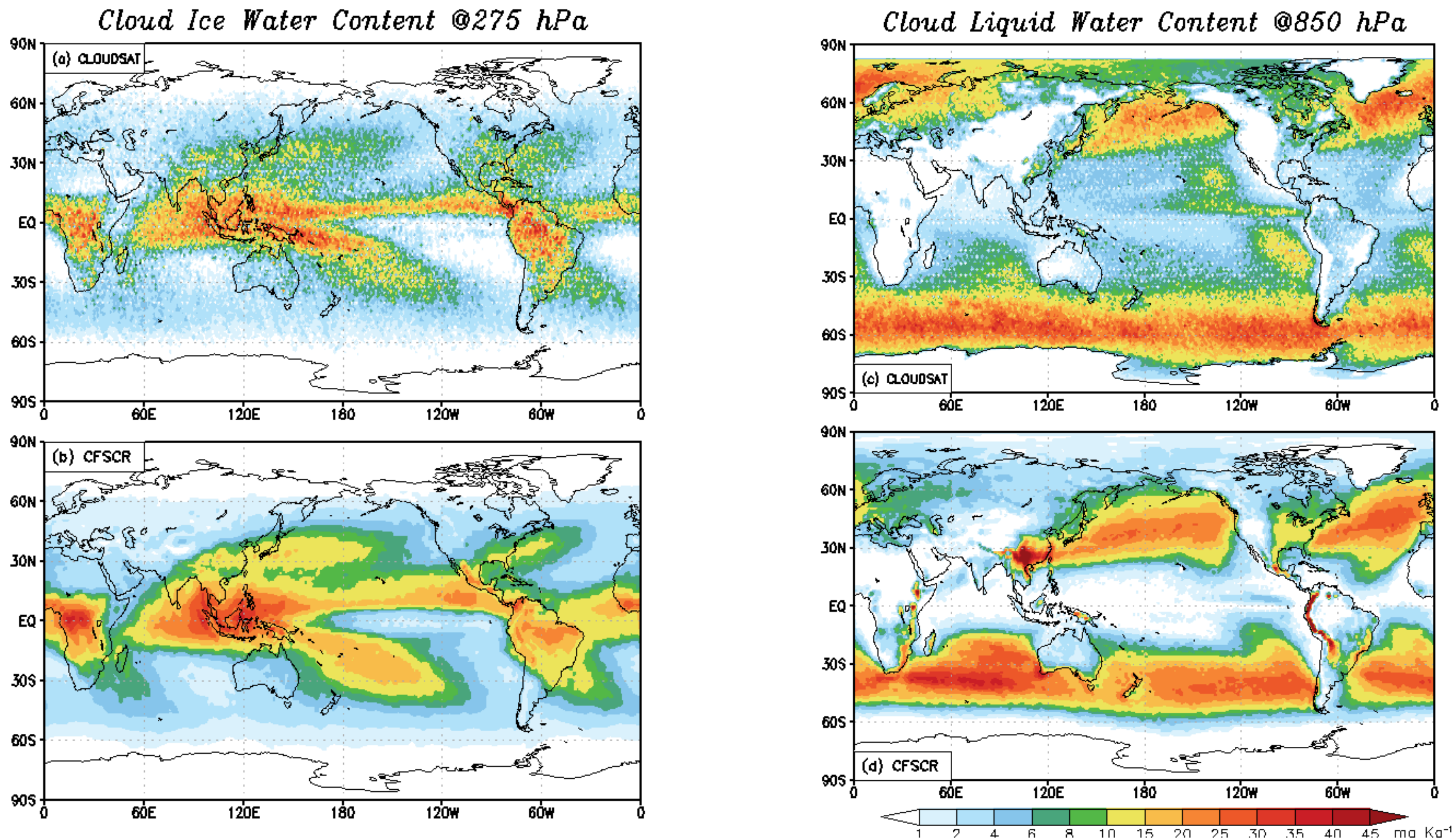

Annual mean isobaric distribution of cloud ice water content (mg kg^{-1}) obtained from (a) CloudSat 2B-CWC-RO, (b) CFSCR (at 271 hPa model level); and cloud liquid water content (mg kg^{-1}) from (c) CloudSat, (d) CFSCR (858 hPa).

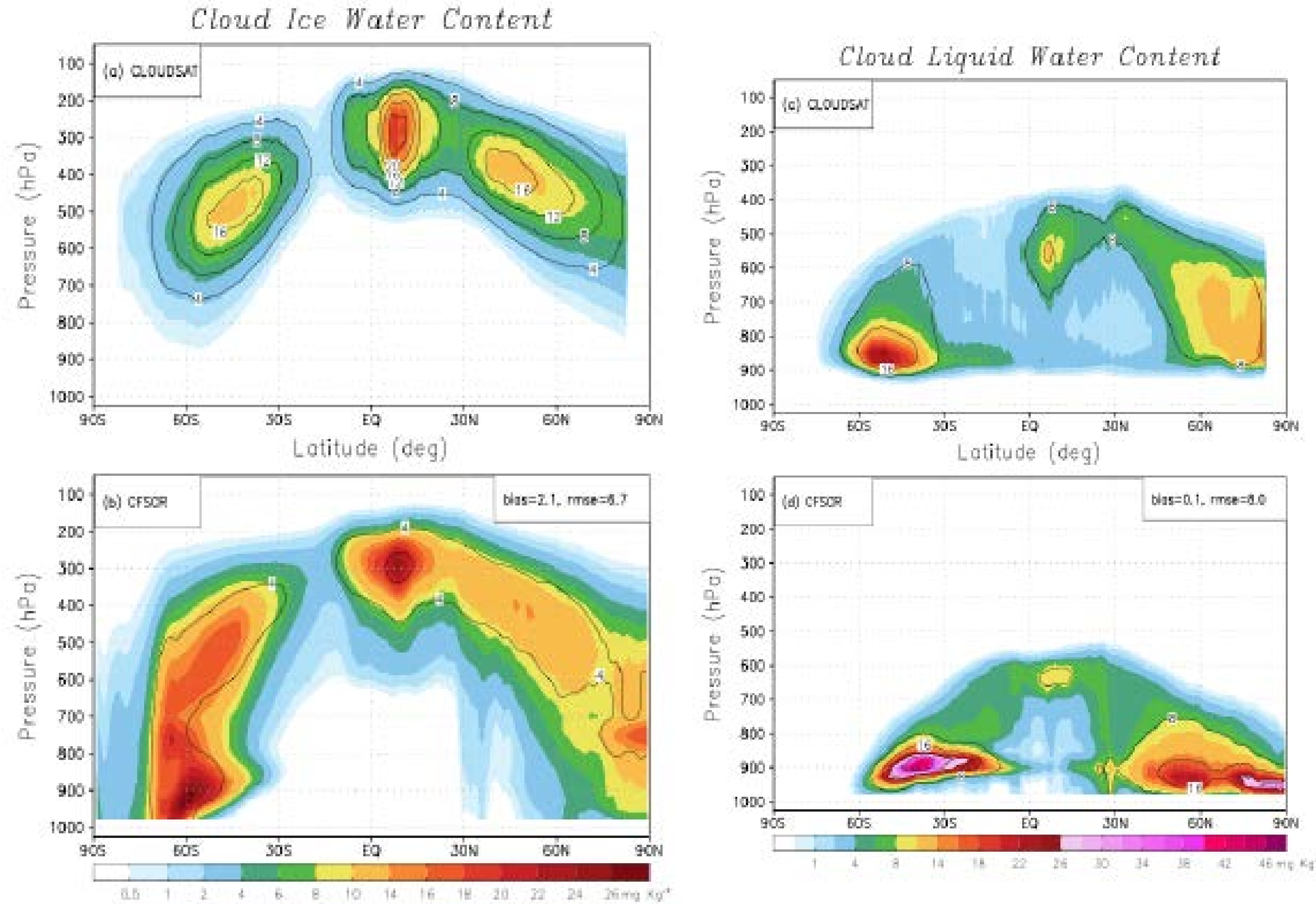
Cloud Ice Water Content
Cloud Liquid Water Content
(a) CLOUDSAT
(b) CFSCR
bias=2.1, rmse=6.7
(c) CLOUDSAT
(d) CFSCR
bias=0.1, rmse=8.0
Pressure (hPa)
Latitude (deg)
90S 60S 30S EQ 30N 60N 90N
100 200 300 400 500 600 700 800 900 1000
0.5 1 2 4 6 8 10 14 16 18 20 22 24 26 mg Kg⁻¹
1 4 8 14 18 22 26 30 34 38 42 46 mg Kg⁻¹

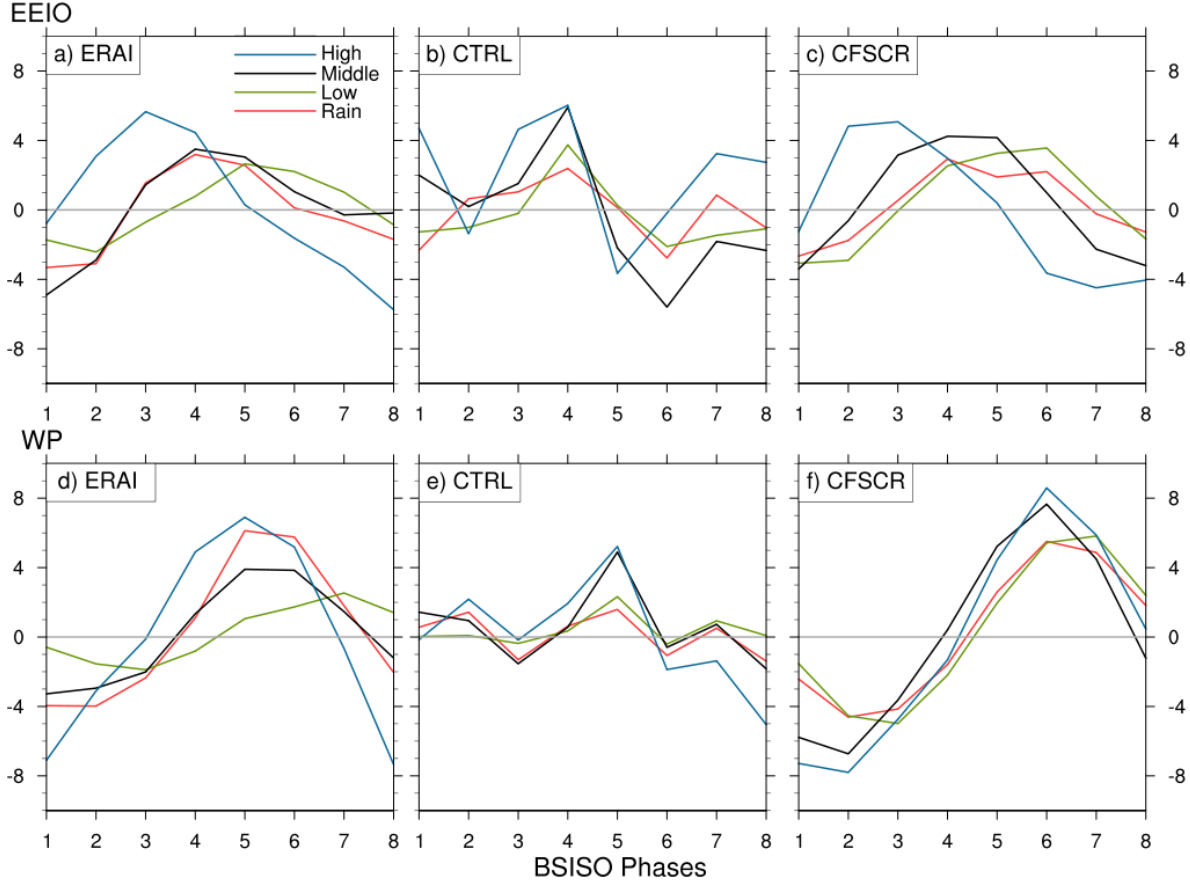

Evolution of anomalous low, middle and high cloud fractions (%, left axis) and rainfall anomalies (mm day-1, right axis) associated with BSISO1 convection over EEIO (top panels) and WP (bottom panels) for (a-b) observation, (c-d) CTRL and (e-f) CFSCR.

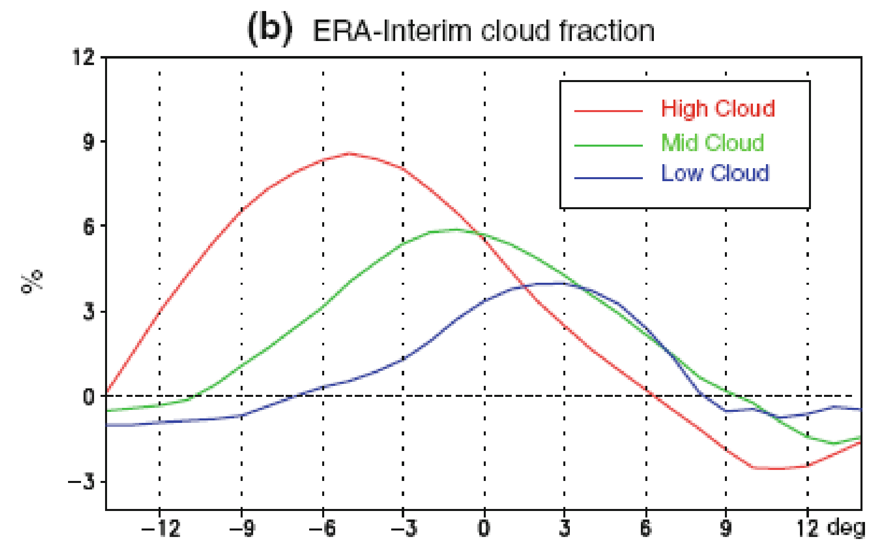

Jiang et al. 2011

Vertical distribution of clouds (JJAS) averaged over 80-90E and 90 to 100E

CFS

CFS-CR

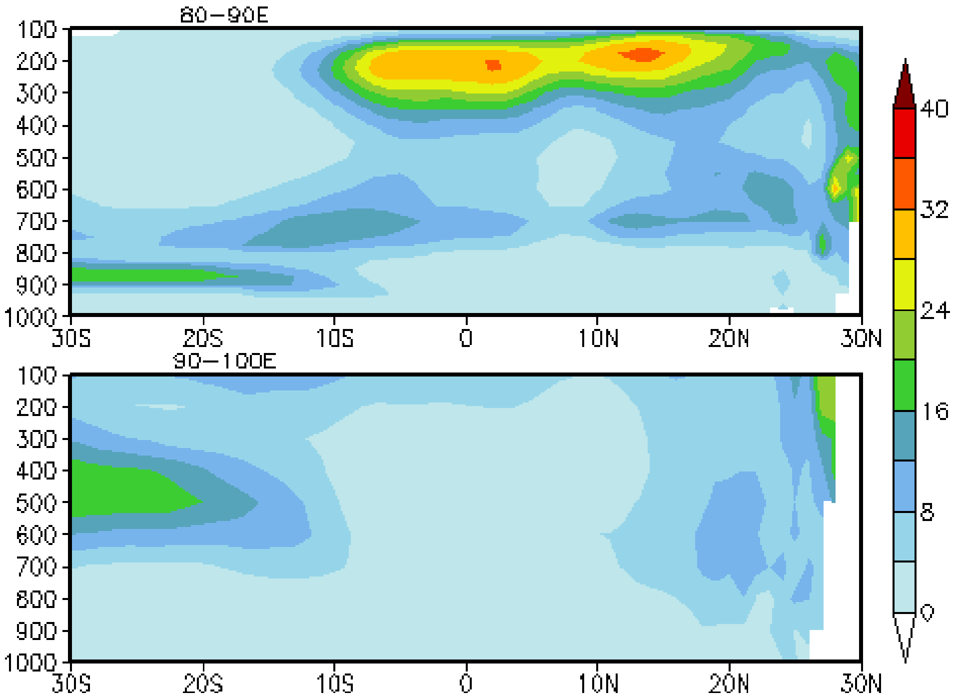

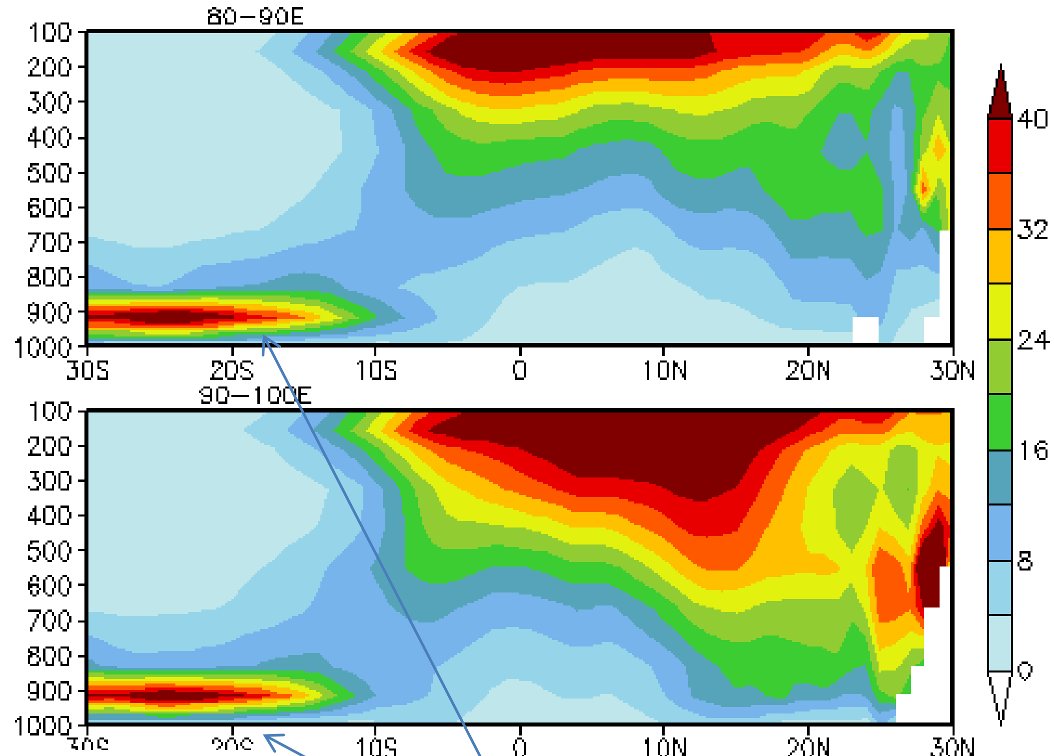

Jun -- Sept. (2006 -- 2010)

(a)

Vertical distribution of clouds

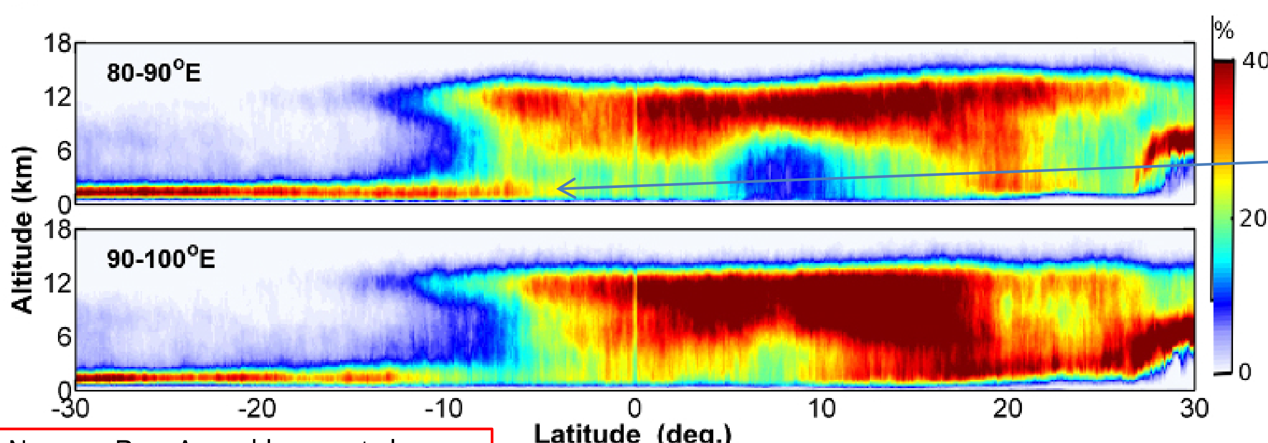

Low Cloud captured by CFS-CR as seen in Cloudsat observation. CFSv2 does not capture

T. Narayan Rao, Aneeshkumar et al.

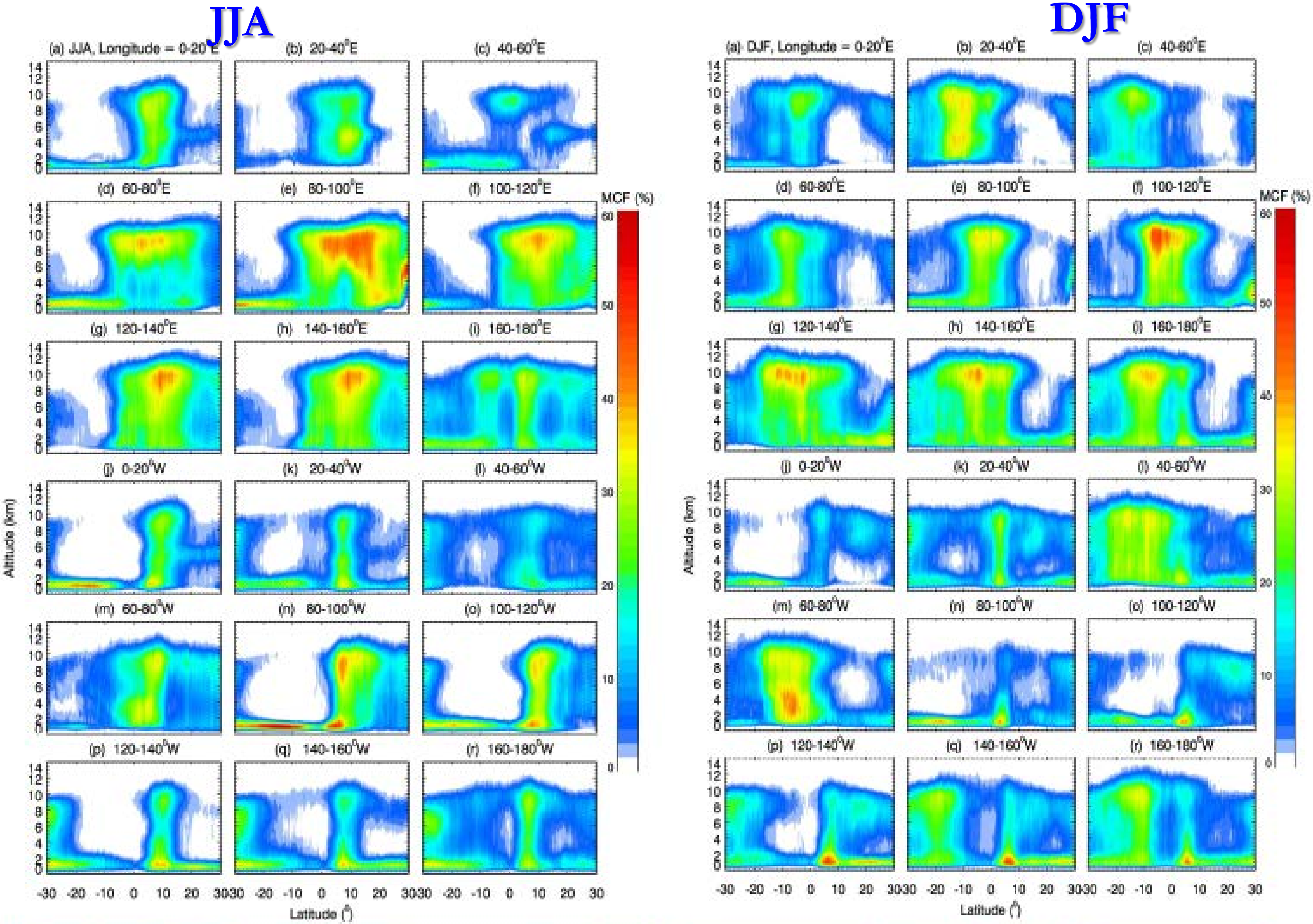

Fig. 1 Mean Cloud Fraction (longitude cross-section of 0-20 ⁰) during summer (JJA) and Winter (DJF) seasons represents the characteristic features associated with Ascending and Descending limbs of Walker and Hadley Cells.

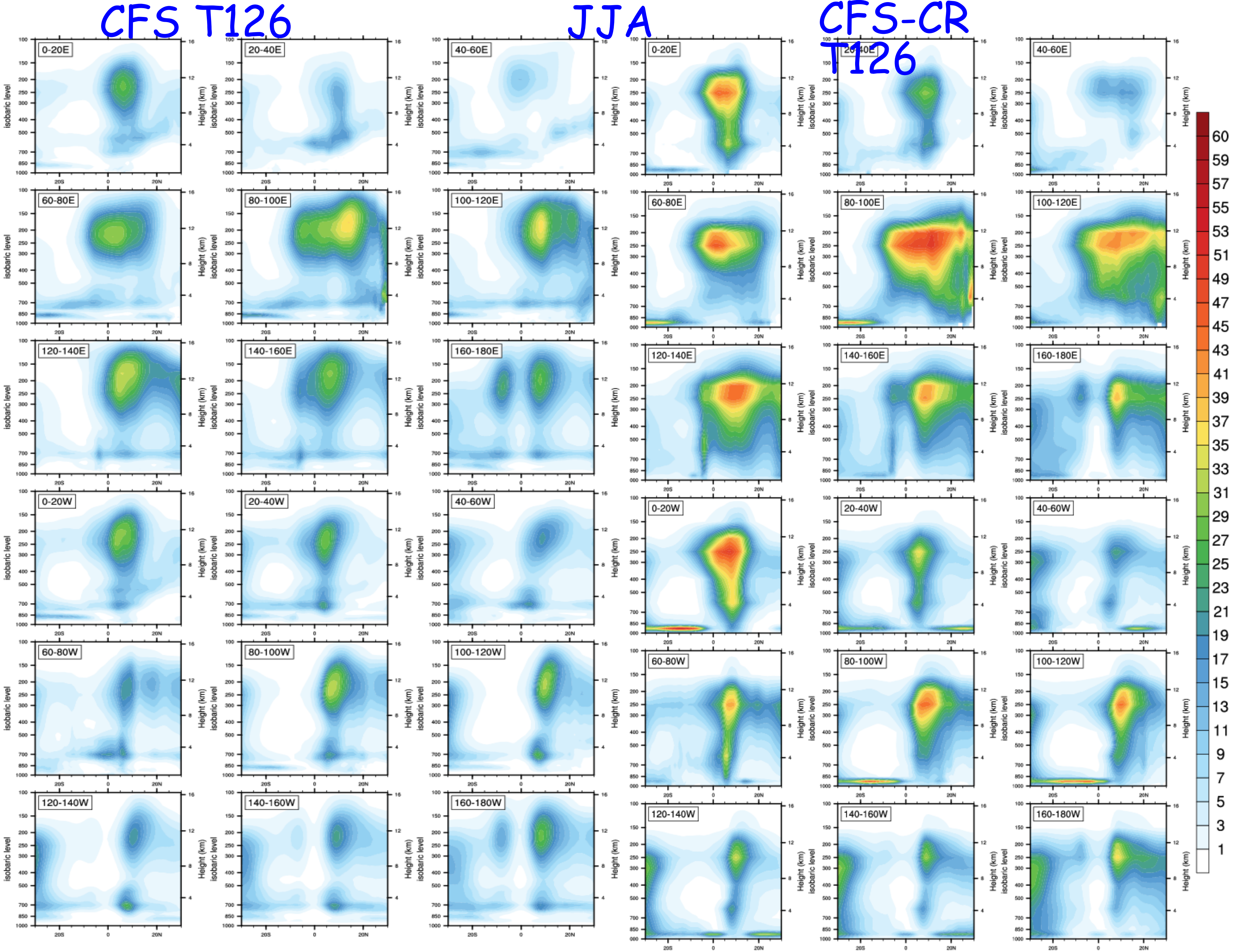

CFS T126
JJA
CFS-CR T126
0-20E
20-40E
40-60E
60-80E
80-100E
100-120E
120-140E
140-160E
160-180E
0-20W
20-40W
40-60W
60-80W
80-100W
100-120W
120-140W
140-160W
160-180W
isobaric level
Height (km)
20S
0
20N
60
59
57
55
53
51
49
47
45
43
41
39
37
35
33
31
29
27
25
23
21
19
17
15
13
11
9
7
5
3
1

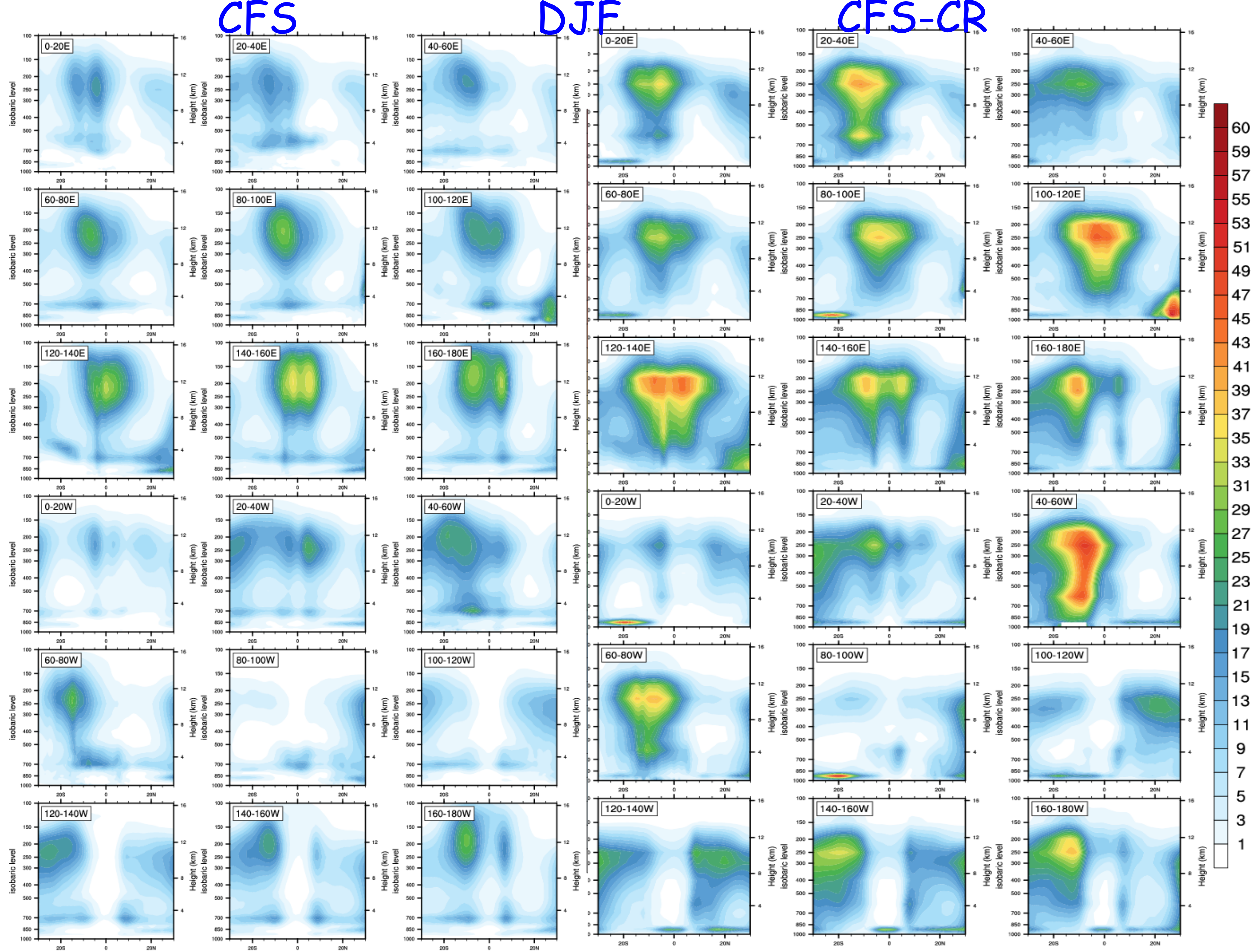
CFS
DJF
CFS-CR
0-20E
20-40E
40-60E
60-80E
80-100E
100-120E
120-140E
140-160E
160-180E
0-20W
20-40W
40-60W
60-80W
80-100W
100-120W
120-140W
140-160W
160-180W
isobaric level
Height (km)
20S
0
20N
60
59
57
55
53
51
49
47
45
43
41
39
37
35
33
31
29
27
25
23
21
19
17
15
13
11
9
7
5
3
1

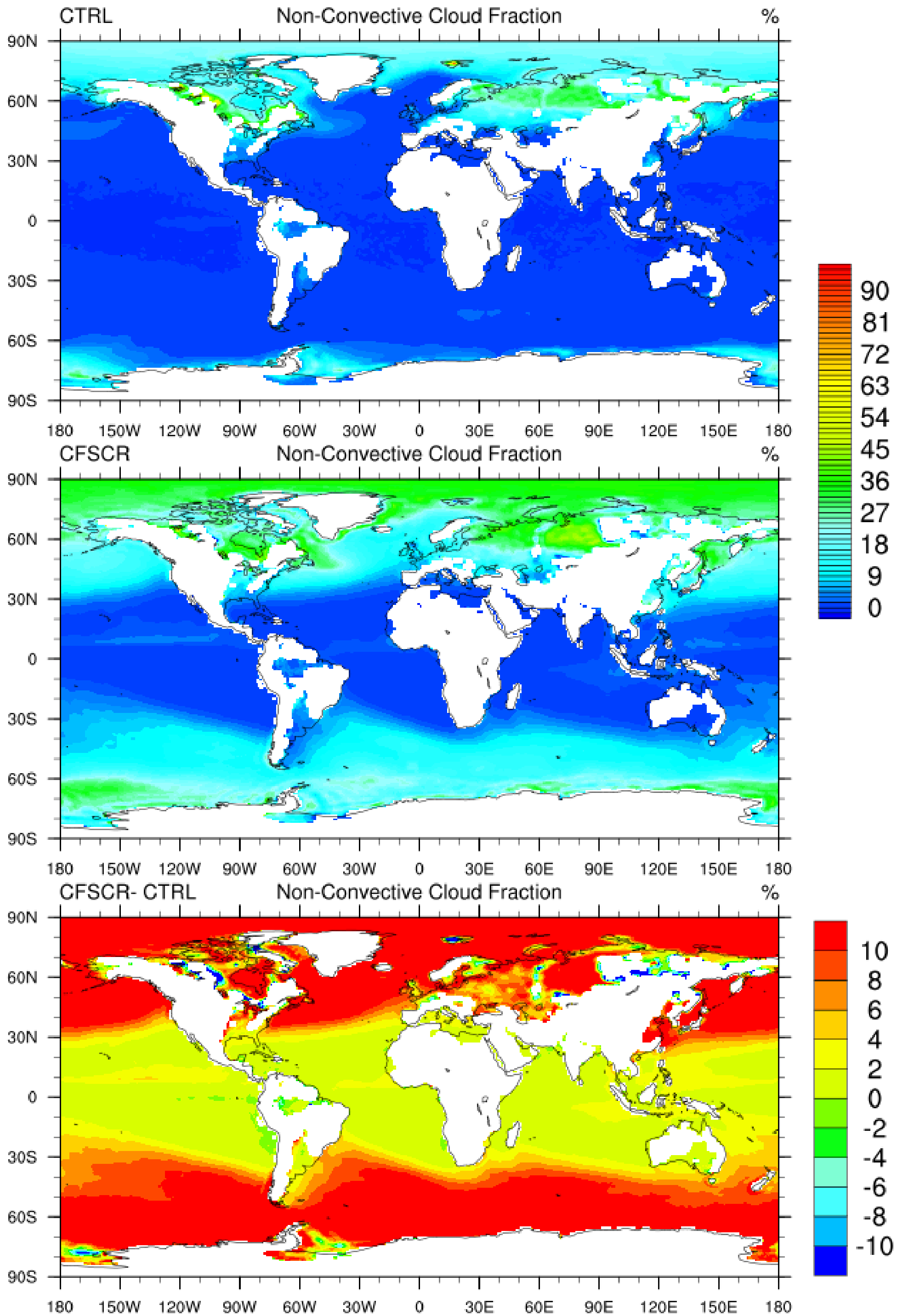

CTRL
Non-Convective Cloud Fraction
%
CFSCR
Non-Convective Cloud Fraction
%
CFSCR- CTRL
Non-Convective Cloud Fraction
%
90N
60N
30N
0
30S
60S
90S
180
150W
120W
90W
60W
30W
0
30E
60E
90E
120E
150E
180
90
81
72
63
54
45
36
27
18
9
0
10
8
6
4
2
0
-2
-4
-6
-8
-10

Amount of total rainfall contributed by different categories

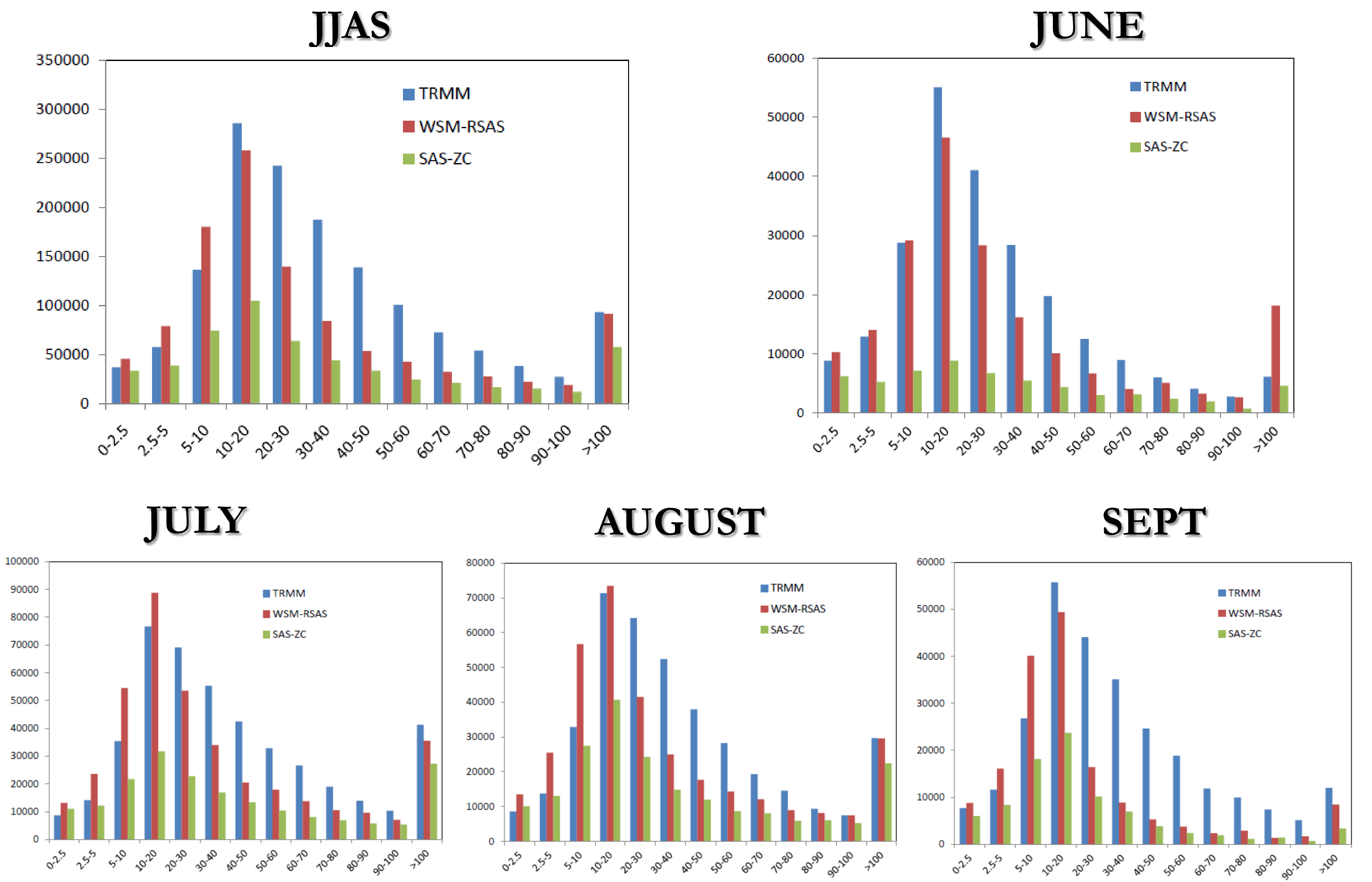

Total cloud water path corresponding to different rainfall categories

JJAS

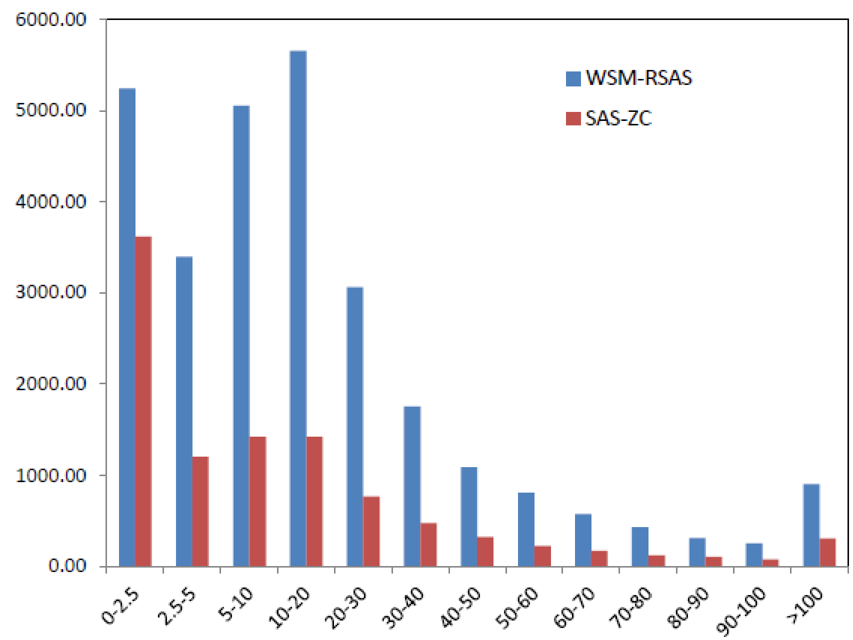

JUNE

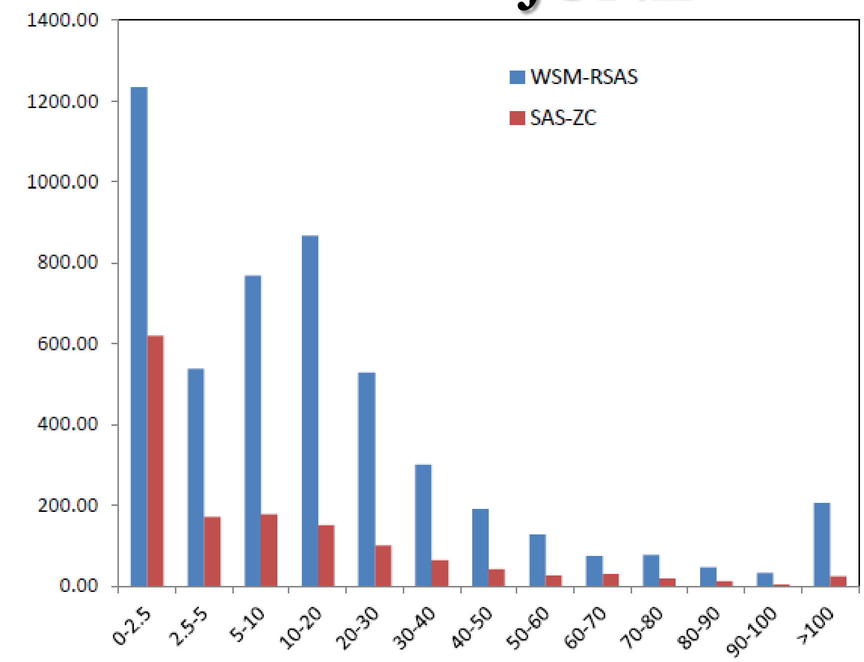

JULY

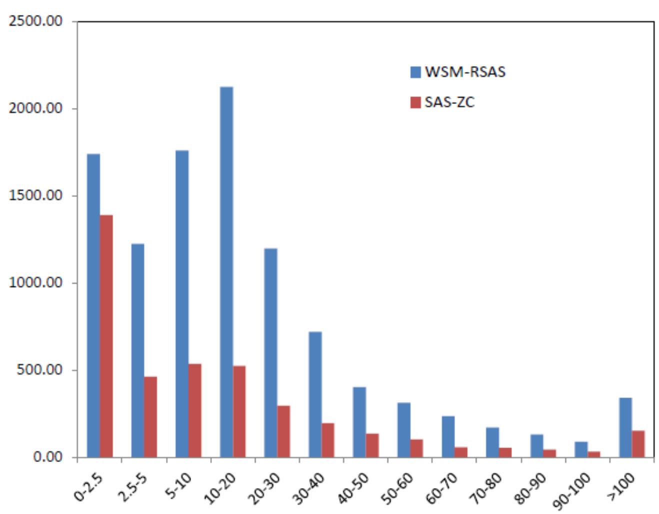

AUGUST

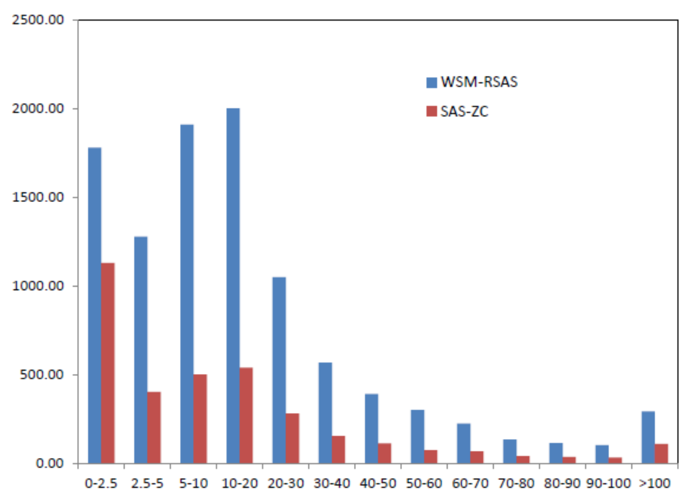

SEPT

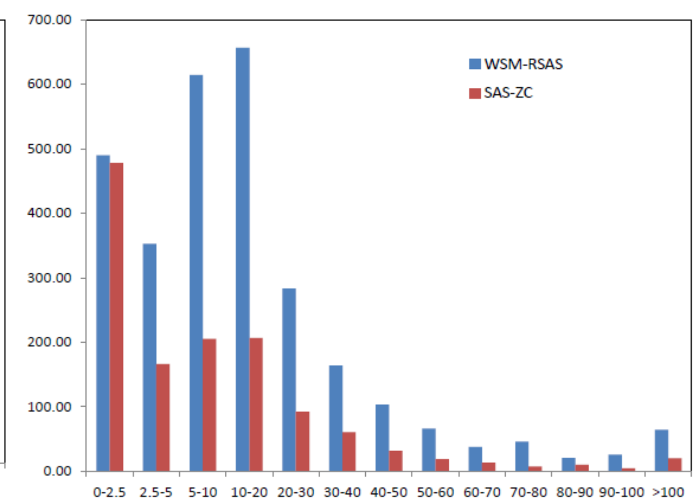

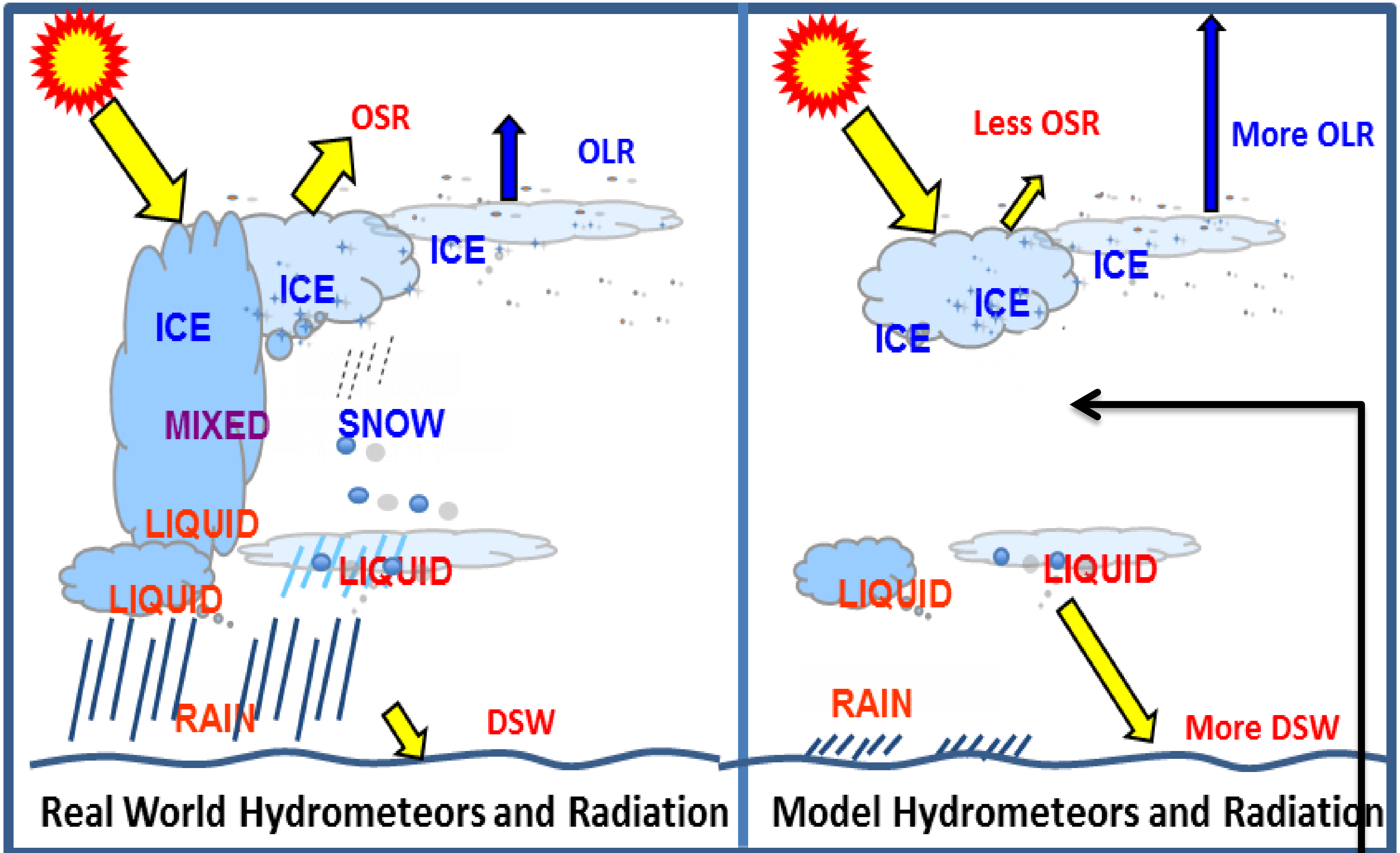

Bridging the Gap in CFSv2 using modified Microphysics: WSM6

SCHEMATIC OF GEFS (SL) T574 L64 RUNNING AT IITM

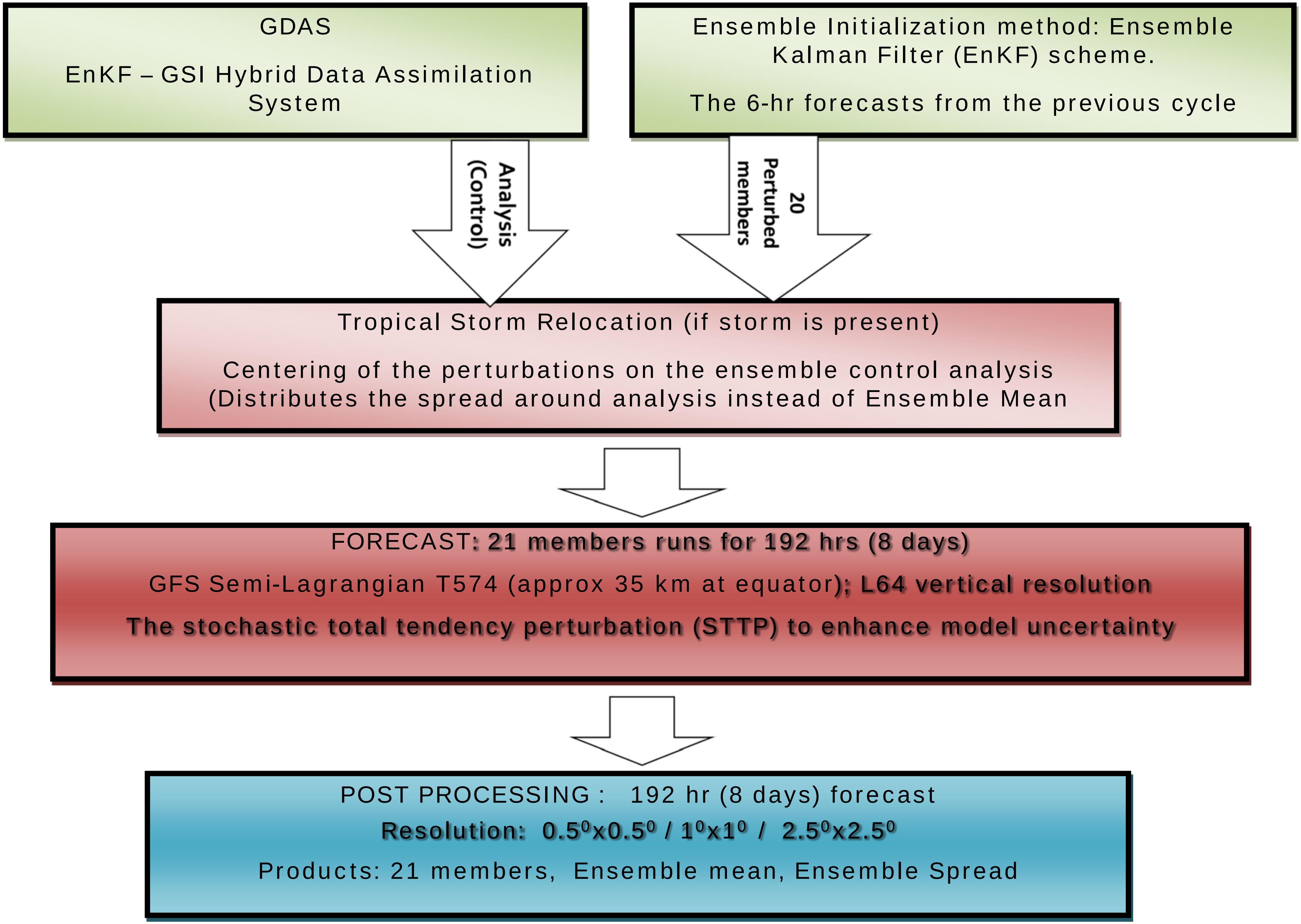

SCHEMATIC OF GFS (SL) T1534 L64 RUNNING AT IITM

GDAS

EnKF – GSI Hybrid Data Assimilation System

Analysis

FORECAST: GFS Semi-Lagrangian T1534 (approx 12 km at equator)

L64 vertical resolution

Runs for 240 hrs (10 days)

POST PROCESSING

120hr (10 days) forecast

Resolution: **Regular grid and Gaussian grid at different resolutions**

0.125^0x0.125^0 / 0.25^0x0.25^0 / 0.5^0x0.5^0 / 1^0x1^0

JJAS 2016 rainfall BIAS (mm/day)

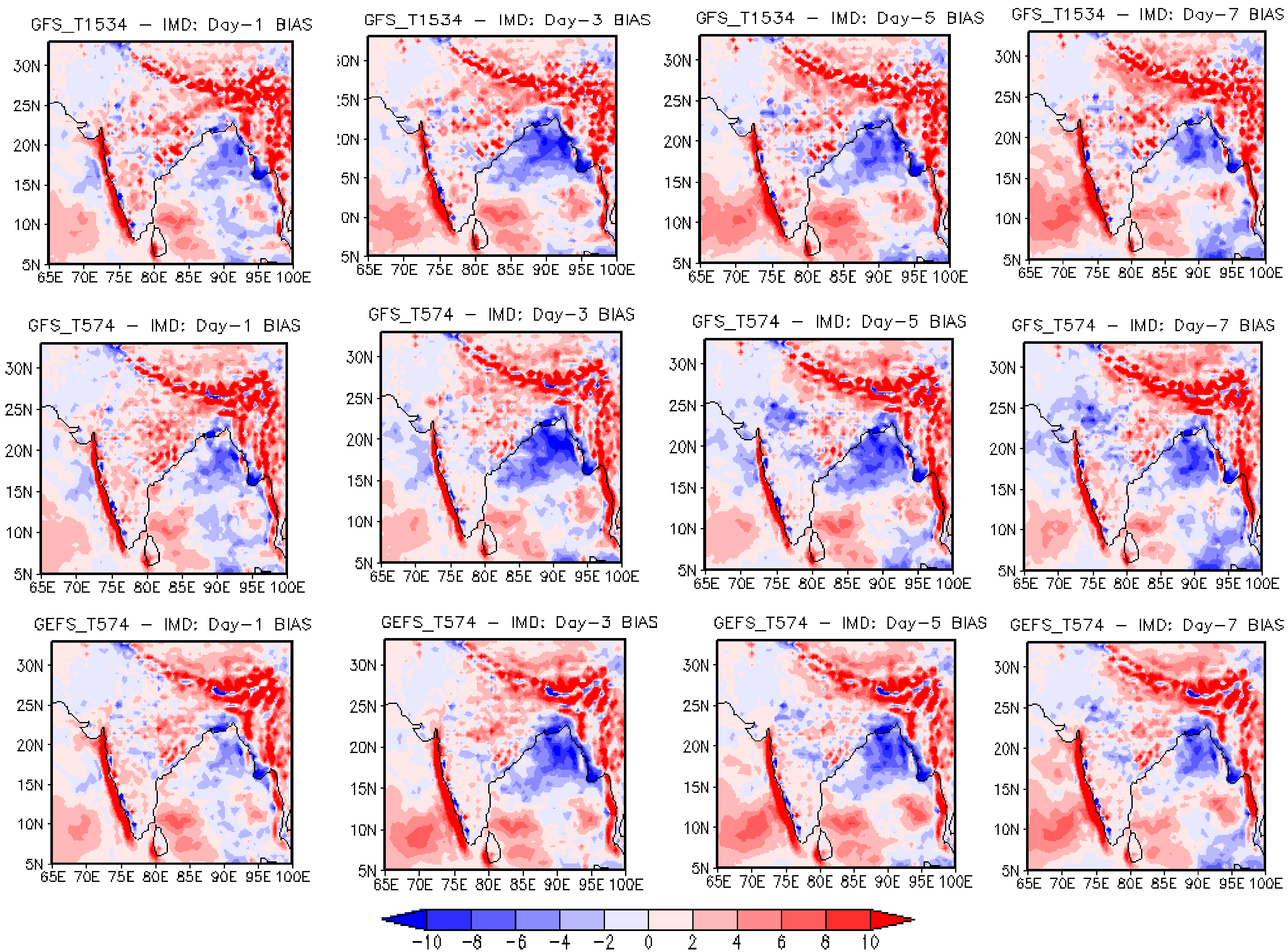

All India land points Rainfall (cm): JJAS

X-axis: cm/day
Y-axis: cm

Day-1

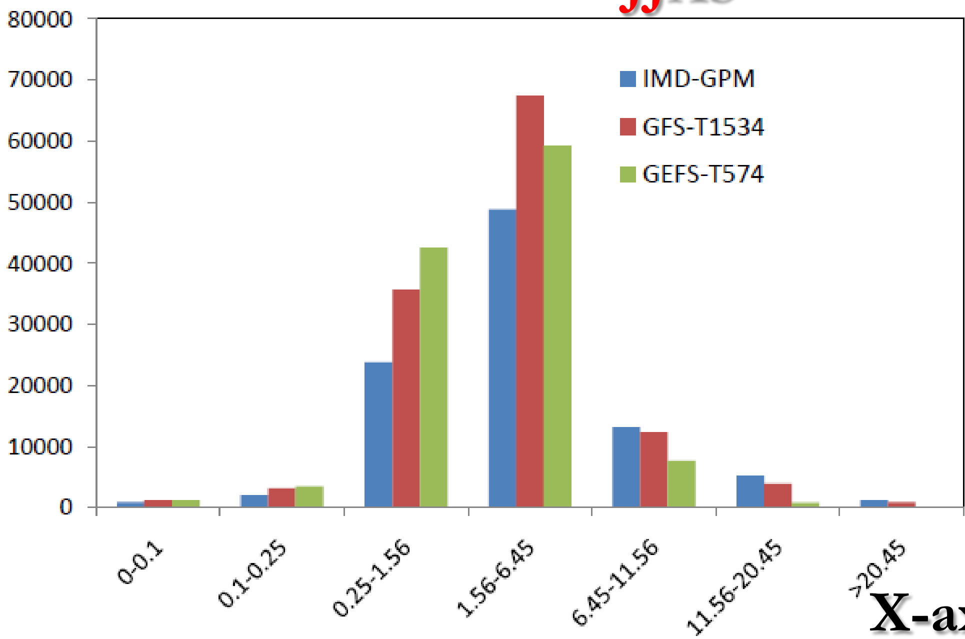

Day-3

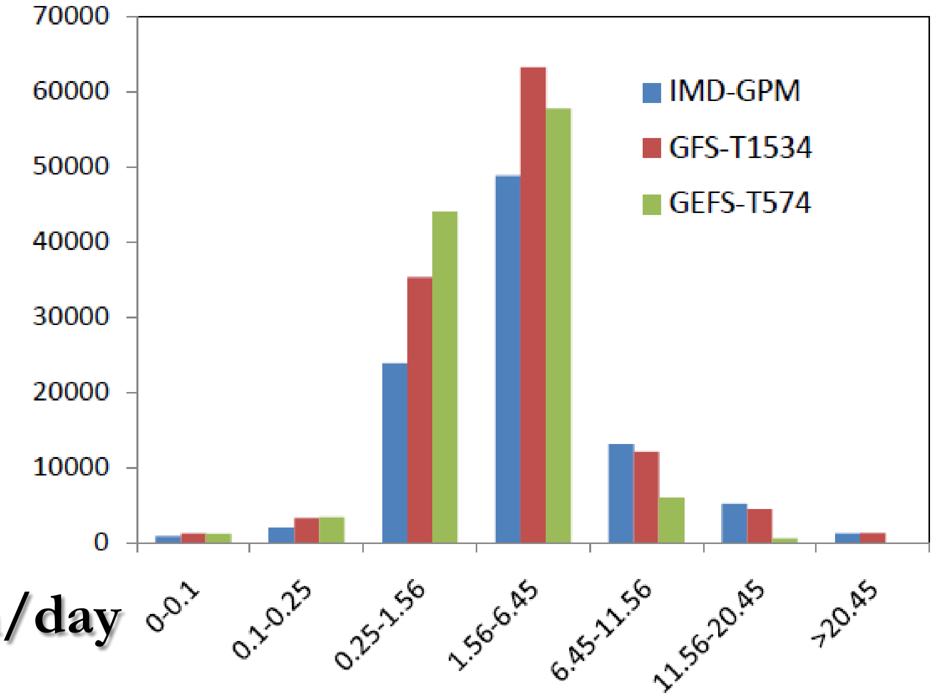

Day-5

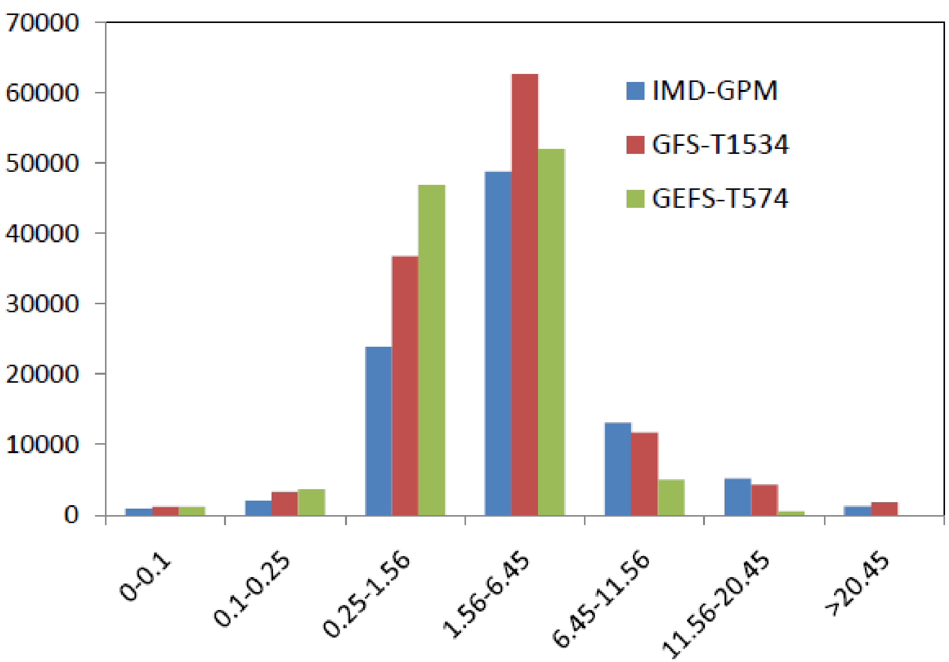

Day-8

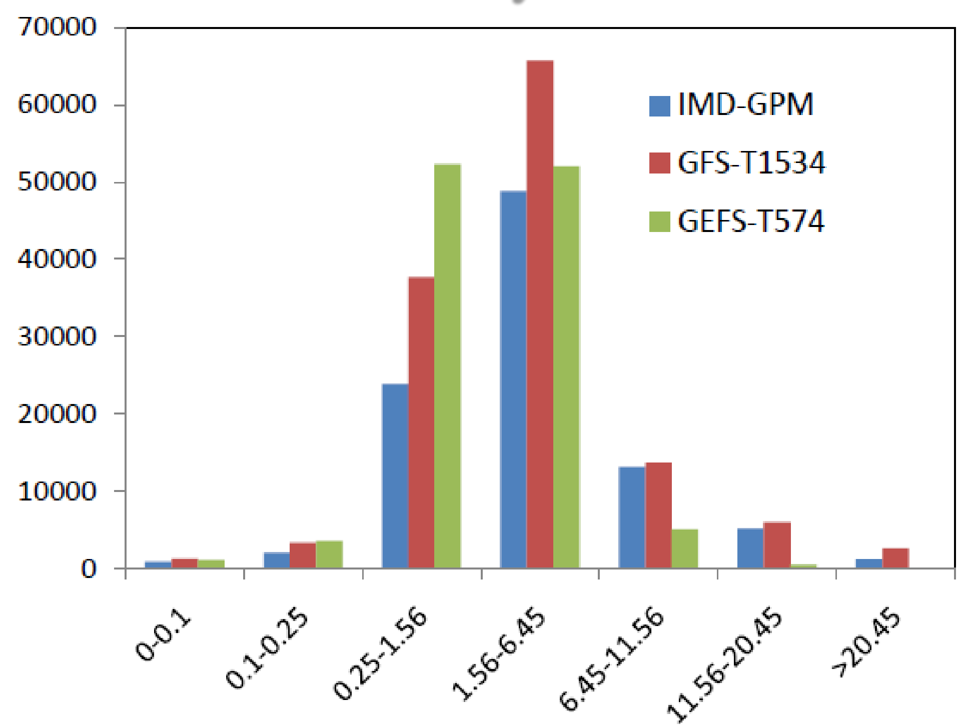

Recent very heavy rainfall over west coast predicted by GEFS T574 (30 km) with the probability

Forecast Valid for 23 Sept 2016 IC:22 Sept 2016

OBSERVATION

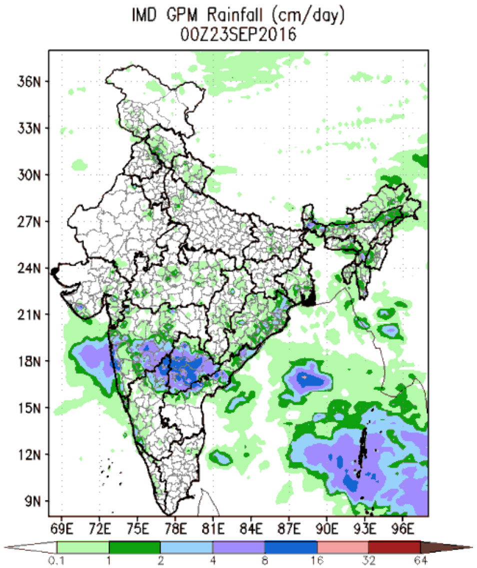

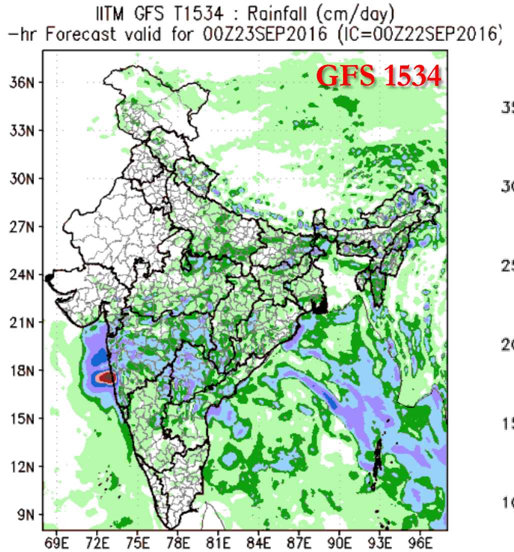

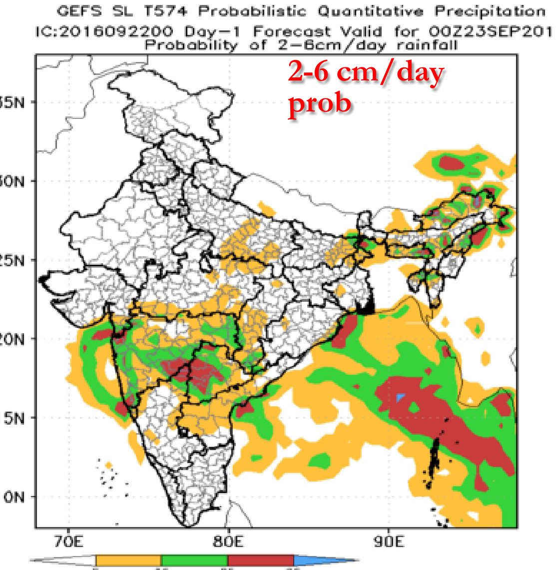

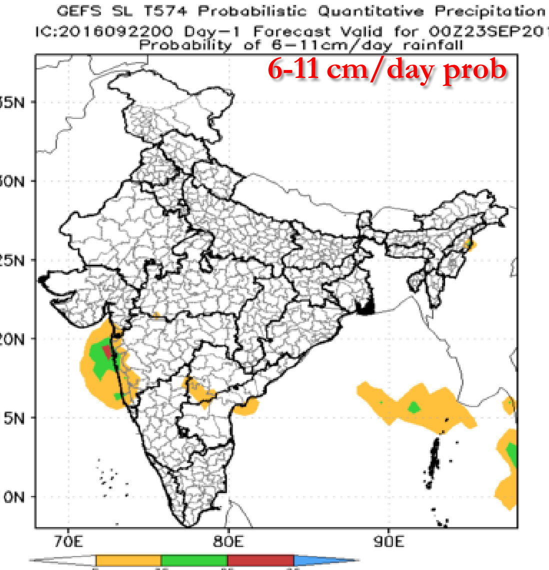

As per the IMD records, the 24 hr accumulated station rain on 23 Sep 2016 over

Colaba

(18.9067 N/ 72.8147 E) 45mm

SantaCruz

(19.0823 N/72.8407 E) 40 mm

Harnai, Goa

(17.8154 N/73.0981 E) : 136.7 mm

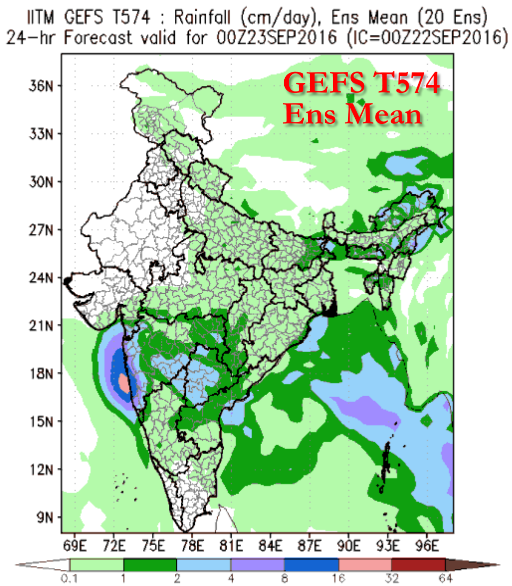

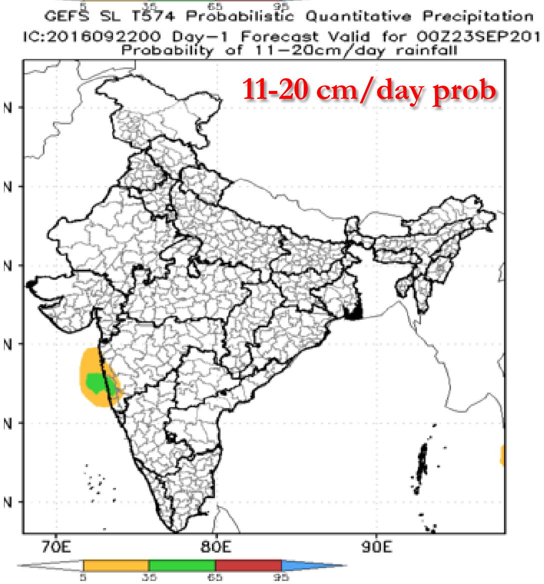

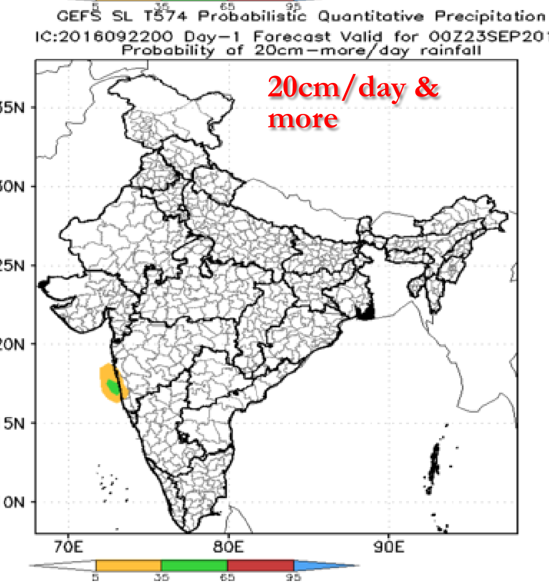

Summary

Improvement of GCM through better representation of cloud processes

Mean as well as Intraseasonal variability improved

Efficient in capturing the low clouds

GFS T1534 shows promise in capturing heavy precip

GEFS T574 efficient in providing probability of heavy rain

Thank You !